Biomarkers of Atherosclerosis

A study of plasma and solid tissues from animal and human models using nuclear magnetic resonance (NMR) technology

Peshang Abdulhannan

Submitted in accordance with the requirements for the degree of Doctor of Medicine

The University of Leeds, School of Medicine

January 2018

The candidate confirms that the work submitted is his own, except where work which has formed part of jointly authored publications has been included. The contribution of the candidate and the other authors to this work has been explicitly indicated below. The candidate confirms that appropriate credit has been given within the thesis where reference has been made to the work of others.

Publications

1- Literature review

"Peripheral arterial disease: a literature review". Abdulhannan P, Russell DA, Homer-Vanniasinkam S. Br Med Bull. 2012; 104: 21-39

Parts of Chapter 1 are based on this publication. P Abdulhannan wrote the initial draft and final version, S. Homer- Vanniasinkam identified the need for this work and edited the initial draft and D Russell edited and commented on the final draft.

2- Abstract

"^{1}H-NMR spectrometric identification of biomarkers of atherosclerosis in the Apolipoprotein-E knockout mouse". P Abdulhannan, S Saha, N Yuldasheva, S Wheatcroft, A Bekhit, D Russell, S Homer-Vanniasinkam and J Fisher. BJS 2014; 101 (S4): 2-49

Parts of chapters 3 and 8 are based on this publication. P Abdulhannan conducted the study and wrote the abstract, S Sakha supervised laboratory work, N Yuldasheva and S Wheatcroft supplied the animal care and preparation for the study, A Bekhit processed some of the samples, D Russell and S Homer-Vanniasinkam edited the final draft and J Fisher supervised the NMR work.

3- Abstract

"^{1}H-NMR Spectroscopic identification of biomarkers of atherosclerosis in patients with carotid artery disease". P Abdulhannan, S. Saha, D Russell, S Homer-Vanniasinkam and J Fisher. BJS 2015; 102 (S5): 3-52

Parts of chapter 5 are based on this publication. P Abdulhannan conducted the study and wrote the abstract, S Sakha supervised laboratory work, D Russell and S Homer-Vanniasinkam edited the final draft and J Fisher supervised the NMR work.

4- Abstract

“High resolution magic-angle-spinning NMR spectrometric identification of biomarkers of atherosclerosis in the Apolipoprotein-E knockout mice plaques (intact solid tissues)”. P Abdulhannan, S Saha, N Yuldasheva, S Wheatcroft, D Russell, S Homer-Vanniasinkam and J Fisher. BJS 2016; 103 (S3): 6–49

Parts of chapter 4 are based on this publication. P Abdulhannan conducted the study and wrote the abstract, S Sakha supervised laboratory work, N Yuldasheva and S Wheatcroft supplied the animal care and preparation for the study, D Russell and S Homer-Vanniasinkam edited the final draft and J Fisher supervised the NMR work.

This copy has been supplied on the understanding that it is copyright material and that no quotation from the thesis may be published without proper acknowledgement.

Acknowledgments

This thesis is dedicated to Kurdistan, a dream yet to become true

Firstly, I would like to thank my supervisor from the University of Leeds, School of Chemistry, Dr Julie Fisher who guided and supported me throughout the first three years of this study. Dr Fisher sadly passed away on the 5th August 2015 and was unable to see the final findings of this work.

I would also like to thank Mr David Russell for his endless patience and continuous support over the past 6 years. His expertise and constructive criticism have been invaluable to me.

"long may The Seagulls fly high"

A special thanks to Professor Shervanthi Homer-Vanniasinkam. You once told me a surgeon must have insight and a sense of humour. I am yet to know which one I lack.

My thanks go to Dr Sikha Saha for her tireless supervision and Dr Nadira Yuldasheva for her meticulous work on the animal sampling. Many thanks to Birmingham University HWB-NMR Unit and Christian Ludwig for supervising and supporting the magic angle spinning NMR experiment.

Many thanks to Dr Lee Roberts for stepping in last minute to save the day.

Finally, I would like to thank my family and friends who have put up with my grumpiness and food demands in difficult times. This work would have not been possible without you.

Pêşeng

Abstract

Biomarkers of Atherosclerosis

A study of plasma and solid tissues from animal and human models using nuclear magnetic resonance (NMR) technology

By Peshang Abdulhannan

Submitted for the degree of M.D., January 2018

Introduction: Current recommendations for surgical management of asymptomatic 50-99% carotid stenosis are guided by two factors, patient's fitness for surgical intervention and the clinical/imaging features associated with an increased risk of late stroke. Despite the advances in imaging modalities and their ability to detect some features of plaque instability, full understanding the pathophysiology of plaque instability will allow early intervention in patients with high risk of developing stroke from the unstable plaque. To date, no serum or urine marker has been shown to predict plaque instability and the risk of future cerebrovascular events.

Aims and methods: The aim of this study was to compare metabolic profiles of plasma and plaques from patients with symptomatic carotid stenosis undergoing endarterectomy, plasma and plaques from patients with symptomatic femoral stenosis, and plasma from patients without carotid or femoral disease (control). We also aim to compare plasma and solid tissues from mammalian model (mice), and further compare them to the human experiment. Nuclear magnetic resonance (NMR) spectroscopy will be used to analyse the metabolic profiles of plasma and plaques, and potentially identify predictive biomarkers of plaque

instability. Animal experiment was carried out using 6 apolipoprotein E–deficient versus 6 control mice. For the human experiment, carotid and femoral plaques alongside plasma and urine samples were collected from 84 patients. NMR analysis was performed on all the samples and further analysis was done on the resulting spectra and correlating data.

Results: The animal experiment showed weak models with inconclusive outcomes. Plasma human experiment also showed weak models and could not confidently establish certain metabolites as atherosclerotic biomarkers. However, similarities were observed between the animal and human models, and 3 metabolites (2-oxoglutarate, choline and taurine) were identified as potential biomarkers. In contrary, human solid tissue experiments have shown much stronger models and clearer results. Spectra gained from these experiments were the first to be described, with no comparable studies in the literature. The most notable finding is the possible effect of taurine on carotid plaques. Taurine signals have been observed in the animal (plasma and solid) as well as human plasma models in this study. Although, they were merely affecting the control groups.

Conclusions: Identifying plaque instability in asymptomatic carotid disease was the centre of this study. Taurine's strong influence on the metabolic profiling of carotid plaques raises the possibility of a potential biomarker of plaque instability. Further work is required regarding the histological examination of plaque sections. An objective assessment of the plaque instability will improve the study outcome and add a different aspect to the current results.

Table of Contents

Acknowledgements……4

Abstract……5

Table of Contents……7

List of Tables……11

List of Figures……13

Abbreviations……18

Chapter 1: Introduction and background……23

1.1 Carotid Atherosclerosis……24

1.1.1 Risk factors……24

1.1.2 Clinical symptoms of carotid artery disease……27

1.1.3 Radiological investigations of CAD……28

1.1.4 Management of carotid artery disease……30

1.2 Peripheral artery disease in the lower limbs (PAD)……35

1.2.1 PAD morbidity and mortality……36

1.2.2 PAD risk factors……37

1.2.3 Clinical presentation of PAD and classification……38

1.2.4 Radiological diagnostic investigations for PAD……39

1.3 Carotid plaque morphology and plaque instability……41

1.3.1 The unstable plaque……43

1.3.2 Predicting plaque instability……46

1.4 The “Omics” era……47

1.4.1 Metabolomics……48

1.4.2 The use of NMR in metabolic profiling……49

1.4.3 Nuclear Magnetic Resonance (NMR) Spectrometry…..51

1.4.4 Data processing…… 58

1.4.5 Previous NMR studies on atherosclerosis…… 59

1.5 Rationale of this study and expected value of results…… 64

Chapter 2: Design and methods…… 66

2.1 Animal sample methods……..66

2.1.1 Blood sample collection…….. 66

2.1.2 Tissue sample collection…… 68

2.2 Human sample methods…….. 70

2.2.1 Patient recruitment……70

2.2.2 Blood sample collection……... 71

2.2.3 Urine sample collection…… 74

2.2.4 Plaque samples protocol…….. 74

2.3 ^{1}H-NMR spectroscopy methods – liquid status…….. 80

2.3.1 Sample preparation…….. 80

2.3.2 ^{1}H-NMR spectroscopy data collection……...82

2.4 ^{1}H-NMR spectrometry methods - solid status…… 83

2.4.1 Sample preparation…….. 83

2.4.2 HR-MAS NMR spectroscopy…….. 84

2.5 Spectral processing…….. 84

2.6 Statistical analysis…….. 86

2.6.1 Multivariate statistical analysis (MVA)……... 86

2.6.2 Univariate statistical analysis…… 87

Chapter 3: NMR analysis of plasma - Animal samples…… 88

3.1 Results……... 88

3.1.1 Analysis of all mice plasma spectra – CPMG Sequence…….. 89

3.1.2 Analysis of all mice plasma spectra – DOSY sequence……...96

3.2 Discussion…….. 102

Chapter 4: NMR analysis of solid tissues - Animal samples……103

4.1 Results……... 103

4.1.1 Analysis of all mice solid tissues spectra – CPMG sequence…… 104

4.1.2 Analysis of all mice solid tissue spectra – 1D NOESY sequence……..108

4.2 Discussion…….. 115

Chapter 5: NMR analysis of plasma - Human samples…… 116

5.1 Results…….. 116

5.1.1 Analysis of all human plasma spectra – CPMG sequence…… 117

5.1.2 Analysis of human plasma spectra (carotid v femoral) – CPMG sequence……126

5.1.3 Analysis of all human plasma spectra – DOSY sequence……..129

5.1.4 Analysis of human plasma spectra (carotid v control) – DOSY sequence…… 133

5.1.5 Analysis of human plasma spectra (carotid v femoral) – DOSY sequence…… 137

5.2 Discussion……. 139

Chapter 6: NMR analysis of plaques - Human samples……...140

6.1 Results……... 140

6.1.1 Analysis of atherosclerotic carotid and femoral plaques – CPMG sequence……141

6.1.2 Analysis of atherosclerotic carotid and femoral plaques – DOSY sequence……. 147

6.2 Discussion……. 153

Chapter 7: Other experiments…….. 154

7.1 Urine experiment……. 154

7.1.1 Analysis of urine samples – NOESY sequence…….. 154

7.2 Histopathological experiment……. 156

Chapter 8: Final discussion and conclusions……. 157

8.1 NMR plasma experiments…….. 158

8.2 NMR solid tissue experiments…….. 160

8.3 Future research…… 162

References…….. 163

List of Tables

Table 1: NASCET criteria for carotid artery stenosis evaluation---------- 29

Table 2: Comparison of BMT and CEA---------- 33

Table 3: Fontaine's and Rutherford's classification of PAD---------- 39

Table 4: Terms Used to Designate Different Types of Human Atherosclerotic Lesions in Pathology---------- 43

Table 5: Advantages and disadvantages of NMR vs MS---------- 50

Table 6: Examples of different spin quantum numbers of isotopes based on their proton and neutron numbers---------- 52

Table 7: Dark regions excluded from spectra prior to binning and normalisation---------- 85

Table 8: Mice weight: comparison between the study and control groups--- 88

Table 9 Chemical shifts responsible for high scores and correlating metabolites PLS-DA – All mice plasma – CPMG---------- 96

Table 10: Chemical shifts responsible for high scores and correlating metabolites. PCA – All mice plasma – DOSY---------- 100

Table 11: Mice weight: comparison between the study and control groups--103

Table 12: Chemical shifts responsible for high scores and correlating metabolites. PLS-DA - All mice solid tissue - 1D NOESY---------- 114

Table 13: Patients demographics and medical background – NMR plasma study---------- 117

Table 14: Chemical shifts responsible for high scores and correlating metabolites. PLS-DA - All human plasma (without Ctrl-078) – CPMG------- 126

Table 15: Chemical shifts responsible for high scores and correlating metabolites. PLS-DA - Human plasma (carotid v control) – DOSY---------- 136

Table 16: Patients demographics and medical background – NMR plaque study---------- 141

Table 17: Chemical shifts responsible for high scores and correlating metabolites. PLS-DA - carotid v femoral plaques – CPMG---------- 145

Table 18: Chemical shifts responsible for high scores and correlating metabolites. PLS-DA - carotid plaques – DOSY---------- 151

Table 19: Chemical shifts responsible for high scores and correlating metabolites. PLS-DA - femoral plaques – DOSY---------- 151

List of Figures

Figure 1: All-cause and CVD morality according to ABPI group, SHS, 1988 to 1999, n=439---------- 37

Figure 2: Plaque progression---------- 42

Figure 3: Energy splitting under the effect of external magnetic field Bo---------- 53

Figure 4: Change of bulk magnetisation vector rotation under the effect of a perpendicular RF pulse

Figure 5: 600 MHz ^{1}H NMR spectrum of urine---------- 56

Figure 6: 600 MHz 1H NMR spectrum of blood sample---------- 57

Figure 7: Blood sample collection from mice---------- 68

Figure 8: Tissue sample collection from mice---------- 69

Figure 9: Blood sample collection from patients---------- 73

Figure 10: Plaque sections at 2 mm intervals---------- 75

Figure 11: Plaque sectioning and processing---------- 76

Figure 12: All mice plasma spectra with highlighted dark regions using CPMG sequence---------- 89

Figure 13: PCA model – All mice plasma – CPMG sequence---------- 90

Figure 14: Score scatter of the PCA model – All mice plasma – CPMG---------- 91

Figure 25: Score column of the PCA model – All mice plasma – CPMG---------- 91

Figure 16: Score scatter of the PCA model – All mice plasma (without sample 37C) – CPMG---------- 92

Figure 17: PLS-DA model – All mice plasma – CPMG sequence---------- 93

Figure 18: Score scatter of PLS-DA model – All mice plasma – CPMG---------- 93

Figure 19: Score column of the PLS-DA model – All mice plasma – CPMG--------- 94

Figure 20: Component 1 loading column of the PLS-DA model – All mice plasma – CPMG---------- 95

Figure 21: Component 2 loading column of the PLS-DA model – All mice plasma – CPMG----------95

Figure 22: All mice plasma spectra with highlighted dark regions using DOSY sequence---------- 97

Figure 23: PCA model – All mice plasma – DOSY sequence---------- 97

Figure 24: Score scatter of the PCA model – All mice plasma – DOSY----------98

Figure 25: Loading column of the PCA model – All mice plasma – DOSY---------- 99

Figure 26: Score scatter of the PLS-DA model – All mice plasma – DOSY---------- 101

Figure 27: All mice solid tissue spectra with highlighted dark regions using CPMG sequence---------- 104

Figure 28: PCA model – All mice solid tissue – CPMG sequence---------- 105

Figure 29: Score column of the PCA model – All mice solid tissue – CPMG---------106

Figure 30: Score scatter of the PCA model – All mice solid tissue (without sample 21X) – CPMG---------- 106

Figure 31: PLS-DA model – All mice solid tissue – CPMG sequence----------107

Figure 32: Valine signal - PLS-DA model – All mice solid tissue – CPMG sequence----------108

Figure 33: All mice solid tissue spectra with highlighted dark regions using 1D NOESY sequence---------- 109

Figure 34: PCA model – All mice solid tissue – 1D NOESY sequence---------- 109

Figure 35: Score scatter of the PCA model – All mice solid tissue – 1D NOESY--- 110

Figure 36: Score column of the PCA model – All mice solid tissue – 1D NOESY-- 110

Figure 37: PLS-DA model – All mice solid tissue – 1D NOESY sequence---------- 111

Figure 38: Score scatter of the PLS-DA model - All mice solid tissue - 1D NOESY--112

Figure 39: OPLS-DA model – All mice solid tissue – 1D NOESY sequence--------- 112

Figure 40: Loading column of the PLS-DA model – All mice solid tissue – 1D NOESY---------- 113

Figure 41: ethanol signal in sample Ctrl-078 (plasma)---------- 118

Figure 42: PCA model – All human plasma (without Ctrl-078) – CPMG sequence--119

Figure 43: Score scatter of the PCA model – All human plasma (without Ctrl-078) – CPMG---------- 119

Figure 44: Score scatter of the PCA model – All human plasma (without samples Ca-010, Ca-011, Ca-015, Ctrl-065, Ctrl-078) – CPMG---------- 120

Figure 45: Score scatter of the PCA model based on gender – All human plasma (without Ctrl-078) – CPMG---------- 121

Figure 46: Score scatter of the PLS-DA model - All human plasma (without Ctrl-078) – CPMG----------122

Figure 47: Score scatter of the PLS-DA model showing the sub-clustering of the femoral endarterectomy group – All human plasma (without Ctrl-078)– CPMG---------- 122

Figure 48: Score scatter of the OPLS-DA model – All human plasma (without Ctrl-078) – CPMG---------- 123

Figure 49: Score column of the PLS-DA model showing the clustering of control samples to the left when arranging the scores in ascending order - All human plasma (without Ctrl-078) – CPMG----------125

Figure 50: Loading column of the PLS-DA model - All human plasma (without Ctrl-078) – CPMG---------- 125

Figure 51: Score Figure 52: Score scatter of the OPLS- DA model - (carotid v femoral) plasma -(without samples Ca-010, Ca-011, Ca-012, Ca-015, Fe-049) – CPMG----127

scatter of the PCA model - (carotid v femoral) plasma – CPMG----------128

Figure 53: Score scatter of the PCA model - All human plasma (without Ctrl-078) – DOSY---------- 130

Figure 54: Score scatter of the PCA model - All human plasma (without Ctrl-078 and Ctrl-065) – DOSY----------131

Figure 55: Score scatter of the PLS-DA model - All human plasma (without Ctrl-078 and Ctrl-065) – DOSY---------- 132

Figure 56: Score scatter of the OPLS-DA model - All human plasma (without Ctrl-078 and Ctrl-065) – DOSY---------- 133

Figure 57: PCA model – Human plasma (carotid v control) – DOSY----------134

Figure 58: Score scatter of the PLS-DA model – Human plasma (carotid v control) – DOSY---------- 134

Figure 59: Loading column of the PLS-DA model – Human plasma (carotid v control) – DOSY---------- 135

Figure 60: Score scatter of the PCA model - Human plasma (carotid v femoral) – DOSY----------137

Figure 61: Score scatter of the OPLS-DA model - Human plasma (carotid v femoral) – DOSY---------- 138

Figure 62: Score scatter of the PCA model - carotid v femoral plaques – CPMG---142

Figure 63: Score scatter of the PCA model - carotid v femoral plaques (excluding the outliers) – CPMG---------- 142

Figure 64: Score scatter of the PLS-DA model - carotid v femoral plaques (excluding the outliers) – CPMG---------- 143

Figure 65: Loading column of the PLS-DA model - carotid v femoral plaques (excluding the outliers) – CPMG---------- 144

Figure 66: PCA model – carotid v femoral plaques – DOSY---------- 147

Figure 67: Score scatter of the PCA model - carotid v femoral plaques – DOSY----148

Figure 68: Score scatter of the PLS-DA model - carotid v femoral plaques –

DOSY---------- 149

Figure 69: Score scatter of the PLS-DA model - carotid v femoral plaques (excluding patient Fe-055) – DOSY---------- 149

Figure 70: Loading column of the PLS-DA model - carotid v femoral plaques –

DOSY---------- 150

Figure 71: NMR spectra of urine sample – NOESY---------- 155

Abbreviations

3D: 3-dimensional

ABPI: ankle brachial pressure index

ACD-Labs: Advanced Chemistry Development - Laboratories

APES: 3-aminopropyl-triethoxysilane

ApoE-/-: apolipoprotein-E knock-out

BMT: best medical therapy

Bo: external magnetic field

C: carbon

CAD: coronary artery disease

CAS: carotid artery stenting

CCA: common carotid artery

CEA: carotid endarterectomy

CI: Confidence Interval

Cit: citrate

CLI: critical limb ischaemia

CPMG: Carr-Purcell-Meiboom-Gill

COPD: chronic obstructive pulmonary disease

CRP: C-reactive protein

CT: computerised tomography

CTA: computed tomography angiography

CVD: cardiovascular disease

D_2O: deuterium oxide

DM: diabetes mellitus

DOSY: diffusion-ordered spectroscopy

EAS: European Atherosclerosis Society

ECG: electrocardiography

EDTA: ethylene-diamine-tetra-acetic acid

EDV: end diastolic velocity

F: fluoride

FID: free induction decay

G: gauge

GA: general anaesthetic

GC: gas chromatography

GPx-1: glutathione peroxidase 1

H: hydrogen

H&E: haematoxylin and eosin

HDL: high-density lipoprotein

HDL-C: high-density lipoprotein cholesterol

HMW: high molecular weight

HR: high resolution

HR-MAS: high-resolution magic angle spinning

IC: intermittent claudication

ICA: internal carotid artery

IL: interleukin

IMT: intima-media thickness

LC: liquid chromatography

LDL: low-density lipoprotein

LH: lithium heparinised

LICAMM: Leeds Institute of Cardiovascular and Metabolic Medicine

LIGHT: Leeds Institute of Genetics, Health and Therapeutics

LDL: low-density lipoprotein

LDL-C: low-density lipoprotein cholesterol

LMW: low molecular weight

Lp-PLA2: lipoprotein-associated phospholipase A2

MAS: magic angle spinning

MCP-1: monocyte chemotactic protein-1

MMPs: matrix metallo-proteinases

MPO: myeloperoxidase

MPs: microparticles

MRA: magnetic resonance angiography

MS: mass spectrometry

N: nitrogen

NaOH: sodium hydroxide

NMR: nuclear magnetic resonance

NOESY: nuclear overhauser effect spectroscopy

NRES: National Research Ethics Service

O_2: oxygen

OPLS-DA: orthogonal partial least squares - discriminant analysis

P: phosphate

PAD: peripheral arterial disease

PAPP-A: pregnancy associated plasma protein A

PCA: principle components analysis

PET/CT: positron emission computerised tomography

PIGF: phosphatidylinositol-glycan biosynthesis class F protein

PFA: paraformaldehyde

PLS-DA: partial least squares - discriminant analysis

PSV: peak systolic velocity

RBCs: red blood cells

RF: radio frequency

S: sulphur

SARS: Society of Academic & Research Surgery

SAA: serum amyloid A

sCD40L: soluble CD4 ligand

SHS: Swedish heart study

sPLA2: secretory type-IIa phospholipase

TG: triglycerides

TIA: transient ischaemic attack

TNF: tumour necrosis factor

VLDL: very low-density lipoprotein

WBCC: white blood cell count

Chapter 1: Introduction and background

Atherosclerosis is a systemic chronic inflammatory response to fatty deposition on the intima, resulting in thickening of the arterial wall and the formation of plaques. Atherosclerosis can affect the heart causing myocardial infarction, the brain causing stroke and the legs causing ischaemia which might lead to amputation. It is considered the main cause of death globally and counts for almost 50% of all deaths in western countries (Hansson, 2005) (Lusis, 2000)
Stroke is one of the most common causes of death worldwide (Mathers, et al., 2009) with carotid artery disease implicated in about 15% of ischaemic strokes (Naylor, et al., 2017).

Acute events associated with carotid atherosclerosis are caused by plaque rupture and the creation of thrombus. Although changes in plaque morphology precede symptoms, understanding of the underlying pathophysiology is still inadequate. Therefore, identifying early biomarkers of plaque instability could potentially avoid these acute events and reduce morbidity and mortality rates related to them.

The aim of this study is to identify biomarkers of carotid plaque instability using Nuclear Magnetic Resonance (NMR) spectroscopy, to be able to identify patients with unstable asymptomatic carotid disease.

This chapter describes carotid and femoral atherosclerosis, risks factors and treatment methods. An explanation of plaque morphology and pathophysiology

is followed by an insight into omics technology and principles of metabolomic profiling using NMR and current advances in solid status NMR studies.

1.1 Carotid Atherosclerosis

Carotid atherosclerosis mainly affects the bifurcation of the common carotid artery and is a combination of focal accumulation of lipid in the intima (atheroma) and thickening of the media (atherosclerosis). Stroke related to carotid artery disease happens mainly due to plaque disruption and distal embolisation (Barnett, et al., 2000).

1.1.1 Risk factors

Risk factors for carotid artery disease (CAD) are similar to those for any atherosclerotic disease. These include non-modifiable factors (Age, sex and family history) and modifiable ones (smoking, hypertension, diabetes mellitus and dyslipidaemia).

1.1.1.1 Age and sex

Several studies have clearly indicated an increased risk of atherosclerosis with increasing age in both men and women (Newman, et al., 1999). Carotid disease incidence in under 50-year-olds is negligible (Kroger, et al., 1999) and rises above 80% in over 90-year-olds (Homma, et al., 2001). The evidence of a gender difference is slightly less clear with some studies suggesting that men are at a higher risk of developing atherosclerotic plaques (Moody, et al., 1990) (Li, et al., 1994).

1.1.1.2 Family history

There have been a few studies emphasising the importance of family history of atherosclerosis on the presence of carotid artery disease (CAD). A recent cohort study of 864 patients with CAD compared to 1698 controls concluded that family history of stroke and of coronary artery disease were each associated with carotid artery disease, suggesting shared genetic and environmental factors contributing to its risk. The study also suggested that sibling history gives greater risk than parental history (Khaleghi, et al., 2014).

1.1.1.3 Smoking

The relation between smoking and the prevalence of CAD is well established (Tell, et al., 1994). In fact, smoking is the single most important risk factor for atherosclerosis (Doll, et al., 2004). Analysing results from 4 large population-based cohort studies suggested that smoking was associated with a significant increase in the incidence of internal carotid artery stenosis, with an odds ratio of 2.3 (95% CI 1.8 – 2.8) for >50% stenosis and of 3 (95% CI 2.1 – 4.4) for >70% stenosis (de Weerd, et al., 2014).

Furthermore, both current and ex-smokers who suffer from chronic infections associated with smoking (such as chronic obstructive pulmonary disease COPD, chronic bronchitis, recurrent upper respiratory tract infection, chronic gastrointestinal infection and chronic skin infection and ulceration) have an increased risk of atherosclerosis with odds ratios of 3.3 and 3.4 respectively (Kiechl, et al., 2002).

1.1.1.4 Hypertension

There is good evidence that hypertension is a powerful predictor of cardiovascular events (Lawes, et al., 2008) (Liu, et al., 2015). A blood pressure above 160/95 mmHg increases the risk of atherosclerosis by 2.5-4 fold (Murabito, et al., 1997) with most studies considering systolic hypertension a significant factor in carotid plaque development and progression (Willeit & Kiechl, 1993) (Su, et al., 2001).

1.1.1.5 Diabetes Mellitus

Diabetes mellitus (DM) has been recognized as one of the main elements for the presence and progression of carotid artery disease. Carotid intima-media thickness (IMT) has been defined as a valuable tool for risk stratification in this population (Bosevski, 2014) (Chambless, et al., 2002). However, this is disputed in some studies which report that DM is associated with plaque progression but not IMT (Van de Meer, et al., 2003).

In other studies, DM has been defined as an independent factor for the presence of high-grade carotid-artery stenosis in the general population (Göksan, et al., 2001) with Type 2 diabetes a considerable risk factor for the progression of atherosclerosis and the increase of carotid IMT (Bosevski & Stojanovska, 2015). The Northern Manhattan Study suggested that diabetes doubles the risk of stroke. It also suggested that the duration of diabetes is independently linked to ischaemic stroke risk (Banerjee, et al., 2012). However, there is no clear evidence of its association with plaque instability (Scholtes, et al., 2014).

1.1.1.6 Dyslipidaemia

The exact association between dyslipidaemia, carotid artery disease and stroke is yet to be fully understood with mixed epidemiological evidence relating cholesterol levels to the incidence and progression of atherosclerosis. Most evidence suggests that high low-density lipoprotein cholesterol (LDL-C) levels or low high-density lipoprotein cholesterol (HDL-C) are independent risk factors for carotid artery atherosclerosis (Fabris, et al., 1994) (Demarin, et al., 2010). The Framingham study linked total cholesterol levels with raised risk of carotid artery disease (O'Leary, et al., 1992b), while some recent studies have indicated that total triglyceride (TG) is an independent risk factor for carotid plaques (Mi, et al., 2016).

The use of lipid-lowering agents (such as statins) has shown a reduction in 10-year stroke risk from 24.1% to 13.4% in patients who were treated conservatively, and from 17.9% to 7.6% in patients who were treated with carotid endarterectomy (Halliday, et al., 2010). A Cochrane review of 18 randomised controlled trials on statins role in preventing cardiovascular disease, showed a significant reduction in stroke rate in patients on statins compared to the control group (Relative risk 0.78, 95% CI 0.68 – 0.89) (Taylor, et al., 2013).

1.1.2 Clinical symptoms of carotid artery disease

Carotid artery symptoms can be classified to hemispheric or retinal. Hemispheric symptoms include hemi-motor/sensory signs and/or evidence of higher cortical dysfunction (dysphasia, visuospatial neglect, etc). This could be in form of stroke which is defined as a focal (occasionally global) loss of cerebral function lasting >24 hours, or a transient ischaemic attack (TIA) which has a similar definition but

the deficit lasts <24 hours. Retinal symptoms comprise transient monocular blindness (amaurosis fugax) or permanent monocular visual loss following central retinal artery occlusion (equivalent to a stroke). The term ‘crescendo’ TIAs is used when the patient suffers repeated neurological events with complete recovery in between.

1.1.3 Radiological investigations of CAD

There have been many studies on the ability of radiological investigations to identify features of plaque instability as well as assessing and detecting atherosclerotic arterial disease. Colour-assisted duplex ultrasound is an important imaging modality for assessing patients with carotid artery disease. It is recommended as a first line investigation for carotid disease (Naylor, et al., 2017). It is non-invasive, safe and inexpensive. It has a sensitivity and specificity for 70 to 90% stenosis of 0.89 and 0.84 respectively while they are 0.36 and 0.91 for 50 to 69% stenosis (Wardlaw, et al., 2006).

Contrast-enhanced ultrasound can further evaluate carotid stenosis morphology and possibly neovascularization of plaque. Although this is promising for predicting plaque instability, it is not widely used and has to be standardized and proven in prospective studies (Shalhoub, et al., 2010). The recommended criteria for ultrasound evaluation of carotid stenosis is based on the NASCET measurement method. It includes recording the peak systolic velocity (PSV) and the end diastolic velocity (EDV) in both internal carotid artery (ICA) and common carotid artery (CCA), then measuring their ratios to determine degree of stenosis (table 1) (Oates, et al., 2009).

Magnetic Resonance Angiography (MRA), on the other hand, is less operator dependent and produces an image of the whole artery. Contrast enhanced MRA has the ability to produce a three-dimensional image of the carotid bifurcation with good sensitivity and specificity for detecting high-grade carotid stenosis (0.94 and 0.93, respectively, for stenosis of 70 to 90%, and 0.77 and 0.97, respectively, for stenosis of 50 to 69%) (Wardlaw, et al., 2006). MRA has been considered a promising modality for predicting plaque instability by detecting the presence of a large necrotic core, the amount of intraplaque haemorrhage and the presence of ulcerated or thinned plaque cap (Kerwin, et al., 2013) (Wasserman, 2010).

Positron Emission Computerised Tomography (PET/CT) scanning has shown some promise as a mean for assessment of plaque instability (Sakalihasan & Michel, 2009). It has been used to allow *in vivo* identification of local activity related to altered or increased cell metabolism in the arterial wall which may be associated with plaque instability (Wu, et al., 2007) . However, it is expensive, not widely available and has the disadvantage of the exposure to ionising radiation which makes it difficult to carry out serial assessments (Mofidi & Green, 2014).

% Stenosis	**PSV ICA (cm/s)**	**PSV (ICA) / PSV (CCA) ratio**	**PSV (ICA) / EDV (CCA) ratio**
< 50%	<125	<2	<8
50 – 69 %	≥125	2 – 4	8 – 10
60 – 69 %	≥125	2 – 4	11 – 13
70 – 79 %	≥230	≥4	14 – 21
80 – 89 %	≥230	≥4	22 – 29
> 90%	≥400	≥5	≥30
Near occlusion	String flow	Variable	Variable
Occlusion	No flow	No flow	No flow

Table 2: NASCET criteria for carotid artery stenosis evaluation (Oates, et al., 2009)

1.1.4 Management of carotid artery disease

1.1.4.1 Best medical therapy

Best medical therapy is centred around reversible risk factors of atherosclerosis with the emphasis on the anti-inflammatory effect of some pharmaceutical agents on the progress of plaque. Patients who present with TIA symptoms should be started on risk factor medications, which may reduce their risk of stroke within the following 90 days for up to 80% (Rothwell, et al., 2007).

1.1.4.1.1 Antiplatelet therapy

Antiplatelet therapy is one of the most important interventions to reduce the odds of recurrent stroke or TIA by up to 22% (Intercollegiate Stroke Working Party of the Royal College of Physicians of London, 2016). Early studies suggested that aspirin (Cyclooxygenase pathway inhibitor) could reduce the risk of long term stroke by up to 25% (Antiplatelet Trialists' Collaboration, 1994). There is also evidence that the use of aspirin and dipyridamole combined reduces the risk of late stroke significantly compared with either of them alone (Diener, et al., 1996) (ESPRIT Study Group, 2006).

ADP inhibitors monotherapy (Clopidogrel, Dipyridamole and Ticlopidine) has also been used, with strong evidence suggesting that clopidogrel significantly reduces the risk of stroke compared to aspirin monotherapy (CAPRIE Steering Committee, 1996). However, combining aspirin and dipyridamole was found to be as effective as clopidogrel monotherapy (ESPRIT Study Group, 2006) (PRoFESS Study Group, 2008). Although, there is no evidence that adding

aspiring to clopidogrel has any advantage compared to clopidogrel monotherapy, with evidence of increased bleeding risk when using both (Diener, et al., 2004). It is therefore recommended that the standard antiplatelet treatment to reduce the risk of recurrent ischaemic stroke or TIA should be clopidogrel 75mg daily as a first line. If clopidogrel is not tolerated, aspirin 75mg daily with dipyridamole 200mg twice daily should be used instead (Intercollegiate Stroke Working Party of the Royal College of Physicians of London, 2016).

In asymptomatic carotid disease, however, there is conflicting evidence regarding antiplatelet therapy. Early studies on aspirin effect on patients with asymptomatic carotid disease suggested no difference in any ischaemic events or death when using aspirin (Côté, et al., 1995). More recent studies in contrast associated antiplatelet therapy with lower rates of stroke and death in patients with asymptomatic 70-99% carotid stenosis (King, et al., 2013). It is currently recommended to use aspirin 75-325mg daily as a first line antiplatelet therapy in patients with asymptomatic carotid stenosis to reduce the risk of myocardial infarction and other cardiovascular events, with clopidogrel reserved for patients with aspirin intolerance (Naylor, et al., 2017).

1.1.4.1.2 Lipid lowering therapy

There is growing evidence that the effect of statins is not just cholesterol lowering but they also thought to have a role in carotid plaque stability. The UK Heart Protection Study suggested a relative risk reduction of 25 % in stroke and 17% in vascular death when using simvastatin 40mg daily (Heart Protection Study Collaborative Group, 2011). Other studies suggested that there is a relative risk reduction of 15% in stroke when using atorvastatin 80mg daily (Amarenco, et al.,

2006). Based on these two studies, it is recommended to use statin therapy with atorvastatin 80mg daily in the management of patients with ischaemic stroke or TIA (Intercollegiate Stroke Working Party of the Royal College of Physicians of London, 2016).

Statin therapy is also currently recommended in patients with asymptomatic carotid stenosis to reduce the risk of stroke (Halliday, et al., 2010). However, so far there is insufficient evidence regarding the dosage and intensity of statins (Naylor, et al., 2017).

1.1.4.1.3 Blood pressure control

There is a considerable controversy around the role of blood pressure control on the risk of stroke. However, there is enough evidence to suggest that the use of Angiotensin-Converting Enzyme Inhibitors (ACEi) does lower this risk. Two large randomised trials (PROGRESS and HOPE) studied the effect of ACEi on the risk of stroke in patients with history of ischaemic stroke or TIA (PROGRESS) or vascular disease (HOPE). PROGRESS suggested a relative risk reduction of 28% at 4 years when using perindopril 4mg daily (PROGRESS Collaborative Group, 2001), while HOPE suggested a 32% relative risk reduction in stroke when using ramipril 10mg daily (The Heart Outcome Prevention Evaluation Study Investigators, 2000).

It is currently recommended that patients who had an ischaemic stroke or TIA should maintain their systolic blood pressure <130mmHg to effectively reduce their risk of recurrent stroke (Intercollegiate Stroke Working Party of the Royal College of Physicians of London, 2016). Although there are no randomised trials

to study the effect of blood pressure control on preventing stroke in patients with asymptomatic carotid stenosis, it is still recommended to maintain their blood pressure <140/90mmHg, based on a meta-analysis of 25 blood pressure randomised controlled trials (Naylor, et al., 2017).

1.1.4.2 Surgical and endovascular interventions

Randomised controlled trials on managing carotid artery disease have suggested treating symptomatic carotid disease (50-99% stenosis) with carotid endarterectomy with the maximum benefit in patients with 70-99% stenosis, provided the peri-operative risks do not exceed the benefits from this intervention (North American Symptomatic Carotid Endarterectomy Trial Collaborators (NASCET), 1991).

Table 3 summarises the results from three large trials (European Carotid Surgery Trialists' Group 1998; North American Symptomatic Carotid Endarterectomy Trial NASCET 1998; and the Veteran Affairs Trial 1991), comparing best medical therapy (BMT) to carotid endarterectomy (CEA) in symptomatic carotid disease. (Naylor, 2015).

	5 years ipsilateral stroke prevention	
Stenosis	BMT	CEA
<30%	9.8%	12.1%
30-49%	18.1%	14.8%
50-69%	18.2%	13.6%
70-99%	26.2%	10.4%

Table 2: Comparison of BMT and CEA (Naylor, 2015)

However, controversy arises in asymptomatic carotid disease. A large randomised trial from the USA (ACAS 1995) strongly recommended carotid endarterectomy in asymptomatic lesions causing > 60% stenosis. However, data from this trial and another large randomised trial from the UK (ACST 2004) suggested that intervening on asymptomatic carotid stenosis may only provide a modest reduction in stroke risk from 2% per year to 1% per year (Executive Committee for the Asymptomatic Carotid Atherosclerosis Study, 1995) (MRC Asymptomatic Carotid Surgery Trial (ACST) Collaborative Group, 2004). This was widely criticised, and the results of those two trials are probably too historical now to guide practice (Naylor, 2015). A second Asymptomatic Carotid Surgery Trial (ACST-2) and a second European Carotid Surgery Trial (ECST-2) are currently undergoing to try and answer this question.

The question of whether modern medical therapy (including statins) is equivalent or superior to carotid endarterectomy or stenting was not yet been addressed by well-designed, appropriately funded, prospective, multicenter, and randomized trials (Ricotta, et al., 2001). Carotid artery stenting (CAS) is a more recently developed therapeutic alternative to carotid endarterectomy (CEA) for the treatment of carotid artery disease. It can be performed under sedation and preserves the cranial nerves which are at risk of palsy in CEA cases.

The results from trials comparing the two in symptomatic patients have been conflicting (Rosenfield, et al., 2016). The use of stenting in asymptomatic patients has been studied in the Asymptomatic Carotid Trial (ACT I). Although the long-term effectiveness of CAS is not inferior to that of CEA, however, the trial suggested a 30-day risk of stroke or death of 2.9% in stenting compared to 1.7%

with endarterectomy (Rosenfield, et al., 2016). Similar results were shown in the CREST trial too (Brott, et al., 2010). These results illuminate the fact that the peri-procedure risk of stroke is almost twice as high with CAS than with CEA. Furthermore, many studies show that small silent infarctions (picked on diffusion-weight MRI scan) are more common after CAS than after CEA, with some reporting micro emboli presence on transcranial doppler scan during stent placement (Spence, et al., 2016).

The recommendation is that CAS should currently be considered for patients with indication for carotid revascularization and high surgical risk or unsuitable for open surgical, and patients who have a preference for stenting (Intercollegiate Stroke Working Party of the Royal College of Physicians of London, 2016)

In general, most of the studies have shown that with modern intensive medical therapy the annual risk of stroke in patients with asymptomatic carotid artery disease is around 0.5% which is lower than either carotid artery stenting (CAS) or endarterectomy (CEA) (Marquardt, et al., 2010) (Naylor, 2011). This highlights the importance of identifying patients with asymptomatic carotid atherosclerosis and at high risk of stroke or death, so that we can offer them intervention before they develop symptoms.

1.2 Peripheral artery disease in the lower limbs (PAD)

PAD is a term used to describe the impairment of blood flow to the extremities usually as a result of atherosclerotic stenotic or occlusive disease (Schirmang, et al., 2009) (Flu, et al., 2010). Generally speaking, the presence of symptoms in PAD depends on the metabolic demands of the ischaemic tissue during exercise,

the degree of collateral circulation and the size and location of the affected artery (Hills, et al., 2009).

The incidence of PAD varies in the general population from 3-10% in people younger than 70 years to 15-20% in people older than 70 years (Norgren, et al., 2007). However, approximately 40% of PAD patients are asymptomatic, while only 10% of them present with typical intermittent claudication (Schirmang, et al., 2009) (Hiatt, 2001). One third of PAD patients will have a complete occlusion of a major artery to the leg at first presentation (Norgren, et al., 2007) (Fowkes, et al., 1991).

1.2.1 PAD morbidity and mortality

Only about 25% of patients with intermittent claudication (IC) will significantly deteriorate, most frequently (7% to 9%) in the first year following diagnosis compared with 2% to 3% per year thereafter (Norgren, et al., 2007). The reported incidence of critical limb ischaemia (CLI) is around 200-400 new cases every year per million population (Rothwell, et al., 2004), and approximately 1 out of every 100 patients with IC will present with CLI per year (Ubbink, 2004).

Although major amputation is a relatively rare outcome of claudication, with only 1% to 3% of claudicants needing it over a 5-year period (Norgren, et al., 2007), limbs with ulceration due to arterial insufficiency treated without revascularization will have a 19% risk of amputation at 6 months and 23% risk at 1 year (Marston, et al., 2006). Cardiovascular risk varies with the severity of PAD and is closely correlated to both reduced and increased ankle brachial pressure index (ABPI). The relationship between ABPI and mortality over a period of 10 years in the

Strong Heart Study is shown in figure 1 (Resnick, et al., 2004). Mortality in claudicants at 5, 10 and 15 years is 30%, 50% and 70% respectively and similar rates are found in asymptomatic patients. 25% of CLI patients will die within a year of diagnosis (Norgren, et al., 2007).

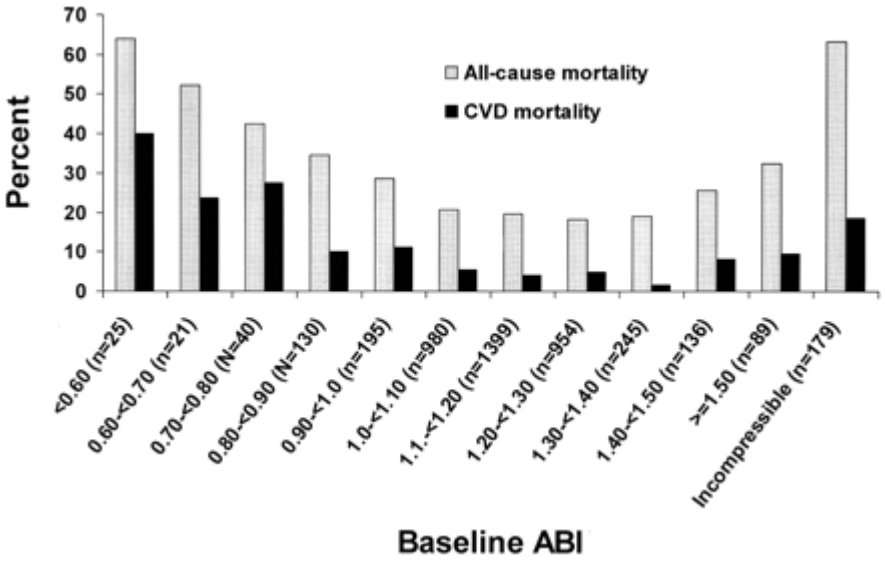

Figure 1: All-cause and CVD morality according to ABPI group, SHS, 1988 to 1999, n=439 (Resnick, et al., 2004)

1.2.2 PAD risk factors

Similar to carotid artery disease, PAD risk factors can be divided into non-modifiable (race, male gender and increasing age) and modifiable (smoking, diabetes mellitus, hypertension and dyslipidaemia). Other modifiable risk factors for PAD include hypercoagulable and hyperviscous states; hyperhomocysteinaemia; systemic inflammatory conditions and chronic renal insufficiency (Norgren, et al., 2007). Overall, PAD increases with smoking, African-American ethnicity, renal insufficiency, diabetes mellitus, and hypercholesterolaemia (Selvin & Erlinger, 2004) while it has been documented

that developing critical limb ischaemia (CLI) is more likely with ABPI of less than 0.7, age over 65 years, smoking, and hypercholesterolaemia (Hirsch AT, 2006).

1.2.3 Clinical presentation of PAD and classification

Although 65-75% of patients with PAD are asymptomatic, the classic presenting symptom is intermittent claudication which is usually described as muscle cramps, fatigue or pain in the lower legs induced by exercise and rapidly relieved by rest; often the symptom location indicates the level of arterial involvement (Schirmang, et al., 2009). Less commonly, patients may present with critical limb ischaemia. The European Society of Vascular Surgeons defined CLI as a recurring ischaemic rest pain requiring analgesia for more than two weeks or ulceration or gangrene of foot or toes with ankle systolic pressure < 50 mmHg or toe systolic pressure < 30 mmHg (Fontaine's III and IV) (Norgren, et al., 2007).

Fontaine's classification, proposed in 1954, remains a popular way of staging PAD. It divides patients into groups according to their clinical presentation. A similar clinical classification developed more recently by Rutherford has the advantage of including haemodynamic data, helping to ensure that any rest pain or tissue loss is directly related to PAD (Table 3) (Becker, et al., 2011).

Another classification of PAD could be made according to the duration of symptoms. Patients could present with Acute Limb Ischaemia (less than 24 hours duration), Sub-acute Limb Ischaemia (more than 24 hours and less than two weeks) or Chronic Limb Ischaemia (symptoms more than two weeks in onset).

Fontaine's		Rutherford's	
Stage	Clinical presentation	Stage	Clinical presentation
I	Asymptomatic	0	Asymptomatic
II	Intermittent claudication	1	Mild claudication
	IIa - on walking > 200 m	2	Moderate claudication
	IIb - on walking < 200 m	3	Severe claudication
III	Rest pain	4	Rest pain
IV	Ulceration or Gangrene	5	Minor ischaemic ulceration
		6	Severe ischaemic ulcers or frank gangrene

Table 3: Fontaine's and Rutherford's classification of PAD

1.2.4 Radiological diagnostic investigations for PAD

Colour-assisted duplex ultrasound scan is safe, non-invasive and non-expensive and, if done by an expert hand, able to provide anatomical as well as functional information (Norgren, et al., 2007). It is often used in surveillance following angioplasty or reconstruction. However, the accuracy of this investigation is highly operator-dependent. Other disadvantages include the length of examination and the challenge in imaging crural arteries.

Magnetic resonance angiography (MRA) and computed tomography angiography (CTA) could be used to confirm and localise suspected disease, especially where intervention is being considered. Both techniques have been shown to be sensitive and specific for PAD evaluation (Catalano, et al., 2004). They are similar in terms of diagnostic accuracy, clinical outcome and ease of use (Ouwendijk, et al., 2005).

Although MRA is a more expensive investigation than CTA, it has the advantage of avoiding the nephrotoxic iodinated contrast material and radiation, as well as the ability to provide rapid high-resolution 3D images of the abdomen, pelvis and lower limbs in one setting. As a result, MRA has become the preferred imaging technique for the diagnosis and treatment-planning of patients with PAD in many centres. However, MRA is contraindicated in patients with implanted devices such as pacemakers and metallic clips and in those with claustrophobia (Ouwendijk, et al., 2005). Previous arterial stents cause signal dropout making assessments of patency or in-stent stenosis difficult. In addition, a retrospective study showed a link between the contrast agent used for MRA, gadolinium, and nephrogenic systemic fibrosis (NFS) (Sadowski, et al., 2007).

Even though catheter-based digital subtraction angiography is considered the ‘gold standard’ investigation for PAD (Norgren, et al., 2007) (Sritharan & Davies, 2006), this is usually only performed when a concurrent endovascular intervention is anticipated due to its invasive nature. The risks related to catheter angiography include nephrotoxicity induced by the iodinated contrast, allergic reaction to the contrast, arterial dissection, arterial spasm, embolization and access site complications such as haematoma, pseudoaneurysm and arterio-venous fistula (Norgren, et al., 2007).

The use of non-toxic contrast agents such as gadolinium (Waybill & Waybill, 2001) and carbon dioxide (Hawkins, et al., 2009) has been recommended in patients with renal impairment to reduce the risk of nephrotoxicity seen with conventional contrast media (Aspelin, et al., 2003).

The National Institute for Health and Care Excellence in the UK (NICE) recommended duplex ultrasound as first-line imaging to all people with peripheral arterial disease for whom revascularisation is being considered. It further recommended to offer contrast-enhanced magnetic resonance angiography (or CTA if MRA is contraindicated) to patients with PAD who need further imaging (after duplex ultrasound) before contemplating revascularisation (NICE, 2012).

Considering the progressive occlusive disease aetiology of PAD, these investigations can help in assessing the severity of atherosclerotic stenosis or the presence of occlusion in the arteries, which will then allow the prediction and evaluation of PAD prognosis, as well as planning interventions when indicated.

1.3 Carotid plaque morphology and plaque instability

The development of atherosclerosis commences in the teenage years as a result of endothelial dysfunction with formation of a fatty streak, an inflammatory lesion that affects the intima, causing the formation of foam cells. This progresses with time to development of a fibro-proliferative atheroma and finally advanced lesion, containing a necrotic lipid core covered by a fibrous cap which may thin and rupture (Bartholomew & Olin, 2006). Acute events associated with carotid atherosclerosis are caused by plaque rupture and the creation of a thrombus rather than its haemodynamic effect on the arterial blood flow. Studies have also suggested that carotid and femoral plaques show different morphology in comparable groups of patients (Herisson, et al., 2011).

Although, changes in plaque morphology precede symptoms, understanding of the underlying pathophysiology is still inadequate. However, carotid plaque

instability has been well described histopathologically and there are different classifications of atherosclerotic lesions in place. Every plaque has a fibrotic cap containing lipid-filled macrophages, collagen and smooth muscle cells, and a core of necrotic mass and lipids. The progression of plaques (Figure 2) starts with an initial damage to the endothelium which increases the permeability of the intima to lipoproteins that leads to the formation of fatty streak (DiCorleto & Chisolm, 1986). Subsequent development and breakdown of lipoproteins result in the invasion of leucocytes into these fatty streaks to hunt for the breakdown products which in turn converts them into lipid-rich macrophage foam cells, resulting in the formation of atheroma (Stary, et al., 1995). The atheroma then acquires a lipid-rich necrotic centre from foam cell apoptosis and a surrounding fibrotic layer evolved from the proliferation of the smooth muscle cells within the intima (Fostegard, et al., 1990). More advanced lesions then occur with the help of neo-vascularisation of the atheroma (Virmani, et al., 2000).

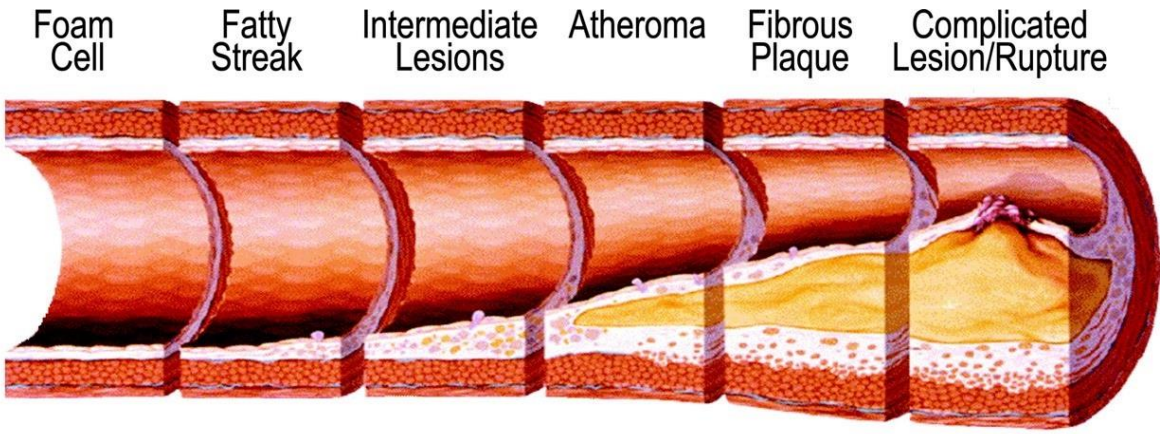

Figure 2: Plaque progression (Stary, et al., 1995)

The American Heart Association classified atherosclerotic lesions according to their histological progress into 6 types (Table 4) (Stary, et al., 1995).

Type I		Initial lesion
Type II	**Type IIa**	Progression-prone type II lesion
	Type IIb	Progression-resistant type II
Type III		Intermediate lesion (pre-atheroma)
Type IV		Atheroma
Type V	**Type Va**	Fibroatheroma (type V lesion)
	Type Vb	Calcific lesion (type VII lesion)
	Type Vc	Fibrotic lesion (type VIII lesion)
Type VI		Lesion with surface defect, and/or hematoma-hemorrhage, and/or thrombotic deposit

Table 4: Terms Used to Designate Different Types of Human Atherosclerotic Lesions in Pathology

Further histological studies have shown more manifestation of fibrous cap atheroma and cholesterol in carotid plaques compared to more fibrocalcific plaque in femoral arteries, with morphological studies also showing a higher prevalence of osteoid metaplasia in femoral arteries (Herisson, et al., 2011).

1.3.1 The unstable plaque

Unstable plaques have certain features including an intense inflammatory process within the plaque, angiogenesis, and intra-plaque haemorrhage with gradual thinning of the fibrous cap, subsequent loss of plaque cap integrity and ulceration (Mofidi & Green, 2014).

1.3.1.1 Inflammation

Inflammation is thought to play an important role in the initiation, the progression and the instability and rupture of plaques (Libby, 1995). Studies suggest that mature plaques contain variable amounts of inflammatory cells, concentrated mainly in lipid-rich lesions that can be found in the thinned cap or/and the shoulders of the lesions (Davies, et al., 1993). The presence of monocyte-derived macrophages and T-lymphocytes at the site of plaque rupture has been well documented (Koenig & Khuseyinova, 2007). These inflammatory cells have the ability to produce cytokines, chemokines, and growth factors, which lead to the proliferation of smooth muscle cells, plaque progression and the degradation and weakening of the fibrotic cap (Shah, 2003).

When compared to femoral plaques, carotid plaques have more macrophages and T-cells which is consistent with a more inflammatory phenotype. Moreover, symptomatic carotid plaques predominantly display M1-macrophages (macrophages that encourage inflammation), while femoral plaques mainly have M2-macrophages (macrophages that decrease inflammation and encourage tissue repair) (Shaikh, et al., 2012).

1.3.1.2 Angiogenesis

The presence of newly formed blood vessels (angiogenesis) has been described as part of the plaque development (O'Brien, et al., 1994). In addition, the density of these vessels in carotid plaques has been linked with plaque instability and intra-plaque haemorrhage (Virmani, et al., 2006).

More importantly, angiogenesis is considerably increased in carotid plaques from symptomatic patients compared to asymptomatic plaques (McCarthy, et al., 1999).

It is also thought that symptomatic carotid plaques have larger, more irregular and immature newly-formed vessels, which makes them more prone to haemorrhage and eventually plaque rupture (Folkman, 1995). Although it has been suggested that the lipid core in the plaques can be the stimulator of the angiogenesis process (Silverman, et al., 1985), it is difficult to explain the absence of angiogenesis in some asymptomatic carotid plaques when examined histologically (McCarthy, et al., 1999).

1.3.1.3 Intra-plaque haemorrhage and cap thinning

Many studies have shown that intraplaque haemorrhage is associated with plaque instability and the occurrence of neurological events, with some reporting its presence in up to 95% of ruptured plaques (Carr, et al., 1996). It is thought that intraplaque haemorrhage leads to rapid changes in plaque volume and the necrotic core which increases plaque instability risk (Von Maravic, et al., 1991). Although the source is uncertain, intraplaque haemorrhage may occur from fissures within the cap which allows the entrance of blood into the plaque (Davies & Thomas, 1985), or as a result of the rupture of newly-formed vessels within the plaque with some studies recording an increased vessels density correlating with the presence and amount of intraplaque haemorrhage (Moreno, et al., 2006) (Türeyen, et al., 2006).

1.3.2 Predicting plaque instability

Predicting changes in advanced atherosclerotic lesions before the event occurs has always been a great challenge with most available screening and diagnostic methods being insufficient. Identification of biomarkers of plaque instability could allow early recognition of disease, and consequently preventative measures could be applied to avoid acute events and reduce atherosclerosis related mortality, morbidity and cost of treatment of advanced disease.

Many studies have attempted to find reliable, accurate and easy to detect biomarkers of atherosclerosis. C-Reactive Protein has been suggested in a few studies as a potential biomarker and yet its value in our clinical practice is yet to be proven, mainly because of its lack of specificity (Koenig & Khuseyinova, 2007). Non-invasive detection of radio-labelled Annexin A5 - a plasma protein with a strong affinity for phosphatidylserine expressed by apoptotic cells - has been explored as a technique that can predict carotid plaque instability in studies with only small number of patients (Kietselaer, 2004) (Corsten, et al., 2007).

The use of different imaging modalities to predict plaque changes and instability in asymptomatic patients has also been investigated thoroughly over the last two decades. These modalities mainly focused on detecting carotid plaque ulceration as a key feature for plaque instability (Yuan, et al., 2017). Although each modality may be able to detect a variety of plaque instability characteristics, none can identify and reliably predict all of them (De Feijter & Nieman, 2011).

Metabolomic and proteomic profiling has become an increasingly used and powerful technique for the detection of biological markers of disease (Rochfort, 2005).

Not many studies have assessed atherosclerotic arterial disease using plasma or urine samples from patients with symptomatic atherosclerotic disease in addition to plaque extraction to identify potential biomarkers. Analysing plaques without extraction (solid state tissues) is still in its infancy and, supported by very promising results from trials on cancerous cells, could well provide realistic, reliable and clinically valuable biomarkers, provided these markers can be measured systemically.

1.4 The "Omics" era

The Omics science includes proteomics, genomics and metabolomics. While genomics and proteomics provide extensive information regarding the genotype, they give quite limited information regarding molecular phenotype. One major problem with these types of studies is reproducibility and several efforts to improve it have been published (Boja & Rodriguez, 2012).

Mass spectrometric analysis is usually used to detect a mixture of the large number of proteins in biological samples to identify potential biomarkers of a disease (Proteomics studies). Due to the wide range of proteomics obtained from each sample and considering its low reproducibility rate, it is becoming increasingly important to study targeted proteomics to help in understanding mechanisms and pathways of the disease (Boja & Rodriguez, 2012).

Metabolomics studies on the other hand looks into low molecular weight composites in a sample or tissue which are the closest link to phenotype (Wishart, 2007). It is a newer 'omics' science that can establish differences between healthy and diseased samples in their metabolomic profiling.

Nuclear Magnetic Resonance (NMR) Spectroscopy has the ability of detecting almost all the metabolites in a sample. It is a non-invasive technique that allows repeated measurements with the great value of reproducibility and analysing intact tissues. However, NMR sensitivity has always been an issue and one way to increase it is by using higher resonance frequency to reduce the amount of noise affecting signals. Availability of such devices, in addition to their costs, has limited research projects carried out in this field.

1.4.1 Metabolomics

The metabolome was first described by Oliver and colleagues as “the quantitative complement of all of the low molecular weight molecules present in cells in a particular physiological or developmental state” (Oliver, et al., 1998). Metabolites are regarded as the end product of metabolism, and there is an estimate of at least 3000 metabolites in the human metabolome (Dunn, et al., 2007) (Lewis, et al., 2008).

Metabolomics or metabolic profiling can be defined as “the quantitative measurement of the metabolic response of living systems to pathophysiologic stimuli or genetic modification” (Goodacre, et al., 2004) (Nicholson, et al., 1999). Living systems always try to preserve homeostasis when exposed to a stimulus (disease, drugs, etc). This disturbs the normal ratio of metabolites and changes the biofluid and tissue profile (Lindon, et al., 2006). Metabolite normal ratio is precise to each individual, but the loss of homeostasis is considered to be the first stage of disease progress (Van Der Greef & Smilde, 2005).

The difference between metabolomics (with “L”) and metabonomics (with “N”) is still arguable but most nuclear magnetic resonance (NMR) spectroscopy researchers initially used the later terminology. Metabolomics is mainly concerned with profiling all metabolites in normal conditions, while metabonomics expands it to include biochemical distress caused by a disease or drug (Hollywood, et al., 2006). In practice, however, there is a great degree of overlapping between the two terms and they are essentially identical (Robertson, 2005).

The term “Metabolomics” will be used in this report as it is now more commonly used amongst researchers.

1.4.2 The use of NMR in metabolic profiling

Although the idea of metabolic profiling was introduced a long time ago (Gates & Sweeley, 1978), it was only through technological analytical innovations in recent decades, namely gas chromatography-mass spectrometry (GC-MS), that quantitative measurement could be performed (Van Der Greef & Smilde, 2005). Also, the immense advances in the science and technology of nuclear magnetic resonance (NMR) spectroscopy in the last two decades permitted its use in the field of metabolic profiling (Emwas, 2015). Nicholson and colleagues were the first to explain metabolomics and they further established the application of pattern recognition techniques to data obtained from NMR spectroscopy (Lenz & Wilson, 2007) (Nicholson, et al., 1999) (Nicholson, et al., 1984).

Nowadays, NMR spectroscopy alongside mass spectroscopy (combined with liquid chromatography mass spectrometry LC-MS or gas chromatography mass

spectrometry GC-MS) are widely used in metabolic profiling. Each has its advantages and disadvantages and joining the two would provide more detailed analysis (Fancy, et al., 2006).

Table 5 summarises the main differences between NMR and MS (Viant, et al., 2009) (Lindon & Nicholson, 2008) (Emwas, 2015).

	NMR	**MS**
Reproducibility	High	Low
Sample preparation	Easy	Difficult
Sample preservation	Good	Poor
Sensitivity	Low	High
Metabolic recognition	Universal	Narrow
Separation techniques	Always the same	Variable

Table 5: Advantages and disadvantages of NMR vs MS

Although there has been a significant improvement in NMR sensitivity, this remains its weakest point, and it can sometimes limit the detection of low molecular weight metabolites (Emwas, 2015) (Dunn, et al., 2007). This mainly occurs because they are masked by either the large water signal associated with biofluids, or high molecular weight metabolites activities within the magnetic field. Though, adjusting pulse sequences can potentially minimise the effect of these two problems when studying low molecular metabolites (Saude, et al., 2006).

1.4.3 Nuclear Magnetic Resonance (NMR) Spectrometry

1.4.3.1 Brief history

NMR was first described by Isidor Rabi in 1938 and he was awarded the Nobel Prize in Physics for his work in 1944. The use of the technology on liquids and solids was then introduced in 1945 by 2 independent groups of physicists – Bloch and colleagues at Stanford University and Purcell and colleagues at Harvard. They also shared the Nobel Prize in Physics in 1952. Jacobson and colleagues carried out the first biological investigation using NMR technology in 1954. Since 1960, the technology has been routinely applied in organic chemistry for molecular structuring with major advances happening since the 1970s including computing and pulse-Fourier transform methods.

High resolution NMR spectroscopy has recently been widely used in identification of biomarkers of disease, while using Magic Angle Spinning for tissue analysis has allowed monitoring dynamic processes and giving information on compartmentisation.

1.4.3.2 Principles of NMR spectroscopy

When nuclei are exposed to a magnetic field, they absorb and reproduce electromagnetic energy. The strength of this magnetic field (in Hertz) and the properties of the nuclei determine the resonance frequency of this energy. The use of NMR as an analytical tool allows examining these magnetic properties of the nuclei by the application an external magnetic field (Bo) and further agitating it by an electromagnetic pulse, usually a perpendicular 90^{o} radio frequency (RF) pulse (Claridge, 1999).

All Isotopes have a specific number of protons and neutrons which affects the stability of the nucleus. When the spins of the protons and neutrons are not balanced, the overall spin (*I*) generates a magnetic dipole along the spin axis, and this is called the nuclear magnetic moment (μ). Therefore, the isotopes that contain an even number of protons and neutrons have an overall spin of zero, while isotopes with an odd number of either or both have a central and rotational magnetic moments which make them of nonzero spin (half integer spin and an integer spin respectively). Examples shown in table 6. The two most commonly used isotopes for NMR studies are ^{1}H and ^{13}C. (Skoog, et al., 1998).

No or protons	No of neutrons	Spin quantum number (*I*)	Examples
Even	Even	0	^{12}C, ^{16}O, ^{32}S
Odd	Even	1/2	^{1}H, ^{19}F, ^{31}P
Even	Odd	1/2	^{13}C
Odd	Odd	1	^{2}H, ^{14}N

Table 6: Examples of different spin quantum numbers of isotopes based on their proton and neutron numbers

1.4.3.2.1 Principle of relaxation

In quantum mechanics, when applying an external magnetic field (Bo) on a nucleus with an overall spin *I*, its nuclear magnetic moment will have (2*I*+1) possible orientations, either strengthen or oppose Bo. This means the energy levels split and each can be given a magnetic quantum number (*m*). (figure 3) (Claridge, 1999).

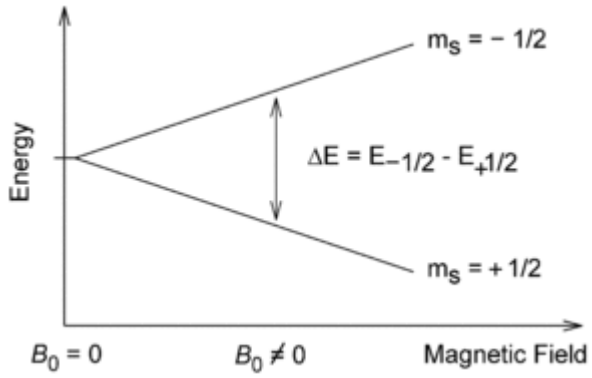

Figure 3: Energy splitting under the effect of external magnetic field Bo

The magnetic moment of a nucleus in the lower energy level does not oppose Bo, and its axis of rotation will *precess* around the magnetic field. The frequency of this precession is called Lamor frequency. On the other hand, a nucleus in the higher energy level will oppose Bo and absorb the energy, which then changes the angle of precession. The 'bulk magnetisation vector' represents the combination of all vectors for nuclei. The rotation of this bulk vector under the effect of RF pulse changes from axis *z* towards the *x-y* plane (figure 4) (Edwards, 2009) (Derome, 1987).

When agitating these nuclei which make up the bulk magnetisation for the correct length of time, those energy levels may become equal and no further absorption of radiation will happen. This is called *saturation* (Claridge, 1999). Therefore, *relaxation* process comes into function to ensure the return of nuclei to the lower energy level (Derome, 1987).

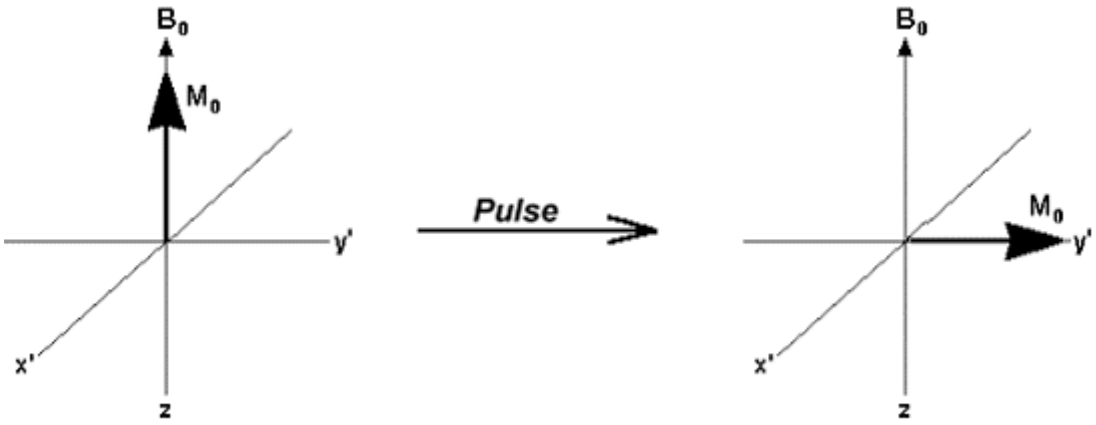

Figure 4: Change of bulk magnetisation vector rotation under the effect of a perpendicular RF pulse

There are two main relaxation processes; spin-lattice (Longitudinal) and spin-spin (transverse). Spin-lattice relaxation happens because of the interaction between nuclei in the higher energy level and the components of the lattice field caused by motion of neighbouring nuclei. This leads to energy loss and recovery to the ground state. The time needed for this is called longitudinal relaxation time (*T1*). Spin-spin relaxation happens because of the interaction between the neighbouring nuclei allowing the transfer of energy amongst them. All spins will have a similar frequency under the same Bo, but different magnetic quantum states due to the inhomogeneity of Bo. Therefore, some spins will be exposed to greater magnetic fields depending on its region (isochromat) within the sample and will process quicker than others. Transverse relaxation time (*T2*) permits the equalisation of all vectors and a zero-net magnetisation eventually (Claridge, 1999) (Derome, 1987).

Ideally, relaxation rates should be fast enough to reduce saturation, without losing the NMR spectra by being too fast (Claridge, 1999). To remove the Bo inhomogeneity effect and measure an accurate *T2* value, 180^{o} spin-echo pulse

sequence can be used. This helps with observing resonances from low molecular weight (LMW) molecules, which are normally much narrower than the high molecular weight (HMW) ones (Claridge, 1999) (Derome, 1987). An example of spin-echo pulse sequence is the Carr-Purcell-Meiboom-Gill (CPMG) sequence which will be used in this research. The Carr-Purcell pulse sequence uses many repetitions of short inter-pulse delays (τ) and 180^{o} pulses resulting in the intensity of the echoes decaying according to $T2$ but because of the large number of echoes, the loss between each echo due to diffusion is small (Derome, 1987).

1.4.3.2.2 NMR spectra

The basis of obtaining NMR spectra depends upon the fact that large molecules have short *T2* times, while small molecules have long *T2* times (Derome, 1987). A typical NMR spectrum, therefore, contains thousands of sharp lines which correlate to different metabolites and vary according to these times and the sample used in the experiment. Urine samples, for example, have mainly low molecular weight metabolites, while plasma and serum samples usually have both low and high molecular weight metabolites with a wide range of signal line widths (Beckonert, et al., 2007). Examples of urine and blood NMR spectra are shown in figure 5 and figure 6.

1.4.3.2.3 Chemical shifts

Chemical shifts of the NMR frequency happen because of the ‘shielding’ effects of the electrons surrounding the nuclei. This causes the magnetic field at the nucleus to be different than the actual external magnetic field (Bo). This difference is called ‘nuclear shielding’. It allows, in turn, the exploration of the chemical structure of molecules. Chemical shifts are usually stated in parts per million

(ppm) to make it easier to illustrate the position of the resonances in an NMR spectra (Edwards, 2009) (Claridge, 1999) (Derome, 1987).

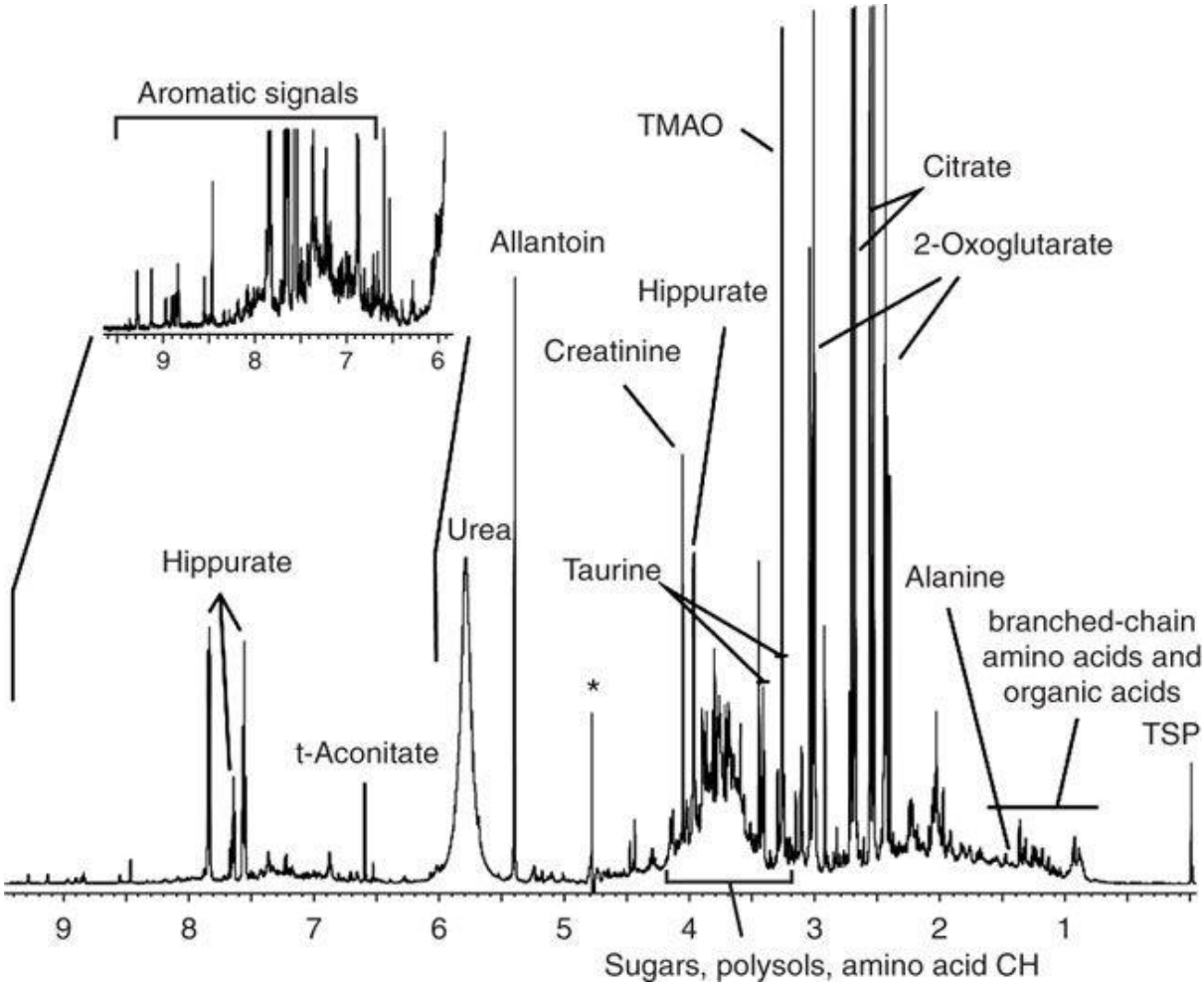

Figure 5: 600 MHz ^{1}H NMR spectrum of urine (Beckonert, et al., 2007)

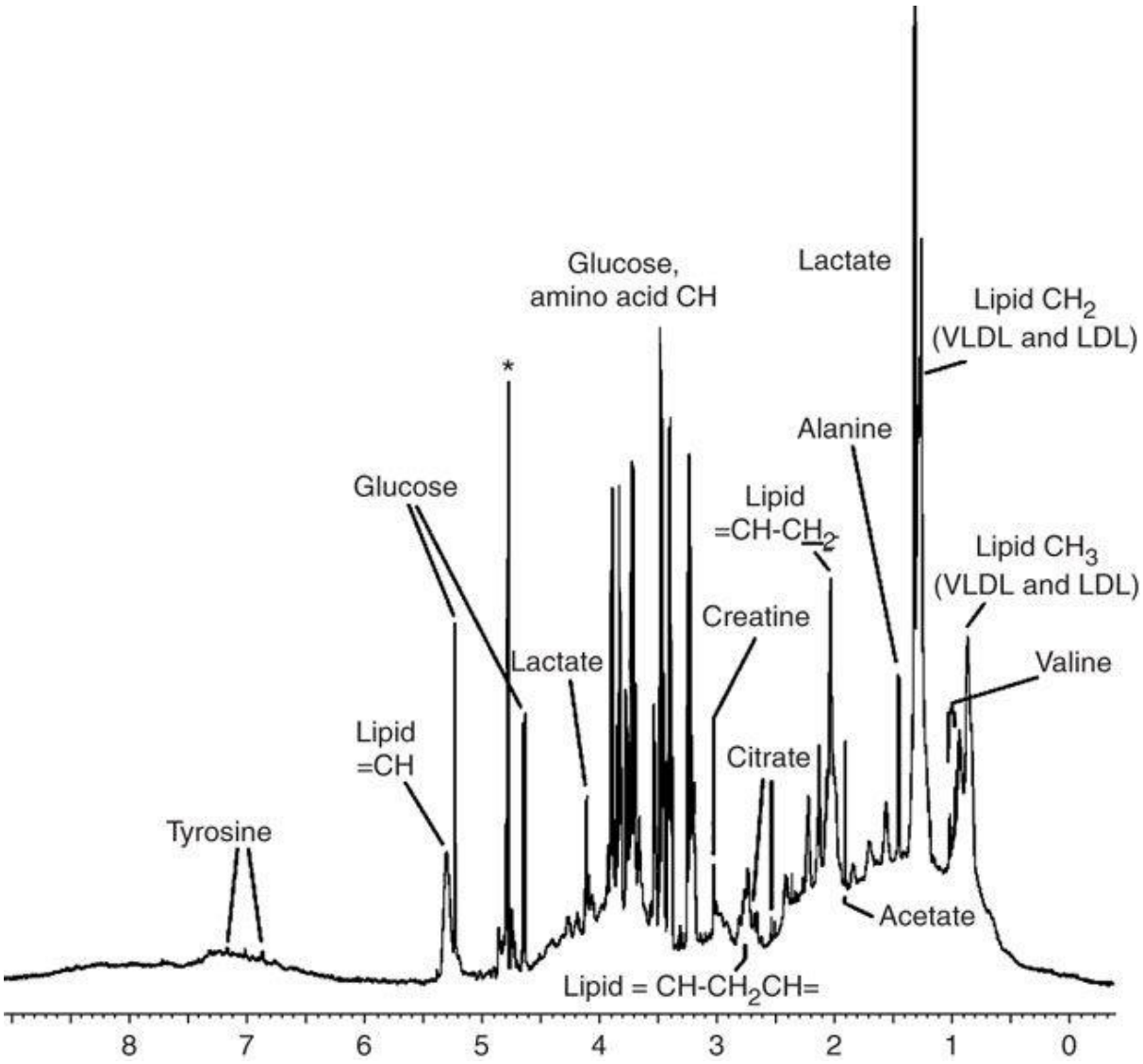

Figure 6: 600 MHz 1H NMR spectrum of blood sample (Beckonert, et al., 2007)

1.4.3.3 High resolution magic angle spinning NMR

The advancements in high-resolution ^{1}H magic angle spinning HR-MAS NMR spectroscopy has made it possible to gain high-resolution NMR data on small pieces of intact tissues (Garrod, et al., 1999). Rapid spinning of the sample at an angle of 54.7° helps reducing the loss of information caused by line broadening seen in nonliquid samples such as tissues (Beckonert, et al., 2007).

1.4.4 Data processing

Metabolomics studies produce more measured variables than the actual number of samples (Trygg, et al., 2007). Thus, acquired data requires reduction, normalisation and scaling prior to analysing. This is mainly to allow accurate and adequate comparisons between the variables, and therefore make results amenable to multi-variate analysis (Craig, et al., 2006).

1.4.4.1 Data reduction (Binning)

This is usually achieved through the process of bucketing (binning). The spectra are divided into equal sized small bins to account for the small changes in chemical shifts between samples and to ensure comparable signals. The most commonly used bin size is 0.04 parts per million (ppm) (Craig, et al., 2006). Some studies used even smaller sizes to account for much smaller chemical shift differences (Holmes, et al., 1994) (Spraula, et al., 1994). The disadvantage of binning is that it sometimes can integrate two opposite peaks in the spectra, therefore not reflecting the intensity of either of them correctly (Jahns, et al., 2009).

1.4.4.2 Normalisation and scaling

Data are usually organised in a table where each row is attributed to a certain sample or experiment, while the column reflects a particular measurement within that experiment.

Normalisation of data is typically a table row operation while scaling is a table column one (Craig, et al., 2006). Normalisation is used to ensure data from all samples are comparable, commonly by removing the effect of varying dilution of

samples. The most common method is by normalising to the sum of the integrals of the whole spectrum, where each bin integral is divided by the spectrum integral and the sum of all the new integrals is set to one (Webb-Robertson, et al., 2005).

Scaling, on the other hand, is used to express the variation in metabolites with low intensity. Mean-centering is often carried out prior to scaling to allow multi-variate analysis of concentration variances around zero rather than around the concentration mean of metabolite (Van den Berg, et al., 2006). This can be done by subtracting the column mean from each value in it (Craig, et al., 2006).

1.4.5 Previous NMR studies on atherosclerosis

There have not been many NMR based metabolomic profiling studies investigating atherosclerotic biomarkers of carotid disease. No previous studies have used solid status NMR to compare intact plaques from various regions of the body and only four NMR based metabolomic studies have attempted to establish atherosclerosis biomarkers in mammalian models.

1.4.5.1 Animal based studies

Four animal studies used Nuclear Magnetic Resonance (NMR) technology to assess atherosclerotic metabolomes in hamsters and mice.

Martin and colleagues carried out the first study examining the suitability of plasma metabolomics to determine the severity of diet-induced atherosclerosis in 48 male Golden Syrian hamsters (Mesocricetus auratus), divided into six groups and fed with different experimental diets. Changes in amino acid and lipid metabolism associated with atherogenesis were demonstrated and animals were

able to be distinguished based on their dietary treatments. Promising atheropositive biomarkers (such as lipids and N-acetyl-glycoproteins) and atheronegative biomarkers (such as glutamine, proline, glycerol and creatine) were identified in this study, although they were thought to be valid only for the specific diets used in the study (Martin, et al., 2009).

Leo and colleagues studied NMR-based metabolomics of urine from 16 apolipoprotein-E knockout mice. The mice were divided into two groups, captopril-treated and untreated. Urine samples obtained from the apolipoprotein-E deficient mice were then analysed using 1H-NMR. The groups were able to be differentiated according to their NMR spectra and urine levels of xanthine and ascorbate were identified as potential markers of plaque formation (Leo & Darrow, 2009).

Yang and colleagues studied the metabolomic profiling of 40 apolipoprotein-E knockout mice divided into four groups according to the duration of high fat feeding using ^{1}H-NMR spectroscopy. The study suggested choline, glycine and glucose as potential biomarkers for the early diagnosis of atherosclerosis (Yang, et al., 2014).

Li and colleagues were the first to analyse plasma, urine and tissue of western diet fed low density lipoprotein receptor knockout (LDLR-/-) mice, using both Gas Chromatography / Mass Spectrometry (GC-MS) and NMR spectrometry. Although, they did not identify a specific biomarker of atherosclerosis, they did identify that metabolisms of fatty acids and vitamin-B3 together with gut microbiota plays an important role in atherosclerosis development. This is

considered to be a novel molecular pathophysiological mechanism of atherosclerosis (Li, et al., 2015).

Other animal studies mainly used mass spectroscopy technology. Mayr and colleagues identified 79 altered protein species during various stages of atherogenesis, using a combination of 2-dimentional gel electrophoresis and mass spectrometry profiling of aortas from apolipoprotein-E knock-out mice (Mayr, et al., 2005).

Zha and colleagues studied metabolomic characterisation of early atherosclerosis in 24 Golden Syrian hamsters divided into three groups based on body weight, using Gas Chromatography / Mass Spectrometry (GC/MS). Twenty-one compounds were identified as markers involved in the development to atherosclerosis with amino acid metabolism and fatty acid oxidation significantly being disturbed in the process (Zha, et al., 2009).

While Zhang and colleagues used Ultra-Fast Liquid-Chromatography coupled with Ion Trap-Time of Flight (IT-TOF) Mass Spectrometry (UFLC/MS-IT-TOF) metabolomic approach to study the plasma and urine of 18 male Wistar rats allocated into two groups, high fat diet and common diet fed. Around 20 potential biomarkers were identified in the study. The results showed abnormal metabolism of bile acids, Lysophosphatidylcholines and amino acids in atherosclerosis rats (Zhang, et al., 2009).

More recently, Jové and colleagues published a study on the plasma metabolome and circulating and aortic lipidome of 31 male Golden Syrian hamsters divided

into two groups (atherogenic diet vs normal diet), using Liquid Chromatography / Mass Spectrometry (LC/MS) analysis. The results showed the existence of several previously unreported changes in lipid and amino acid metabolism. Taurocholic acid, a sodium salt in the bile of mammals, was suggested as a potential plasma biomarker of early atheromatous plaque formation (Jové, et al., 2013).

1.4.5.2 Human based studies

An early study using ^{1}H-NMR analysis of human serum suggested that it was possible to predict the presence and severity of coronary artery disease (CAD) as more than 90% of CAD patients could be differentiated from patients without CAD from their metabolomic profiling (Brindle, et al., 2003). This has not been reproduced and subsequently challenged by a later study determining the predictive power of NMR for angiographically defined CAD. The study suggested that predictions for normal coronary arteries and diseased ones were only accurate in 61.3% of patients treated with statins (Kirschenlohr, et al., 2006).

At least 24 metabolites were identified as significantly modified in the patients with atherosclerotic disease in a study which combined GC/MS and NMR spectroscopy to analyse metabolomics of plasma in humans with stable carotid atherosclerosis (n=9) compared with healthy controls (n=10). Those were mainly associated with the insulin resistance pathway (Teul, et al., 2009). In another study using only GC/MS for metabolomics analysis of plasma from 16 patients with stable atherosclerosis compared with 28 healthy controls, researchers demonstrated that fatty acid metabolism, especially palmitate, could be a phenotypic biomarker for clinical diagnosis of atherosclerosis (Chen, et al., 2010).

In the Young Finns Study - a large epidemiological study of Cardiovascular Risk in 4309 subjects - data from serum NMR metabolomic spectral profiles were analysed to predict early atherosclerotic changes in healthy young adults. Three different metabolic phenotypes linked with high carotid intima-media thickness (IMT) were identified, all of which showed disturbances of lipid metabolism (Würtz, et al., 2011).

Early attempts to combine proteomic and metabolomic techniques to reveal protein and metabolite alterations in individuals with atherosclerotic disease were encouraged by the fact that 2-D gel electrophoresis proved to be highly complementary to (NMR) spectroscopy (Mayr, et al., 2004). Only one study to date has used microparticles (MPs) derived from carotid artery plaques in patients undergoing carotid endarterectomy for metabolomic and proteomic analysis. Metabolomic study was done by liquid state HR-NMR spectroscopy while LC/MS was used for proteomic analysis. This study was the first to explore the protein distribution as well as metabolite content of MPs. Combining proteomics, metabolomics, and Immunomics had a great advantage and indicated to the role of MPs in inflammation, which is a key determinant of plaque instability (Mayr, et al., 2009).

Jové and colleagues used LC/MS to analyse plasma samples from 131 TIA patients. The study identified lysophosphatidylcholine (LysoPC) as a potential biomarker of stroke recurrence, which will in turn enhance other predictive methods for stroke recurrence following TIA (Jové, et al., 2015).

In a recent small study, organic and aqueous extracts obtained from carotid plaques in patients with symptomatic stenosis (n = 5) and asymptomatic stenosis

(*n* = 5) were analysed, using two ultra-performance liquid chromatography coupled to mass spectrometry metabolic profiling methods. The study showed a higher presence of metabolites related to the eicosanoid pathway (such as arachidonic acid and arachidonic acid precursors) in symptomatic patients (Vorkas, et al., 2016).

1.5 Rationale of this study and expected value of results

No studies have previously compared the results of metabolomic analysis of plasma, urine and plaques from the same subject. Also, no studies have attempted to define differences in the metabolic profile between patients with symptomatic and asymptomatic carotid artery disease to detect plaque instability or identify the “high risk patient”.

Furthermore, no studies have compared metabolomic profiles of plaques and plasma from different origins (carotid vs femoral in this study).

Finally, no studies have correlated data obtained from human samples to mammalian model of atherosclerosis, which is a worthy of investigation.

In this research, we aim to study the metabolic profiles of human carotid atherosclerosis plaque, plasma and urine in patients with symptomatic carotid disease. We also intend to compare this to the metabolic profiles of human femoral atherosclerosis plaque, blood and urine in patients with claudication, and the metabolic profiles of human blood and urine in patients with no carotid

disease (control). In addition, this will be studied in a mouse model of atherosclerosis.

We hope that this study may clarify the pathophysiological pathways involved in the final stages of development of plaque instability, and whether this is a local effect within the plaque or can be identified systemically in plasma or urine. Studies on a mammalian model of atherosclerosis may also guide future studies to further understand the disease mechanism and may lead to identification of novel therapeutic strategies targeted against development of plaque instability.

This project could also advance the possibility of identifying a candidate biomarker for point-of-care risk assessment of stroke. This would potentially allow the development of a urine dipstick or blood test to identify high risk carotid plaques or high-risk patients who would most benefit from intervention to their carotid plaque prior to developing clinical symptoms.

Chapter 2: Design and methods

2.1 Animal sample methods

6 Apo-E knockout mice vs 6 Controls (Harlan-Olac, Bicester, UK) were used for the study). All mice were males and born on the 9th October 2011. All animals were fed high fat (western) diet until the 13th March 2012 (12 weeks). The apolipoprotein E–deficient (ApoE−/−) mouse is popular because of its tendency to spontaneously develop atherosclerotic lesions on a standard high fat diet (Meir & Leiterdorf, 2004).

Animals were labelled as follow: 17X – 18X – 19X – 20X – 21X – 22X - 35C – 36C – 37C – 38C – 39C – 40C.

The housing and care of the animals, and all the surgical procedures carried out on them for this study, were in accordance with the UK Home Office regulations. Animals care, feeding and preparation was done by S Wheatcroft from the Leeds Institute of Cardiovascular and Metabolic Medicine (LICAMM) at the University of Leeds. Dr N Yuldasheva (from LICAMM) did the anaesthetising of the animals (by inhalation of Isoflurane with Oxygen), harvesting and samples acquisition, in addition to embedding solid tissue samples in paraffin ready for sectioning.

2.1.1 Blood sample collection

All blood samples were collected by Dr N Yuldasheva from the inferior vena cava of each animal. Approximately 900 µl was obtained from each animal. There were divided into 3 parts; 700 µl in Lithium heparinised (LH) tube, 100 µl in EDTA (ED)

tube and 100 µl in Citrate (Cit) tube (Figure 7). It was not possible to obtain any blood from animal 40C as the inferior vena cava collapsed immediately after cannulating and Dr N Yuldasheva was not able to aspirate any blood from it. Therefore, this was excluded from studies based on blood.

Only plasma collected in LH tubes will be used in this study. All samples were centrifuged (eppendporf FBS29112 Centrifuge 5810 R) at 900 g for 10 mins within two hours of collection. Samples were kept in 4^{o}C until processing. For samples collected in LH tubes, a minimum of 320 µl of plasma (supernatant) was obtained from each animal. Plasma was saved in aliquots in Eppendorf tubes (1.5ml micro tubes; Sarstedt; Leicester, UK, Ref: 72.690), then flash frozen in liquid nitrogen and stored in a freezer at −80°C until analysis.

During preparation, samples 17X, 19X and 22X were mistakenly put into dry ice instead of 4^{o}C ice prior to centrifuging and were therefore haemolysed. I was therefore not able to obtain plasma from these animals. There have been no studies using full blood samples instead of plasma in NMR metabolomic analysis, and if such analysis was tried then it will not be possible to carry out a valid like-for-like comparison with the other plasma samples in this study. These haemolysed samples were still centrifuged (eppendporf FBS29112 Centrifuge 5810 R) at 900 g for 10 mins and divided into 320µl aliquots (2 aliquots from each sample), flash frozen and stored at −80°C.

Figure 7: Blood sample collection from mice

2.1.2 Tissue sample collection

Tissue samples harvesting and embedding in paraffin was done by Dr N Yuldasheva. Animals were anaesthetised using Isoflurane with Oxygen and placed in supine position. A midline incision of chest and abdomen was performed, and internal organs were exposed. The inferior vena cava was cannulated and total blood volume was withdrawn. After the spontaneous stoppage of heart, the arch of aorta was harvested with the brachiocephalic, left common carotid and left brachial arteries attached to it.

The brachiocephalic artery with part of the arch was then separated and saved in 4% paraformaldehyde (PFA) for histological studies as recommended in previous studies (Johnson & Jackson, 2001) (Figure 8). The brachiocephalic is usually 2 mm long with a diameter of 0.5 mm in mice, and reliably develops complex plaques (Bond & Jackson, 2011) (Rosenfeld, et al., 2000).

Due to its small size, it was not possible to harvest the actual plaques from the arch of aorta samples therefore I opted to store the whole sample intact. Arch samples were all flash frozen in liquid nitrogen then kept in -80^{o}C.

Left renal arteries were also harvested from the animals, flash frozen and stored at −80°C until required for analysis. This was due to reports in the literature regarding development of significant atherosclerotic plaques in renal arteries in Apo-E mice (Nakashima, et al., 1994). These samples will be later used to test and develop magic angle spinning NMR.

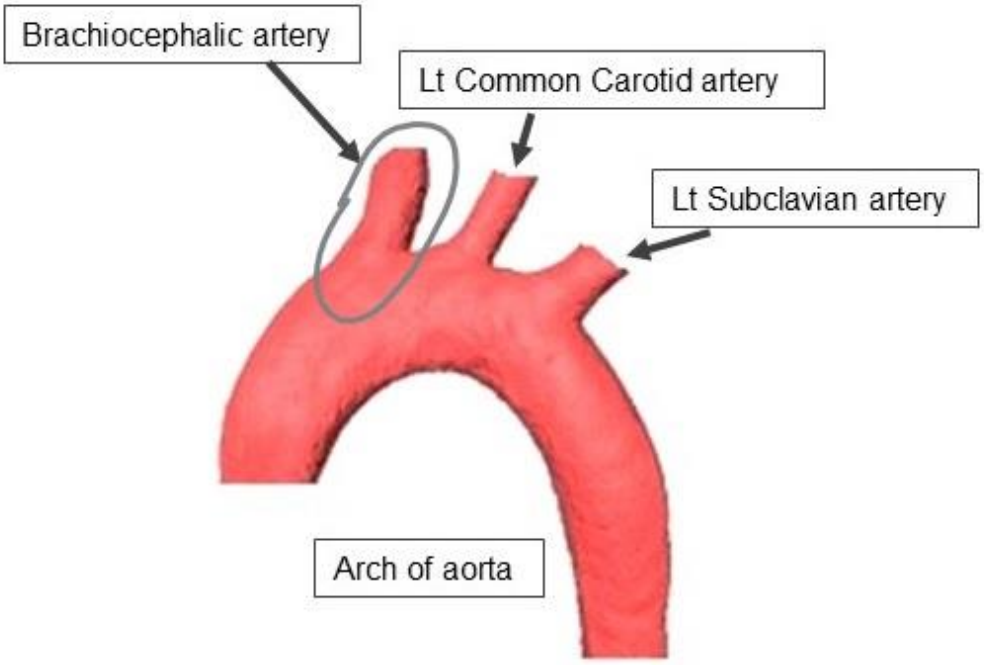

Figure 8: Tissue sample collection from mice

2.2 Human sample methods

2.2.1 Patient recruitment

Ethical approval for studies carried out on human samples in this research was obtained in April 2012 from Yorkshire and the Humber NRES Committee (Reference 11/YH/0425). All patients were recruited from the vascular unit at Leeds General Infirmary between April 2012 till September 2013. Patients were approached at least 24 hours prior to recruiting. A patient information leaflet was given to all patients and written informed consent was obtained for inclusion in the study to allow laboratory tests on blood, urine and plaque samples.

Patient demographics, vascular risk factors, other past medical history and medication history were recorded prior to sampling. Each patient was given a code according to the order of their recruitment, by using the preface (NMR) followed by 3-digit number (Ex: NMR001-NMR002-...).

2.2.1.1 Inclusion criteria

All patients with

- TIA (focal neurological deficit lasting <24 hours),
- minor stroke (focal neurological deficit lasting >24 hours) or
- amaurosis fugax (transient uniocular visual loss)

presenting within 14 days of symptoms associated with a 50-99% internal carotid artery (ICA) stenosis were approached prior to carotid endarterectomy.

All patients with

- claudication symptoms undergoing femoral endarterectomy were approached

Age and sex matched controls were recruited from a cohort of patients presenting to clinic with varicose veins with normal Ankle Brachial Pressure Index (ABPI) and no evidence of significant carotid stenosis for plasma and urine assessment. These patients had a focused carotid duplex to exclude >50% ICA stenosis.

2.2.1.2 Exclusion criteria

- CT evidence of cerebral haemorrhage or lacunar infarcts as the cause for their cerebral events
- Potential cardioembolic source for patient symptoms (cardiac arrhythmia on ECG or 24hr Holter monitoring; atrial thrombus or septal defect on echocardiography)

2.2.2 Blood sample collection

Blood samples were collected and prepared as described by Turner and colleagues (Turner, et al., 2008).

- 20 ml venous blood samples were taken from the antecubital fossa after fasting for a minimum of 6 hours, using a 21 G butterfly needle and a “no-tourniquet” technique to reduce cell crushing which may influence the results

- Blood samples were then put in lithium heparinised 4 ml tubes for the NMR study. There were two tubes from each patient
- A further 3 blood samples were put in a 4 ml EDTA tube, 4 ml citrate tube and a 4 ml Gel clot active tube (for serum samples) respectively. These were not used in this study but kept for future research (figure 9)
- All samples were centrifuged (eppendporf FBS29112 Centrifuge 5810 R) at 900 g for 10 mins within two hours of collection. Samples were kept in 4^{o}C until processing
- Previous protein profiling studies suggested that plasma samples are more stable than serum ones, although the evidence is insufficient. Ideally both should be used, however this would complicate data analysis and the length of each experiment (Luque-Garcia & Neubert, 2007) and we therefore preceded with plasma analysis alone
- Plasma for the NMR study was taken from samples collected in LH tubes, divided into 400µl aliquots in Eppendorf tubes, (1.5 ml micro tubes; Sarstedt; Leicester, UK, Ref: 72.690), flash frozen in liquid nitrogen and stored in a freezer at −80°C ready for analysis
- Centrifuging 8 ml of blood produces around 4-5 ml plasma. Each aliquot has 400 µl of plasma resulting in 10-12 samples from each patient
- Plasma was taken from samples collected in EDTA and citrate tubes, divided into 100-150 µl aliquots in Eppendorf tubes, (1.5 ml micro tubes; Sarstedt; Leicester, UK, Ref: 72.690), flash frozen in liquid nitrogen and stored in a freezer at −80°C ready for analysis
- Serum was taken from samples collected in Gel clot active tubes, divided into 100-150 µl aliquots in Eppendorf tubes, (1.5 ml micro tubes; Sarstedt;

Leicester, UK, Ref: 72.690), flash frozen in liquid nitrogen and stored in a freezer at −80°C ready for analysis

- Centrifuging 4 ml of blood produces around 2-2.5 ml of plasma and serum. Each aliquot will have 100-150 µl of plasma and serum resulting in 10-12 samples from each patient
- Red blood cells (RBCs) (pellet) were also isolated from the samples, divided into 0.5 ml aliquots in Eppendorf tubes (1.5 ml micro tubes; Sarstedt; Leicester, UK, Ref: 72.690), flash frozen in liquid nitrogen and stored at −80°C until required for further studies

Figure 9: Blood sample collection from patients

2.2.2.1 Problems faced while processing blood samples

Initially all samples were placed at 4ºC prior to processing. However, when placing Gel clot active tubes at 4ºC immediately after collection, only a small amount of serum was obtainable. This was due to the inability of the clotting factors in the sample to function at 4ºC. Therefore, it was not possible to separate

the clotted RBCs from serum. As advised by the literature, samples collected in Gel clot active tubes were left at room temperature for 15-20 mins before being placed at 4ºC pending processing (Luque-Garcia & Neubert, 2007).

2.2.3 Urine sample collection

Urine samples were collected and prepared as described by Beckonert and colleagues (Beckonert, et al., 2007).

- 20 ml of mid-stream morning urine sample was collected into sterile tubes containing 15 mM of boric acid
- Sample was placed at 4ºC pending processing
- All samples were centrifuged (eppendporf FBS29112 Centrifuge 5810 R) at 900*g* for 10 minutes at 4°C within two hours of collection
- Supernatant was divided into 1.5 ml aliquots in Eppendorf tubes (1.5 ml micro tubes; Sarstedt; Leicester, UK, Ref: 72.690), flash frozen in liquid nitrogen and stored in a freezer at −80°C until required for analysis.
- Each sample resulted in 14 aliquots

2.2.4 Plaque samples protocol

Protocol was initially drafted recommending the use of a modified surgical technique for carotid endarterectomy to the standard one allowing removal of intact plaque sample (Wijeyaratne, et al., 2002). However, changed provision of carotid endarterectomy meant that urgent surgery was shared amongst consultants, therefore loss of control on quality of samples received.

Femoral endarterectomy was carried out using a standard technique with maximum effort to remove intact plaques similar to the carotid ones.

- Fresh plaque samples were processed within 30 minutes of excision
- Recommendations made by Lovett and colleagues were considered for the preparation of the plaques for histological assessment (Lovett, et al., 2005)
- Transverse sections were taken from each plaque, using a scalpel blade at 1.5-2 mm intervals proximally to distally (common carotid to internal/external carotid) (figure 10)
- Sections were labelled alphabetically in sequence. Alternate sections were either snap-frozen in liquid nitrogen then stored at -80^{o} C for NMR studies, or kept in 4% paraformaldehyde (PFA) for histological studies (figure 11)
- Each plaque was divided into 7-15 sections on average

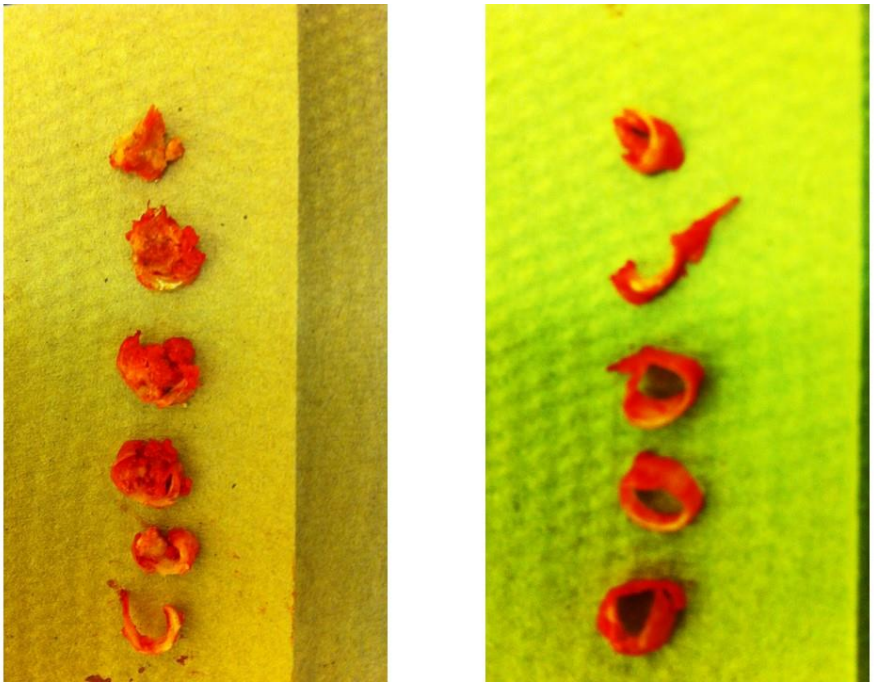

Figure 10: Plaque sections at 2 mm intervals

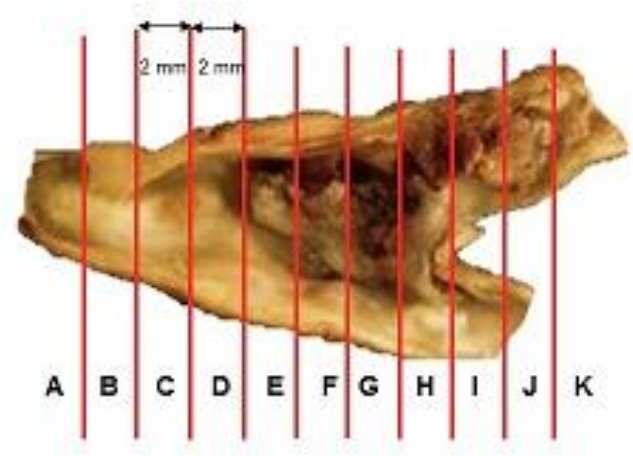

Figure 31: Plaque sectioning and processing

Samples A – C – E – G – I – K were flash frozen in liquid nitrogen and stored in -80ºC for NMR studies

Samples B – D – F – H – J were kept in 4% paraformaldehyde for histological studies

2.2.4.1 Histological methods

Sections kept in 4% PFA were decalcified prior to embedding in paraffin.

2.2.4.1.1 (4%) PFA preparation

This was done by adding equal volumes of 8% PFA and 0.2 M Phosphate buffer (pH=7.4) solutions.

2.2.4.1.1.1 (0.2) M Phosphate Buffer (pH=7.4) preparation

Add 39.2 ml of KH_2PO_4 (1 M) to 160.8 ml of Na_2HPO_4 (1 M). Make up to 1 L by adding distilled water. Measure the pH and adjust by using HCl/NaOH to achieve pH of 7.4.

2.2.4.1.1.2 (8%) PFA preparation

Add 80 g PFA powder to just under 500 ml of distilled water heated at 55^{o}C. Spin the solution at 55^{o}C until transparent. Add NaOH as appropriate (in drips) to fully clear. Top up the solution to 1 L with distilled water.

2.2.4.1.2 Decalcification Protocol

Initially, decalcification was attempted using Ethylene-Diamine-Tetra Acetic Acid (EDTA). Protocol for EDTA preparation was as follow:

- EDTA (free acid) powder (Fisher Scientific UK Ltd) was used
- 0.1 M phosphate buffer (pH=7.1) was prepared by adding 71.5 g of Na_2HPO_4 and 28.5 g of KH_2PO_4 to 1 L of DH_2O
- 10 g of EDTA powder was added to 100 ml of 0.1 M phosphate buffer
- The mixture was stirred for 30 mins at least at 50^{o}C

However, there were two issues with this method:

1- It was not possible to dissolve EDTA powder despite using different methods from the literature as well as local advice from Leeds Teaching Hospitals Labs. Experiment carried out with and without warming up. Adding NaHO (Buffer effect) was trialled with and without warming up. Prolonged stirred (Up to 3 days) was also endeavoured

2- EDTA decalcification has not been used commonly in recent years due to its time-consuming disadvantage compared to formic acid (Prasad & Donoghue, 2013)

The decalcification protocol was changed, and formic acid was used as an alternative. Both EDTA and formic acid have good tissue preservation and staining efficacy regardless of the method used (Sangeetha, et al., 2013).

Formic acid decalcification protocol was adapted from Leeds Teaching Hospitals Histopathology Labs.

- Formic Acid 85% GPC (Atom Scientific) was used to prepare 8.5% by diluting in distilled H_2O (1:9 volume)
- Sample was placed in 8.5% Formic acid and left for 24 hrs
- Chemical end-point test was used at 24 hours and every 12 hours thereafter, until sample was fully decalcified

2.2.4.1.3 Chemical end-point test

- 10-15 drops of concentrated ammonia were added to 5 ml of 8.5% formic acid until litmus paper changed colour to blue (alkali-tic)
- 5 mg ammonium oxalate was diluted in 100 ml distilled H_2O, and 9 ml of it was added to the previously made solution
- The mixture was left for at least 30 mins then compared to a control formic acid sample
- If clear the decalcification was done. Plaque was removed from Formic acid, rinsed with distilled water for a few mins and placed back in 4% PFA ready for paraffin embedding
- If not clear after 30 mins, the formic acid used for decalcification was refreshed and the process was rechecked every 12 hours until clear

2.2.4.1.4 Paraffin embedding protocol

Embedding was carried out using the embedding facility (Leica TP1020) in the LICAMM building at University of Leeds School of Medicine. All samples were treated by the same method.

Steps for embedding were as follow:

- Check if the 1st 70% alcohol container is clear. If not clear, fill the container with 500-600 ml 70% ethanol (EP, BP, 69.5-70.4%, Sigma-Aldrich Company Ltd, Poole, Dorset, UK)
- Place sample in a tissue processing cassette (VMR biopsy cassettes – VMR Internationals, Catalogue No: 720-0290)
- Place cassette in metal sieve
- Raise the embedding machine lid: press button [↑]
- Attach sieve to 1st lid (1st 70% ethanol)
- Select program 3 “used by Dr Yuldasheva research group at LICAMM for embedding”. Make a note of the program used & the time expected to finish (Programme 3 takes 17 hours). When finished, raise the lid, take your samples out and lower the lid again
- Switch on the wax temperature at 65°C one hour before starting embedding
- Use a labelled plastic wax-holder to store the samples
- Use metal moulds to place samples in melted paraffin then wait until cooled to be ready for sectioning

2.2.4.1.5 Processing paraffin blocks

Paraffin blocks were kept at 4^{o}C until sectioning time.

- Each paraffin block was sectioned at 3-5 µm thickness based on calcification (More calcified samples were harder to section at 3 µm so went up to 4 or 5 µm). Occasionally a thicker section (6-8 µm) was taken if there was concern regarding section integrity with thinner, more fragile sections
- All cut sections were then mounted on Polysine glass slides (TWIN Frosted Slides. Catalogue No: MAE-1000-03P. Cell Path) for greater adhesion properties compared to traditional glass slides
- To further enhance adhesion property, Polysine slides were treated with 3-aminopropyl-triethoxysilane (APES). This was done by placing the slides in 2% APES in Acetone (10 mins), distilled water (10 mins) then allowing slides to air dry
- Sections were ready for haematoxylin and eosin (H&E) staining prior to analysis

2.3 ^{1}H-NMR spectroscopy methods – liquid status

2.3.1 Sample preparation

Formerly described ^{1}H-NMR spectroscopy methods for plasma and urine sample processing and analysis by Turner and colleagues, and Hopton and colleagues were used in this study (Turner, et al., 2008) (Hopton, et al., 2010).

All samples were left in the NMR spectrometer for 5 minutes to allow temperature equilibration before optimisation of parameters. 5 mm Norell NMR tubes (S-5-500-7, GPE Scientific Ltd, Leighton Buzzard, Bedfordshire, UK) were used for placing samples in the NMR spectroscopy. All Samples (kept in -80^{o}C) were thawed defrosted by warmth of hand. Samples were then centrifuged (Hettich Mikro 120 (C1204) Centrifuge, angle rotor A1242) at 11992 g for 5 min in room temperature.

2.3.1.1 Plasma samples

350 µl of deuterium oxide D_2O (Sigma-Aldrich Company Ltd, Poole, Dorset, UK) was added to 300 µl of plasma in Eppendorf tube (1.5 ml micro tubes; Sarstedt; Leicester, UK, Ref: 72.690). For animal plasma samples, this was adjusted to 370 µl of D_2O and 250 µl of plasma due to the smaller volumes of the samples obtained. The plasma/ D_2O mixture was vortexed for 5 seconds before transferring 600 µl of it to a 5 mm Norell NMR tube ready for analysis. Samples were kept at 4^{o}C for a maximum of 30 min until placed in the NMR spectroscopy.

2.3.1.2 Urine samples

460 µl of urine in an Eppendorf tube (1.5 ml micro tubes; Sarstedt; Leicester, UK, Ref: 72.690) was added to 230µl of phosphate buffer (0.2 M phosphate buffer solution made up in water). 100 ml of phosphate buffer solution (pH=7.43) contained 2.885g sodium phosphate monobasic (Na_2HPO4), 0.525g sodium phosphate dibasic, (NaH_2PO_4), 0.0172g (1 mM) trimethylsilyl propanoic acid (TSP) and 0.0195g (3mM) sodium azide ($NaN3$) in 20mL of $D2O$ and 80ml of ribonuclease (RNase) free water. The urine/phosphate buffer mixture was

vortexed for 5s before transferring 600 µl of it to a 5 mm Norell NMR tube ready for analysis. Samples kept at 4^{o}C for a maximum of 30 min until placed in the NMR spectroscope.

2.3.2 ^{1}H-NMR spectroscopy data collection

^{1}H-NMR spectra were then measured at a frequency of 499.97 MHz and a temperature of 20°C on a Varian Unity Inova 500 ^{1}H-NMR spectrometer (Varian Inc., Palo Alto, California, USA). All Spectra were saved as a free induction decay (FID) file ready for analysis.

The Carr-Purcell-Meiboom-Gill (CPMG) spin-echo pulse sequence [RD – 90^{o} – $(\tau - 180^{o} - \tau)n$ – acq] was used to suppress signals from macromolecules and other substances with short T_2 values and obtain metabolic profiles for all plasma samples. The relaxation delay (RD) was 2 s, during which water resonance was selectively saturated. For each spectrum, 512 transients were collected into 32,768 pairs of data points with a spectral width of 8,000.00 Hz.

Diffusion-Ordered Spectroscopy (DOSY) pulse sequence was also used for macromolecules for all plasma samples. For each spectrum, 512 transients were collected into 32,768 pairs of data points with a spectral width of 8,000.00 Hz.

The 1D NOESY (one-dimensional Nuclear Overhauser Effect Spectroscopy) pulse sequence [RD – 90^{o} – $t1$ – 90^{o} – t_m – 90^{o} – acq] was used to obtain metabolic profiles for all urine samples. The RD was 2 s, t_m was 1.5 ms and $t1$ was 3 µs. For each spectrum, 512 transients were collected into 16,384 pairs of data points with a spectral width of 8,000.00 Hz.

2.4 ^{1}H-NMR spectrometry methods - solid status

High Resolution Magic Angle Spectrometry NMR (HR-MAS NMR) has been increasingly used for analysing solid tissues due to the advantage of studying intact tissues and the quality of signals obtained compared to other NMR based technologies. This facility was not available at Leeds University. Therefore, collaboration with the Birmingham University Henry Wellcome Building for Biomolecular NMR (HWB-NMR) Spectroscopy Unit was established and this part of the study was carried out there. The protocol for ^{1}H-NMR spectrometry solid status analysis in this study was adapted from Beckonert and colleagues' protocol (Beckonert, et al., 2010), and local protocols used at Birmingham University HWB-NMR unit.

2.4.1 Sample preparation

Preparation of tissue samples was done manually.

- All Samples (kept in -80^{o}C) were thawed at 4^{o}C (ice) for 3-5 minutes
- Samples were positioned in a 12 µl rotor, with 4 µl of D_2O added to each sample as a solvent, and sealed with a rotor cap
- The rotor was then inserted into the HR-MAS NMR spectroscope
- Disposable rotor inserts were used to allow safe and contained handling of tissue in the NMR probe and quick replacement of samples from the rotors
- The sample was kept at 4^{o}C throughout the preparation
- At the end of the process samples were removed from the NMR spectrometer, retrieved carefully and placed in Eppendorfs. Samples were then flash frozen in liquid nitrogen again and kept at -80^{o}C

2.4.2 HR-MAS NMR spectroscopy

A Bruker 500 MHz HR-MAS NMR spectrometer was used for this study. We relied on ^{1}H nuclei because of the high natural abundance and hence short acquisition time (Garrod, et al., 1999). All Spectra were saved as a free induction decay (FID) file ready for analysis.

Parameters of experiment:

- Temperature: 4^{o}C
- Number of scans: 128
- Spinning rate: 4800 Hz
- (P12 = 3 mins, SP1 = 44.277, PL9 = 52, P2 = 9.5)

Spectra achieved using the standard 1D NOESY proton NMR sequence were very weak in the pilot experiment, therefore the Carr–Purcell–Meiboom–Gill (CPMG) sequence was used in addition, to achieve stronger signals.
This pulse sequence can be used to enhance only the contributions from macromolecules or to selectively highlight the signals from the fraction of small molecules without being invasive to the sample integrity in any way (Beckonert, et al., 2007) (Wang, et al., 2003).

2.5 Spectral processing

Protocol for processing and analysing of the acquired spectra was adapted from previous protocols by Turner and colleagues, and Hopton and colleagues (Turner, et al., 2008) (Hopton, et al., 2010). This was also the Standard Operating Procedure in the NMR lab at University of Leeds School of Chemistry.

- An exponential line broadening of 0.5 Hz was applied to each free induction decay (FID), before zero filling to 65,536 points, followed by Fourier transformation
- The resultant spectra were phased, baseline corrected and referenced (α-glucose at 5.24 ppm), using ACD Labs (NMR processor academic edition) software 12.01 (Advanced Chemistry Development, Inc., (ACD/Labs), Toronto, Canada)
- The spectra were then “binned” into 225 segments, each with a width of 0.04 ppm, over the range δ 0 to 10, setting δ 4.8 to zero, to suppress the water peak
- Spectra was normalised to the unit sum of the spectral integral of the whole region examined, to ensure that the spectra were directly comparable
- Prior to binning several dark regions were created to exclude signals from the water region and contaminants that may affect subsequent multivariant analysis. Those dark regions are summarised in table 7

Sample	Dark region	Ppm
Plasma (CPMG sequence)	Highfield	-3.2 → 0.8
	Water	4.68 → 5.2
	Aromatic	5.28 → 13
Plasma (DOSY sequence)	Highfield	-1.5 → 0.6
	Water	4.4 → 5.0
	Aromatic	5.4 → 11
Solid tissue (CPMG sequence)	Highfield	-3.2 → 0.8
	Water	4.6 → 5.16
	Aromatic	5.8 → 13.2
Solid tissue (1D NOESY sequence)	Highfield	-3.2 → 0.5
	Water	4.6 → 5.16
	Aromatic	5.8 → 13.2

Table 7: Dark regions excluded from spectra prior to binning and normalisation

2.6 Statistical analysis

2.6.1 Multivariate statistical analysis (MVA)

MVA has the ability to analyse many associated variables at the same time (Manly, 2005). Besides the standard chemometric techniques such as; principal components analysis (PCA) and partial least squares–discriminant analysis (PLS-DA), other multivariate analysis tools were used for the identification of metabolite signals that allow discrimination between the groups. Example of this is orthogonal partial least squares discriminant analysis (OPLS-DA). All multivariate statistical analyses were performed using SIMCA-P+ software version 14.1 (Umetrics, Umea, Sweden).

The quality of these analyses was evaluated by validation metrics R^2 and Q^2.
R^2 reflects the relevance of information in the data set, while Q^2 is an estimate of the predictive ability of the model. A value of more than 0.5 for both is usually desirable. In general, R^2 should not exceed Q^2 by more than 3 units.
The chemical shifts of interest were analysed and linked to the correlating metabolite based on the chemical shift table published by Nicholson and colleagues (Nicholson, et al., 1995).

2.6.1.1 PCA

Principle component analysis (PCA) models were used to establish whether variables within the data can be differentiated into subgroups. This was demonstrated using scores plot which shows the correlation between observations. Loadings plot, which shows the correlation between variables, was then used to recognise the responsible bins for this differentiation.

2.6.1.2 PLS-DA and OPLS-DA

These models were used to further distinguish between the differentiated groups and create prediction models for other groups. Score plots were used to demonstrate this, while ***w**** loading plots were used to recognise the responsible bins for this differentiation. The results were then cross-validated by running the analysis 4 times after subtracting 1st, 2nd, 3rd, and 4th quarters from the data respectively.

2.6.2 Univariate statistical analysis

This was used to study the statistical significance of results resulting from the multivariate analysis. Student's *t*-test and Welch-Aspin test were used for normal data, based on whether the two groups have equal variances or not respectively. Fisher and Chi-square tests were used for categorical data. Mann-Whitney U test was used for non-parametric data. *P*-values were obtained to determine whether any difference between groups is statistically significant or not. The cut-off for significance used in this study was 0.05. All tests where done in IBM SPSS Statistics 25.0 software (IBM Corporation, New York, USA).

Chapter 3: NMR analysis of plasma

Animal samples

This chapter will describe ^{1}H-NMR spectroscopy analysis of plasma obtained from 8 mice (3 ApoE-/- vs 5 control) using CPMG and DOSY pulse sequences. Samples were prepared as per Section 2.1.1 and 2.3.1.1. Data were collected as explained in Section 2.3.2. Spectra processing was done as per Section 2.5. Statistical analysis was done as per Section 2.6.

Each mouse was given a number followed by a letter for identification purpose. The number was given to each animal according to the animal order of purchase in the University of Leeds Labs. The letter was either X for the study group or C for the control group. All the mice were born on 19th October 2011 and terminalised on 13th March 2012 (21-week-old).

3.1 Results

All animals were weighed immediately prior to terminalisation. There is a statistically significant difference between the two groups which may influence the following results from the NMR analysis. Table 8 details each animal weight in each group.

Study	**Weight (g)**	**Control**	**Weight (g)**	**P-value (*t*-test)**
18X	28.5	35C	36.4	
20X	33.6	36C	37.6	
21X	27	37C	38.6	
		38C	41.8	
		39C	45.5	
Mean ± SD	29.7 ± 3.46	Mean ± SD	39.98 ± 3.68	0.008

Table 8: Mice weight: comparison between the study and control groups

3.1.1 Analysis of all mice plasma spectra – CPMG sequence

3.1.1.1 PCA model

A PCA model was produced for all the spectra obtained from mice plasma using CPMG sequence. Examples of the NMR spectra are shown in figure 12. A Very weak model with only 2 components detected. The goodness of fit R^2X(cum) was 0.489. The predictive ability Q^2X(cum) was -0.0975. The negative value of Q^2X(cum) indicates that this model is not predictive (figure 13).

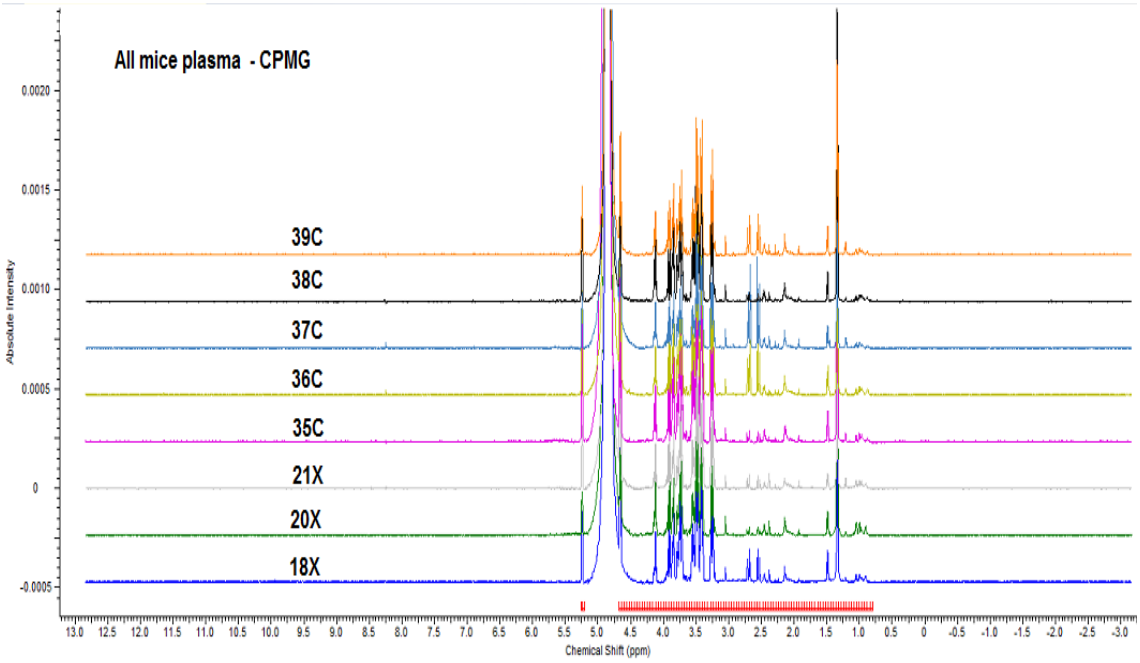

Figure 12: All mice plasma spectra with highlighted dark regions using CPMG sequence. X = chemical shifts (ppm), Y = Absolute intensity.

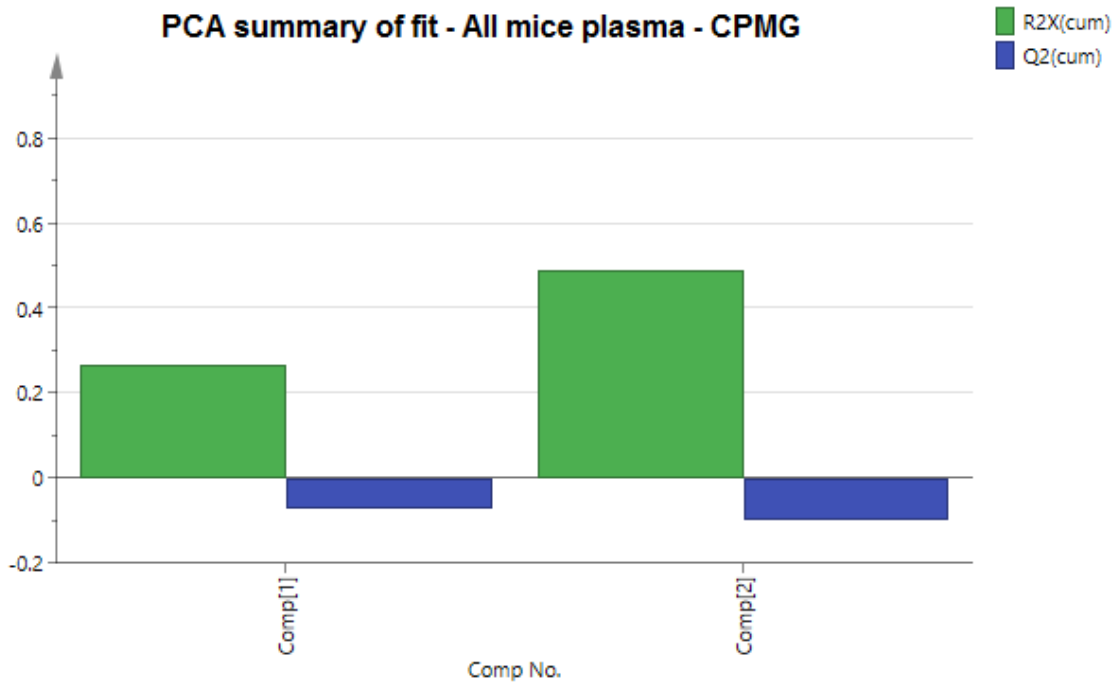

Figure 13: PCA model – All mice plasma – CPMG sequence

Analysing the score scatter, it was obvious that the mice could not be clearly separated based on their metabolites (figure 14). Sample 37C was an outlier from the other control samples which were clustered otherwise, although it was not located outside of Hotelling's T^2 (which defines the normal area resembling the extent of which is bound by the ellipse with 95% confidence) (Eriksson, et al., 2006). 37C behaviour could be another reason for the weakness of this model and the inability of samples separation.

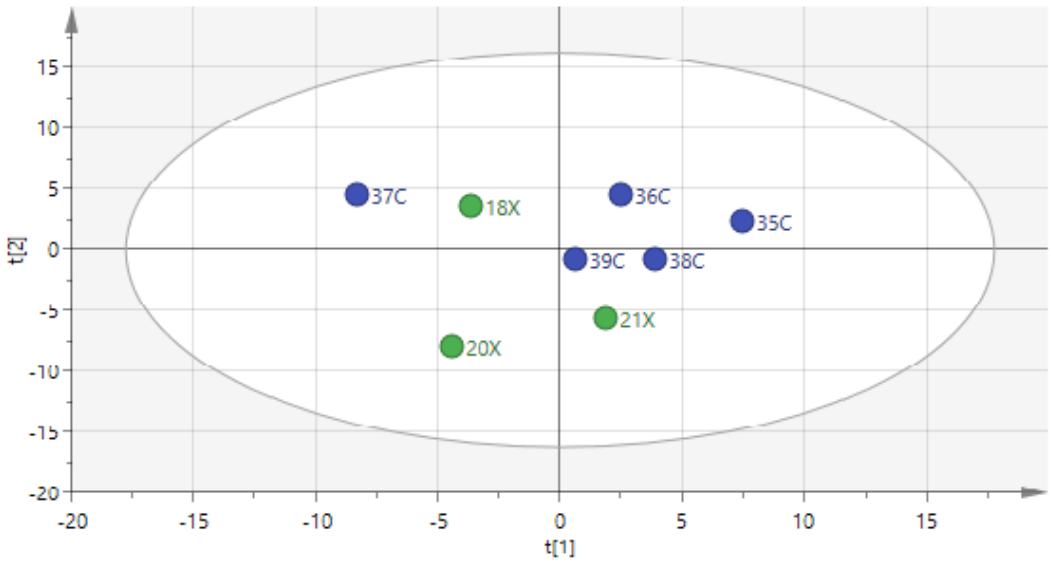

Figure 14: Score scatter of the PCA model – All mice plasma – CPMG

This was further established by looking at the score column (figure 15).

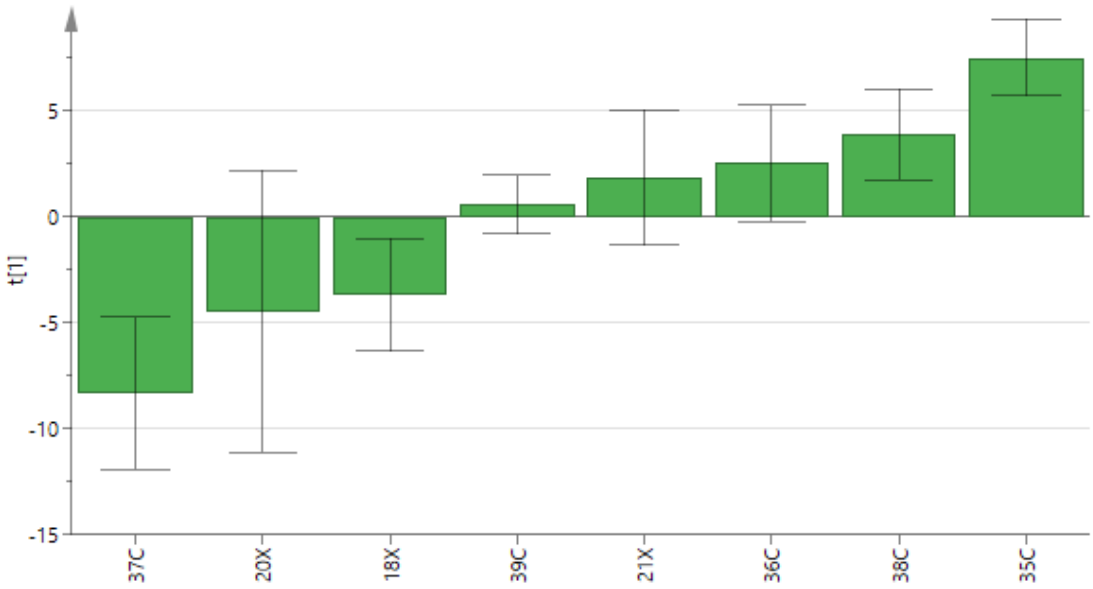

Figure 45: Score column of the PCA model – All mice plasma – CPMG

Removing sample 37C did not improve the model. The goodness of fit R^2X(cum) was 0.522. The predictive ability Q^2X(cum) was -0.11. However, it made the discrimination between study and control samples visible on the score scatter, without affecting the clustering pattern of the study group compared to the control group (figure 16).

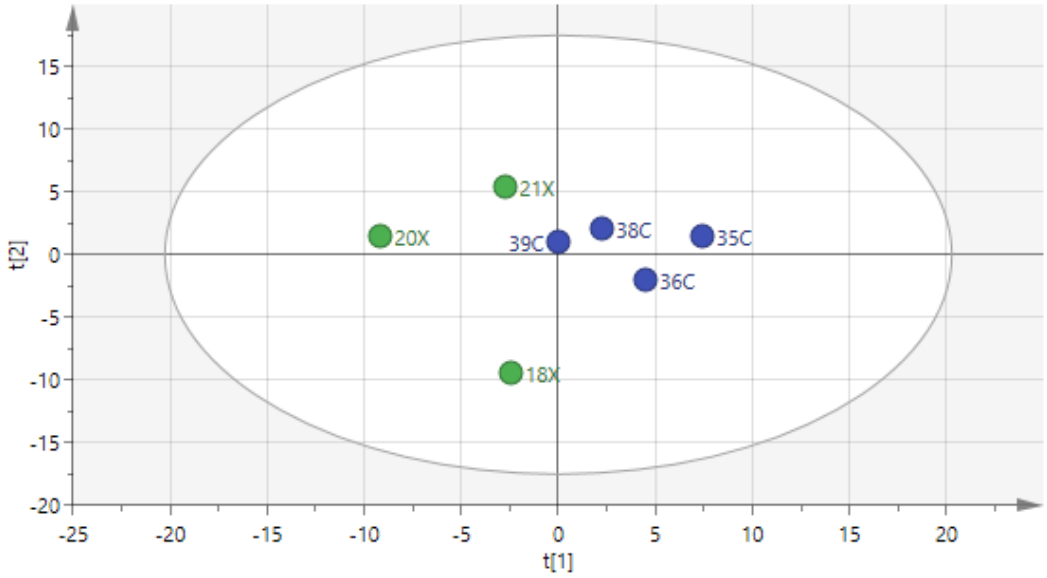

Figure 16: Score scatter of the PCA model – All mice plasma (without sample 37C) – CPMG

3.1.1.2 PLS-DA model

A PLS-DA model was produced, and this was a much stronger model than the PCA with only 2 components detected. The goodness of fit R^2X(cum) was 0.389 and R^2Y(cum) was 0.996. The predictive ability Q^2X(cum) was 0.612 (figure 17). The difference is less than 0.3 between R^2X and Q^2X which means that there is less likelihood that too much noise or outlying data have affected the model (Eriksson, et al., 2006). A Q^2X(cum) value of more than 0.5 means that the model is considered to have a good predictability (Ali, et al., 2012).

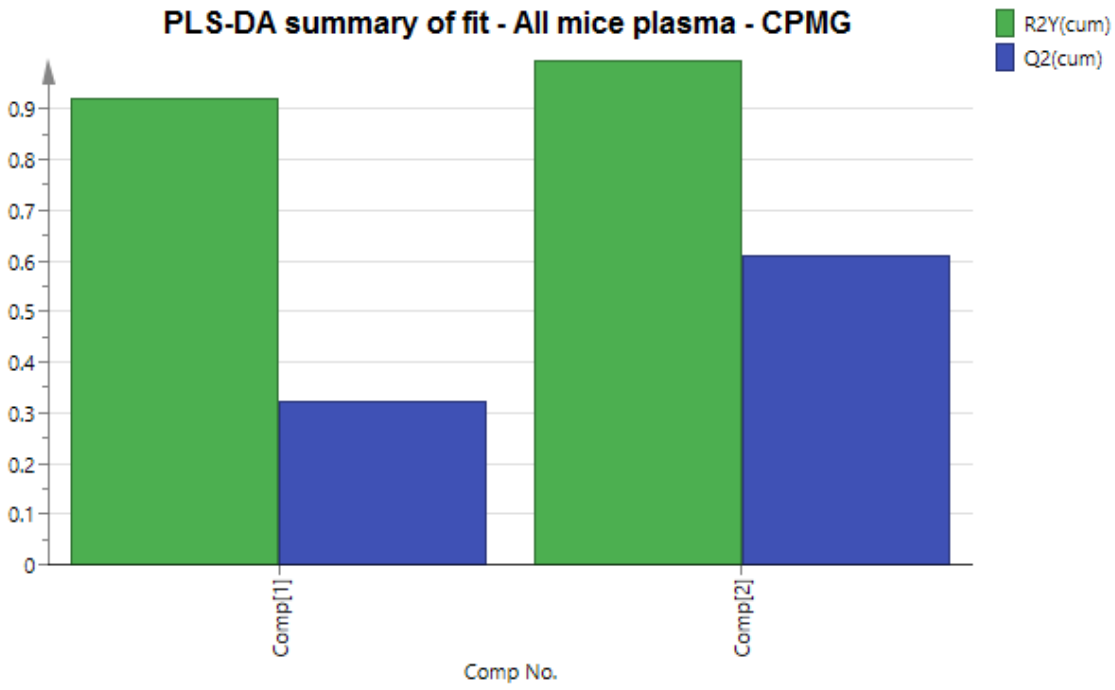

Figure 17: PLS-DA model – All mice plasma – CPMG sequence

The score scatter of this model showed a clear separation between study and control samples (figure 18), with the score column demonstrating the clustering of the samples when arranging the scores in ascending order (figure 19).

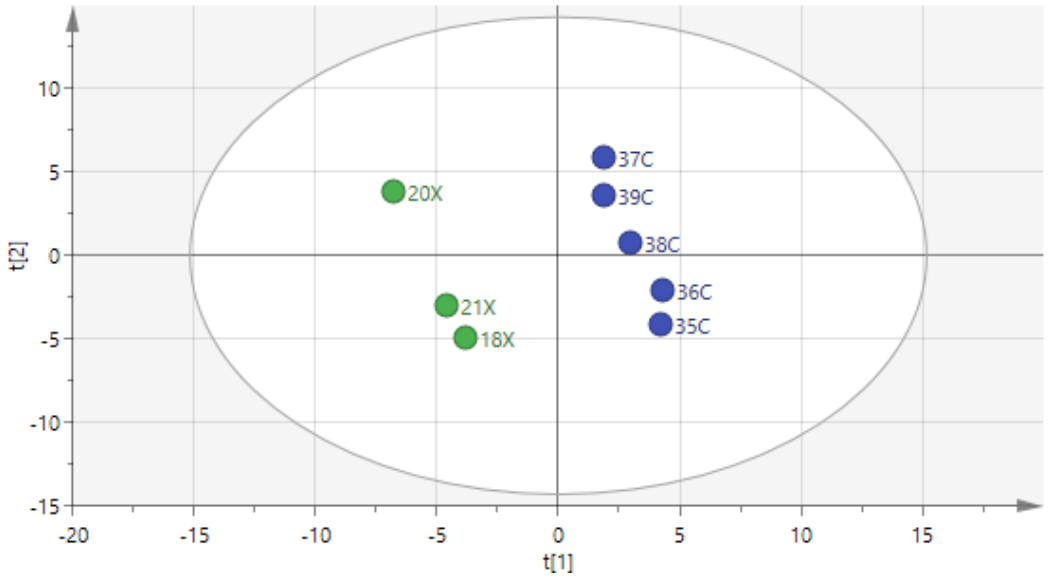

Figure 18: Score scatter of PLS-DA model – All mice plasma – CPMG

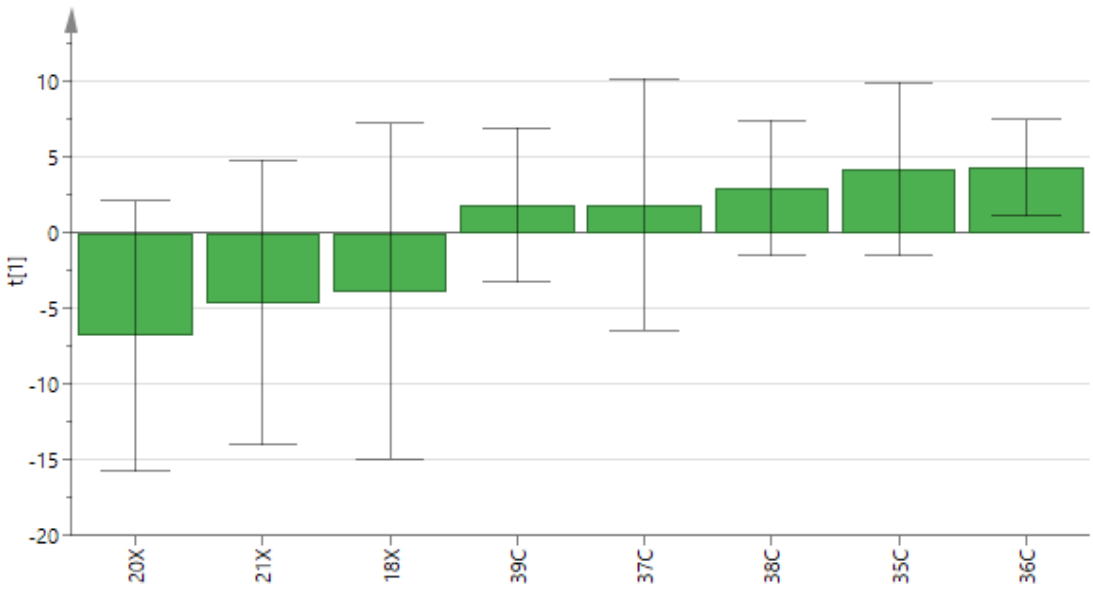

Figure 19: Score column of the PLS-DA model – All mice plasma – CPMG

The matching loading column plots for component 1 and 2 are shown in figures 20 and 21 respectively. These enable the identification of the plasma metabolites which are responsible for the discrimination and clustering of the samples. Table 9 summarises the chemical shifts (bins) that were responsible for differentiating the two groups, and their correlating plasma metabolites responsible for the high scores (95% Confidence Intervals) (Nicholson, et al., 1995).

Bins in the range 0.98-1.06 ppm have a doublet spectral signal are consistent with valine (α-amino acid used in proteins biosynthesis). This was stronger in the study group alongside other protein biosynthetic α-amino acids, such as arginine (3.22 ppm - triplet) and alanine (3.78 ppm - quartet). Although, a doublet valine signal at 3.58 ppm and singlet glutamine (α-amino acid used in proteins biosynthesis) signal at 2.42 ppm were also present in component 2 of the loading plot. On the other hand, 2-oxoglutarate (2.46 ppm - triplet), which is a ketone derivative of glutaric acid, was stronger in the control group. Another strong signal in the control group was taurine (3.26 ppm - triplet) which is 2-

aminoethanesulfonic acid which is a main ingredient of bile and can be found in the colon.

3-hydroxybutyrate (2.38 ppm - singlet) was stronger in the study group. It is usually associated with ketosis, a metabolic state in which the body gains energy from ketone bodies instead of glucose.

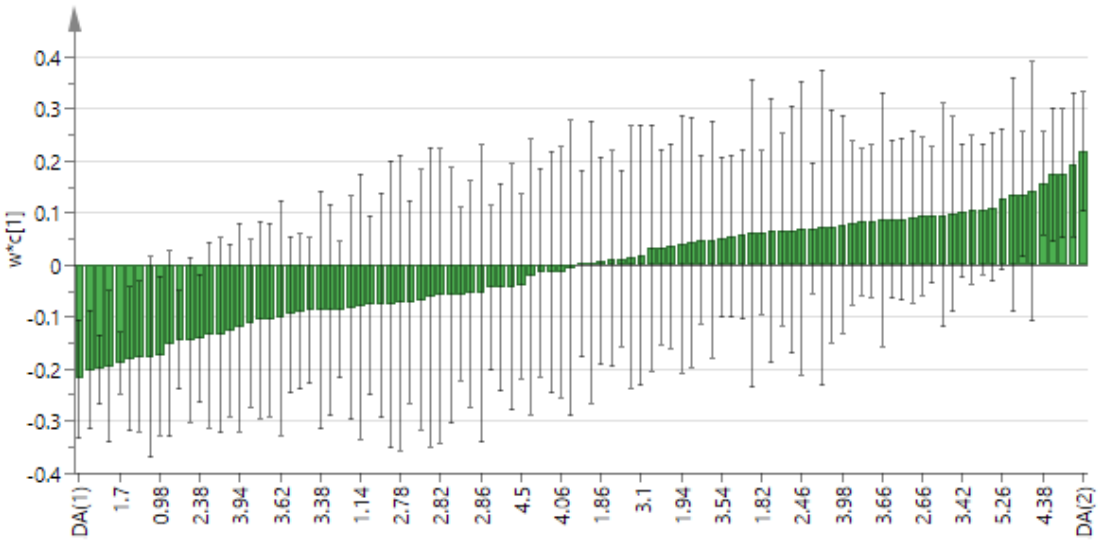

Figure 20: Component 1 loading column of the PLS-DA model – All mice plasma – CPMG

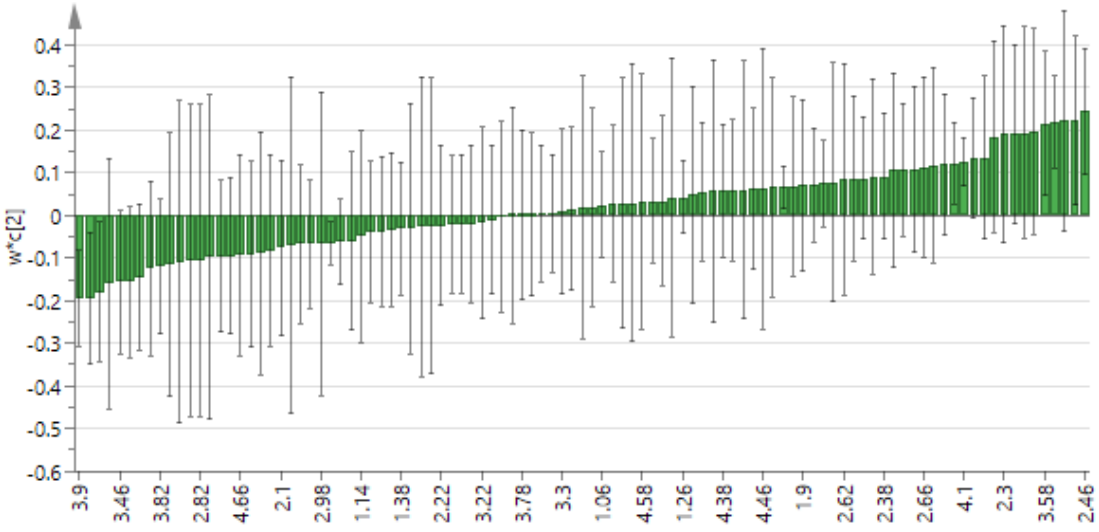

Figure 21: Component 2 loading column of the PLS-DA model – All mice plasma – CPMG

	Component 1			Component 2		
	Bin	Signal multiplicity	Molecule	Bin	Signal multiplicity	Molecule
Study	0.9	m	Lipid	3.38	none	
	0.98	d	Valine	3.74	d	*α*Glucose
	1.02	d	Valine	3.9	d	*β*Glucose
	1.06	d	Valine			
	1.38	d	Lactate			
	1.7	none				
	1.74	none				
	2.38	s	3-hydroxybutyrate			
	3.9	d	*β*Glucose			
Control	0.86	t	Lipid mainly LDL	2.42	s	Glutamine
	3.22	t	Arginine	2.46	t	2-oxoglutarate
	3.26	t	Taurine	2.5	none	
	3.78	q	Alanine	3.58	d	Valine
	4.38	none		4.1	q	Lactate

Table 9 Chemical shifts responsible for high scores and correlating metabolites

PLS-DA – All mice plasma – CPMG (s=singlet, d=doublet, t=triplet, q=quartet, m=complex multiplet)

3.1.2 Analysis of all mice plasma spectra – DOSY sequence

3.1.2.1 PCA model

A PCA model was produced for all the spectra obtained from mice plasma using DOSY sequence. Examples of the NMR spectra are shown in figure 22. This was still a weak model with only 2 components detected. The goodness of fit R^2X(cum) was 0.639. The predictive ability Q^2(cum) was 0.231 (figure 23). The difference was more than 0.3 between R^2X and Q^2 which means that there was more likelihood that too much noise or outlying data was affecting the signals. Analysing the score scatter of this model, the two groups were discriminated

based on their metabolites with no apparent definite outliers (figure 24). Sample C37 still had the tendency to be separated from the clustered control samples, although removing C37 again from the experiment did not alter the plasma metabolites causing this groups discrimination.

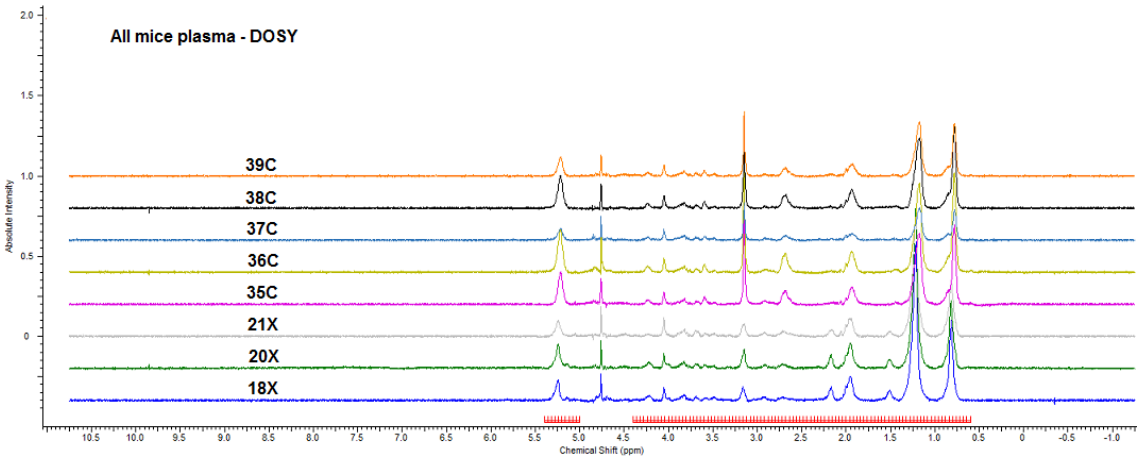

Figure 22: All mice plasma spectra with highlighted dark regions using DOSY sequence. X = chemical shifts (ppm), Y = Absolute intensity.

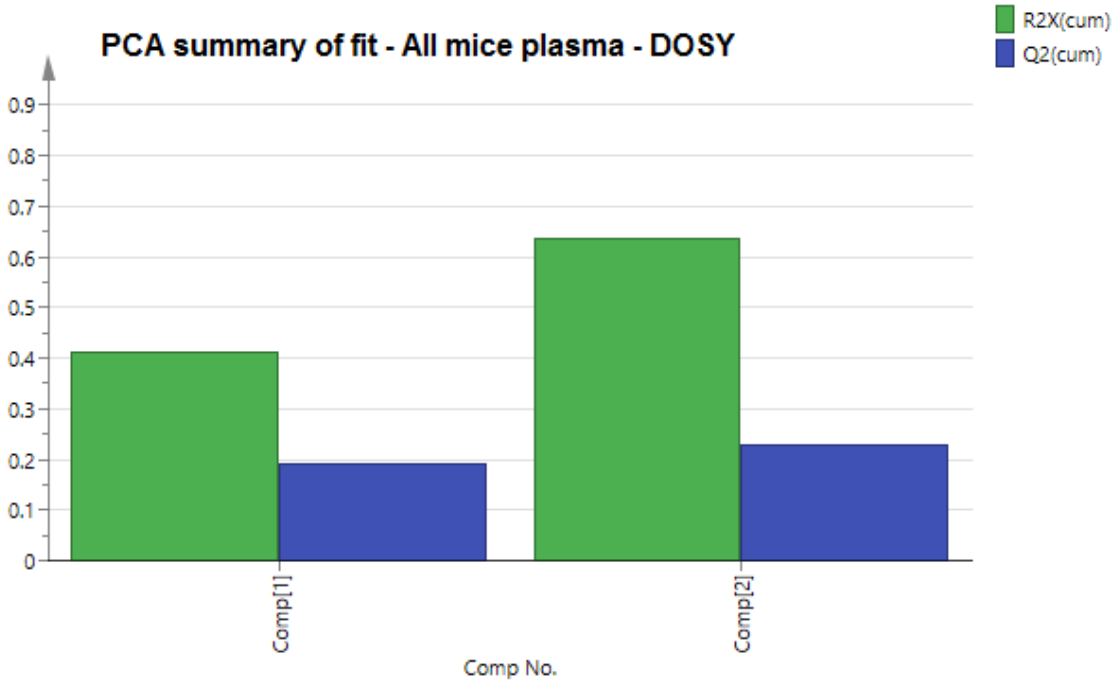

Figure 23: PCA model – All mice plasma – DOSY sequence

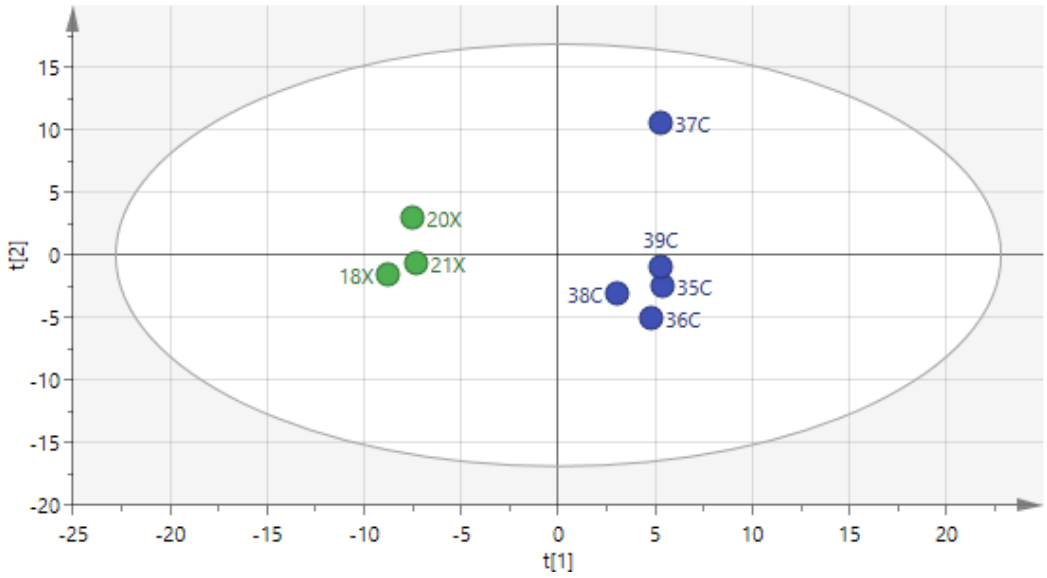

Figure 24: Score scatter of the PCA model – All mice plasma – DOSY

The matching loading column plot for this model produced more than 35 signals potentially causing the discrimination (figure 25). This suggests a probable noise effect which might have influenced the results, and it also makes identifying plasma metabolites which are responsible for samples discrimination more uncertain. Table 10 summarises the chemical shifts (bins) from strongest to weakest that could be responsible for differentiating the two groups, and their correlating plasma metabolites responsible for the high scores (95% Confidence Intervals) (Nicholson, et al., 1995).

It is apparent from the table of chemical shifts in this model that lipid metabolites have stronger signals in the study group, with mainly cholesterol and VLDL (very low-density lipoprotein) affecting their behaviour within the magnetic field. Bins in the range 2.14-2.18 ppm have a complex multiplet spectral signal are consistent with glutamate. Glutamate is considered the richest free amino acid in brain. It is a neurotransmitter which plays an important role during brain growth and learning and memory development (Tapiero, et al., 2002).

The control group however had stronger signals of amino acids predominantly. Although, some of the signals were overlapping which made it difficult to establish which amino acid is causing the shift. Bins in the range 3.14-3.18 ppm have a doublet spectral signal are consistent with tyrosine or histidine. While bins in the range 3.58-3.62 ppm have doublet spectral signals are consistent with valine or threonine. Aspartate (2.62-2.66 ppm - doublet) is another α-amino acid with a stronger signal in the control samples.

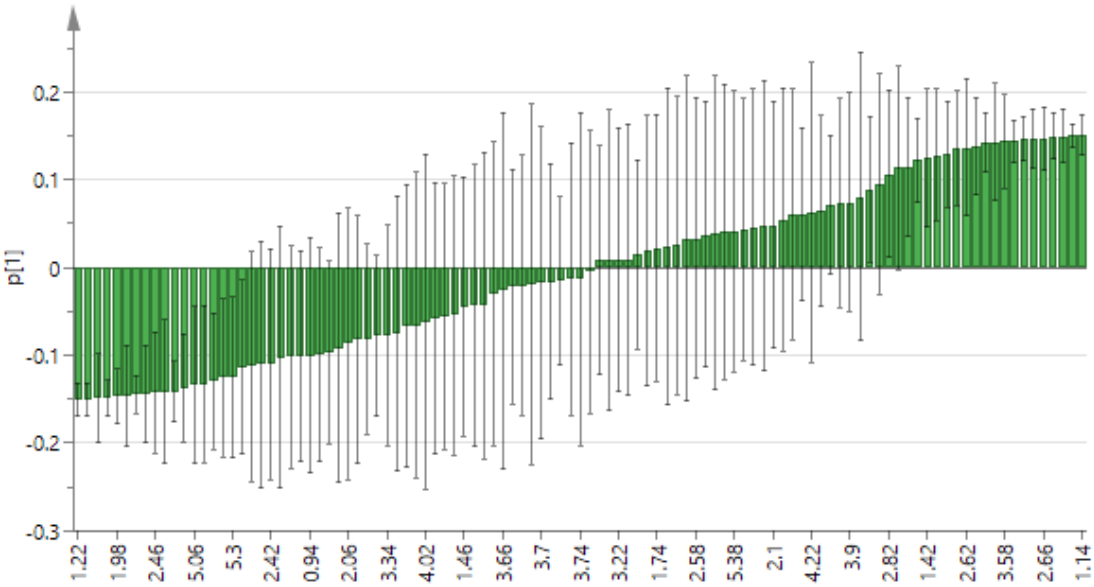

Figure 25: Loading column of the PCA model – All mice plasma – DOSY

Study			Control		
Bin	Signal multiplicity	Molecule	Bin	Signal multiplicity	Molecule
1.22	m	Lipid	1.14	none	
1.26	m	Lipid	3.14	d	Tyrosine Histidine
0.82	m	Cholesterol	1.18	none	
1.3	m	Lipid	0.74	none	
1.98	m	Lipid	2.66	d	Aspartate
1.5	m	Lipid mainly VLDL	0.78	m	Cholesterol
1.34	none		1.9	m	Lysine Arginine
2.18	m	Glutamate	5.18	m	Glyceryl of lipid
2.46	none		3.58	d	Valine Threonine
1.54	m	Lipid mainly VLDL	3.62	d	Valine Threonine
2.14	m	Glutamate	5.22	m	Glyceryl of lipid
1.38	none		2.7	m	Lipid
5.06	none		2.62	d	Aspartate
0.86	t	Lipid mainly VLDL	3.18	d	Tyrosine Histidine
2.5	none		0.7	none	
2.22	none		3.1	none	
5.3	none		1.42	none	
2.02	m	Glutamate	1.1	none	
			1.86	none	
			2.82	none	
			1.02	none	

Table 10: Chemical shifts responsible for high scores and correlating metabolites. PCA – All mice plasma – DOSY

(s=singlet, d=doublet, t=triplet, q=quartet, m=complex multiplet)

3.1.2.2 PLS-DA and OPLS-DA model

A PLS-DA model of this experiment did not add any further information. The model stayed weak with only one component detected. Although, the goodness of fit R^2X(cum) improved to 0.412 with a much higher predictive ability Q^2(cum) at 0.921. The difference in values between R^2 and Q^2 strongly suggested that the signals were affected by noise throughout the experiment. Figure 26 shows the score scatter of this model which again demonstrates group separation.

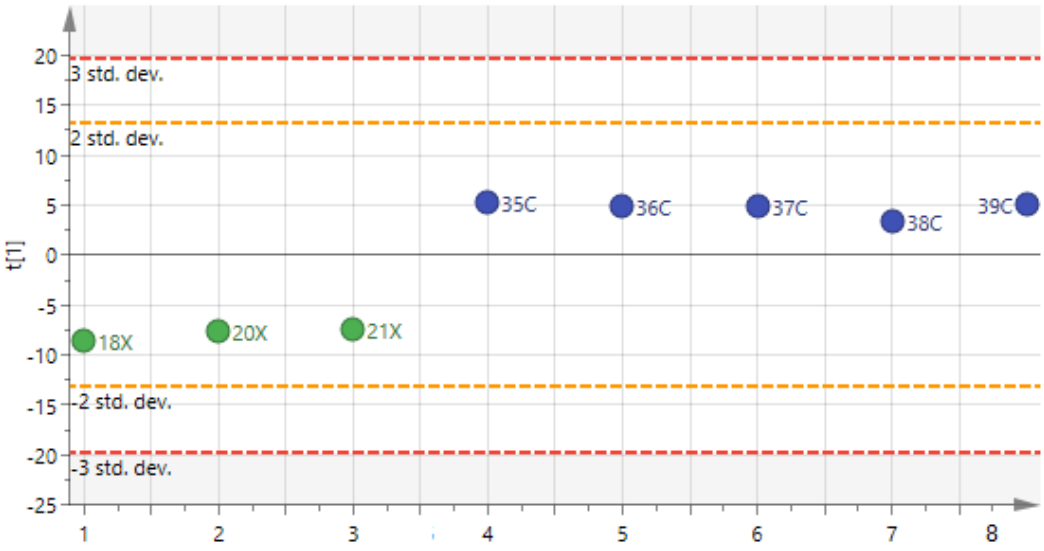

Figure 26: Score scatter of the PLS-DA model – All mice plasma – DOSY

Similarly, the OPLS-DA model did not add any further information, and the strength of the model did not improve with 3 more forced components detected that might be affecting group separation. It is suggested that if more than five PLS/OPLS components are included in the model the training set data generally reproduce excellently (Ali, et al., 2012).

3.2 Discussion

Animal plasma experiments in this study have shown weak results which were difficult to interpret, and it was not possible to generate a model that could confidently establish certain metabolites as atherosclerotic biomarkers.

The effect of lipid signals on the study group was noticeable, although their strong signals might have covered other signals that could represent a significant biomarker. This was more obvious in the DOSY experiment, which is designed for detecting macromolecules. Unfortunately, this was not replicated in the CPMG experiment and with mixed results it was not possible to follow the metabolic pathways that might be responsible for group separation. Similar mixed results were witnessed regarding the effect of amino acids on both groups and therefore difficult to interpret.

Interestingly, taurine signals were more evident in the control group. Taurine is thought to play an important role in supressing the development of atherosclerosis and has preventative influence on cardiovascular diseases and diabetes mellitus complications (Murakami, 2014) (Sarkar, et al., 2017).

This study had a small number of mice (3 study v 5 control) compared to other studies conducted in the same field (Martin, et al., 2009) (Leo & Darrow, 2009) (Yang, et al., 2014). This could be another reason for the models' weakness.

Chapter 4: NMR analysis of solid tissues

Animal samples

This chapter will describe High Resolution Magic Angle Spinning ^{1}H-NMR spectroscopy analysis of aortic arches obtained from 10 mice (5 ApoE-/- vs 5 control) using CPMG and 1D NOESY pulse sequences. Samples were prepared as per Section 2.1.2 and 2.4.1. Data were collected as explained in Section 2.4.2. Spectra processing was done as per Section 2.5. Statistical analysis was done as per Section 2.6.

Each mouse was given a number followed by a letter for identification purpose. The number was given to each animal according to the animal order of purchase in the University of Leeds Labs. The letter was either X for the study group or C for the control group. All the mice were born on 19th October 2011 and terminalised on 13th March 2012 (21-week-old).

4.1 Results

All animals were weighed immediately prior to terminalisation. There is a statistically significant difference between the two groups which may influence the following results from the NMR analysis. Table 11 details each animal weight in each group.

Study	**Weight (g)**	**Control**	**Weight (g)**	**P-value (*t*-test)**
18X	28.5	35C	36.4	
19X	33.1	36C	37.6	
20X	33.6	37C	38.6	
21X	27	38C	41.8	
22X	39	39C	45.5	
Mean ± SD	32.24 ± 4.74	Mean ± SD	39.98 ± 3.68	0.0203

Table 11: Mice weight: comparison between the study and control groups

4.1.1 Analysis of all mice solid tissues spectra – CPMG sequence

4.1.1.1 PCA model

A PCA model was produced for all the spectra obtained from mice aortic arches using CPMG sequence. Examples of the NMR spectra are shown in figure 27. A very weak model again was demonstrated and only 1 component was detected. The goodness of fit R^2X(cum) was 0.442. The predictive ability Q^2(cum) was -0.1. Similar to the animal plasma experiment, the negative value of Q^2(cum) indicates that this model is not predictive (figure 28).

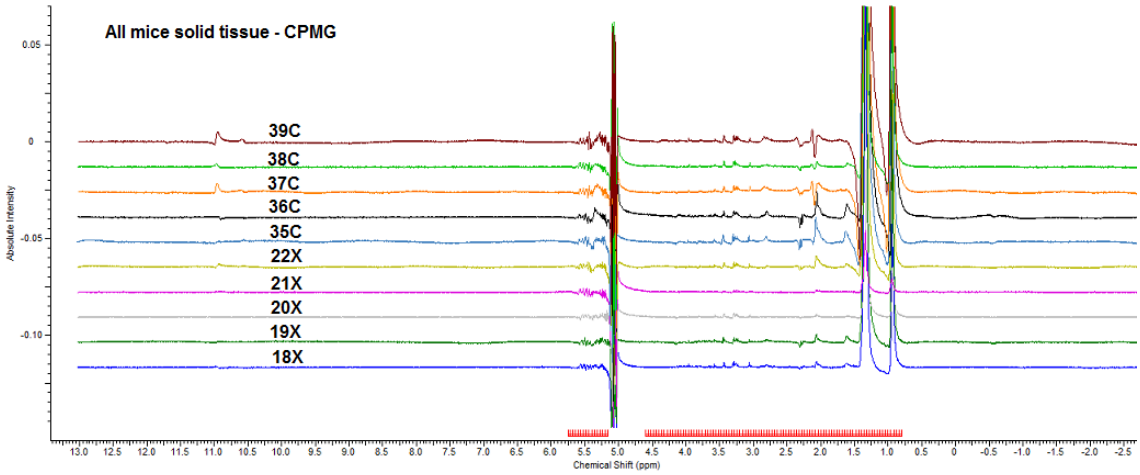

Figure 27: All mice solid tissue spectra with highlighted dark regions using CPMG sequence. X = chemical shifts (ppm), Y = Absolute intensity.

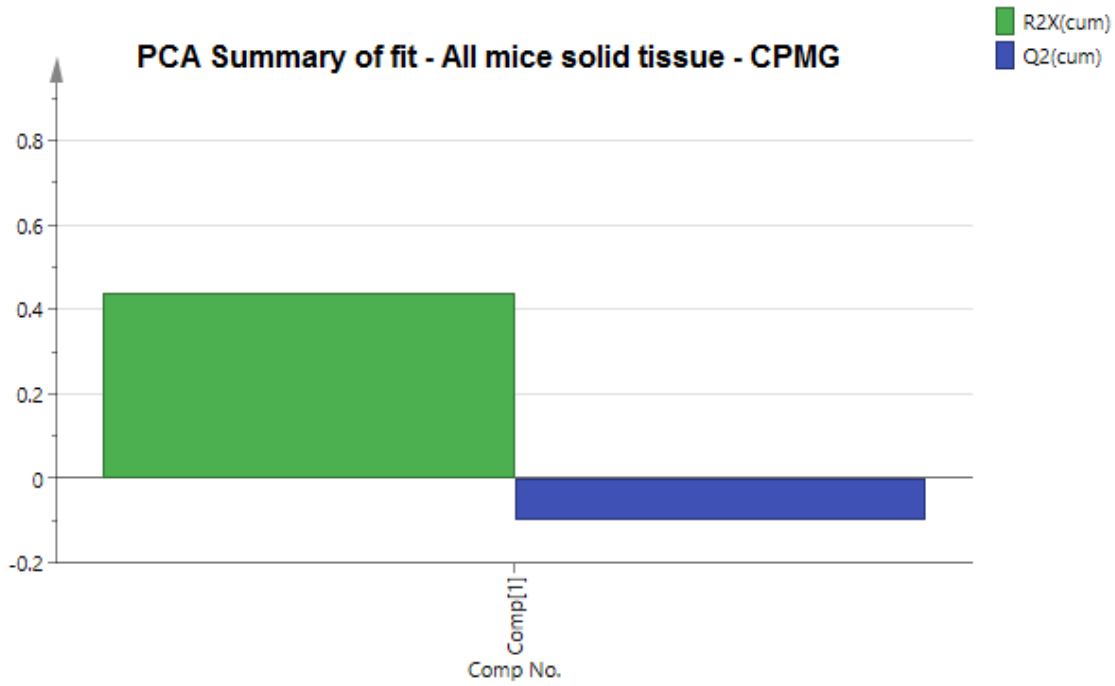

Figure 28: PCA model – All mice solid tissue – CPMG sequence

Analysing the scorer scatter and column, the mice could not be separated based on their metabolites. Sample 21X, however, seemed to have a stronger effect on the study group and could be therefore an outlier (figure 29). This could be one of the reasons for the weakness of this model and the inability of samples separation.

Removing sample 21X did not improve the model. The goodness of fit $R^2\boldsymbol{X}$(cum) was 0.666. The predictive ability Q^2(cum) was -0.0673. However, it did increase the number of detected components to 3, without affecting the clustering pattern of the study group compared to the control group or separating them (figure 30).

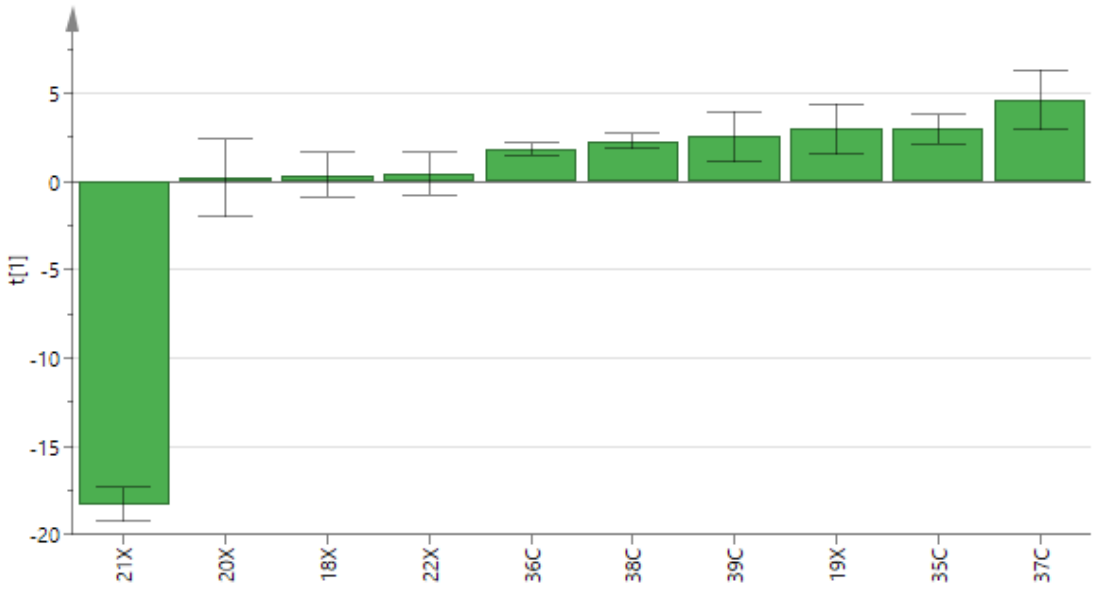

Figure 29: Score column of the PCA model – All mice solid tissue – CPMG

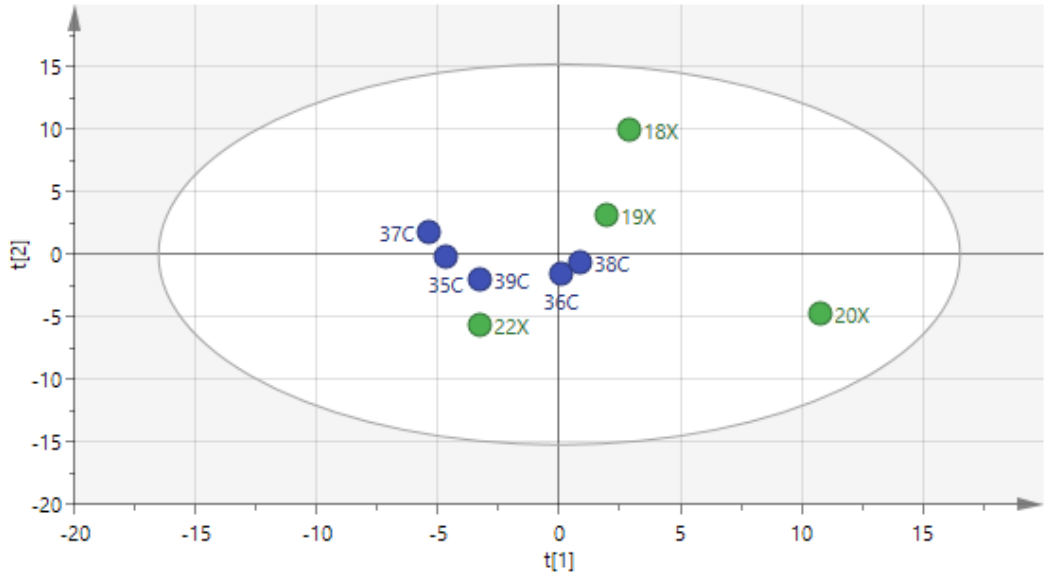

Figure 30: Score scatter of the PCA model – All mice solid tissue (without sample 21X) – CPMG

4.1.1.2 PLS-DA and OPLS-DA models

A PLS-DA model for this experiment was produced, and this was a stronger model than the PCA with only 1 component detected. The goodness of fit R^2X(cum) was 0.399 and R^2Y(cum) was 0.466. The predictive ability Q^2(cum) was 0.221 (figure 31).

Similarly, the OPLS-DA model did not add any further information, and the strength of the model did not improve without being able to force any further components that may affect group separation.

On further analysis of the original spectra and the loading column of this model, there was one area of interest that had higher signals in the study group. This area matched bins in the range 3.54-3.58 ppm. The signal was a doublet which is consistent with valine (figure 32).

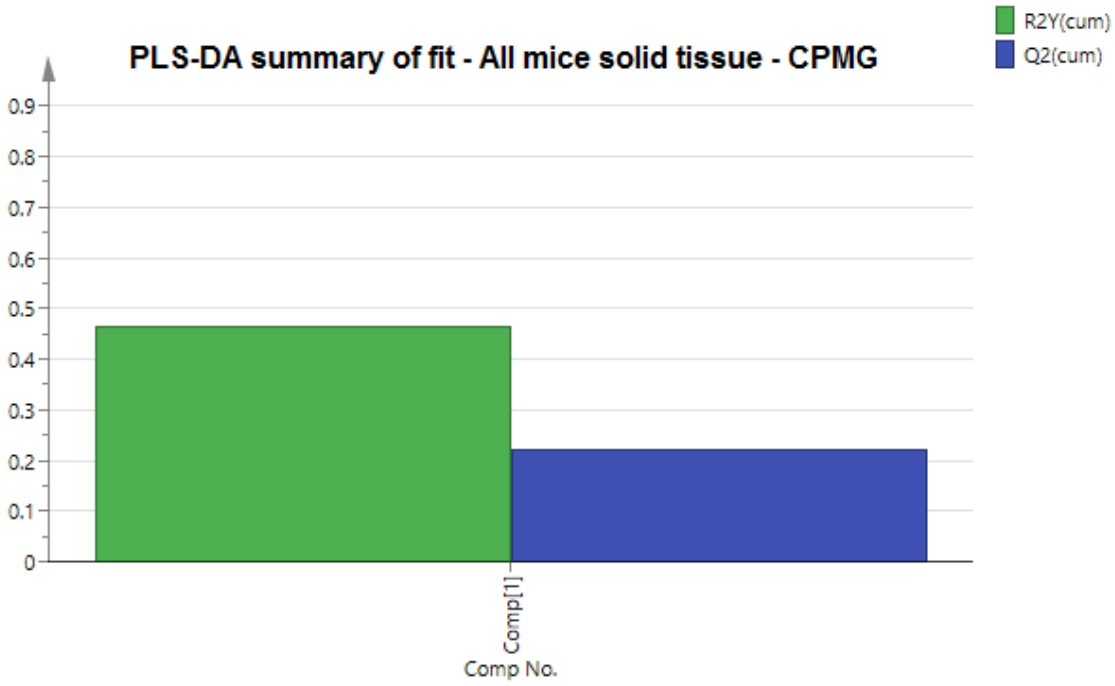

Figure 31: PLS-DA model – All mice solid tissue – CPMG sequence

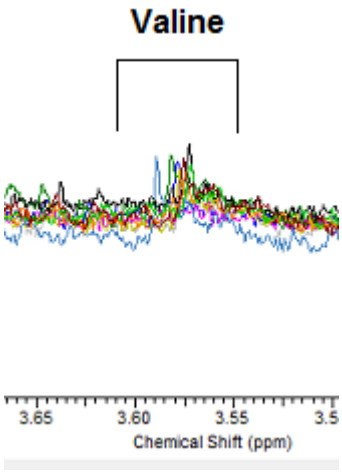

Figure 32: Valine signal - PLS-DA model – All mice solid tissue – CPMG sequence

4.1.2 Analysis of all mice solid tissue spectra – 1D NOESY sequence

4.1.2.1 PCA model

A PCA model was produced for all the spectra obtained from mice aortic arches using 1D NOESY sequence. Examples of the NMR spectra are shown in figure 33. This was a weak model with 3 components detected. The goodness of fit R^2X(cum) was 0.708. The predictive ability Q^2(cum) was -0.0357 (figure 34). The negative value of Q^2(cum) indicates that this model is not predictive.

It was noted, however, that the original spectra obtained using 1D NOESY sequence were easier to process, and produced sharper signals compared to the CPMG sequences. This was in contrast to what was experienced during the NMR analysis and spectra acquisition (section 2.4.2).

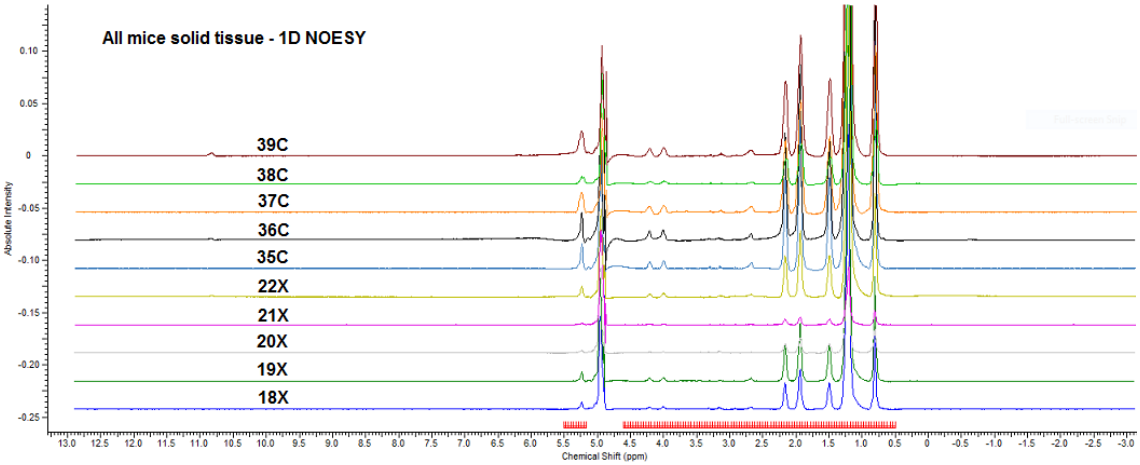

Figure 33: All mice solid tissue spectra with highlighted dark regions using 1D NOESY sequence. X = chemical shifts (ppm), Y = Absolute intensity.

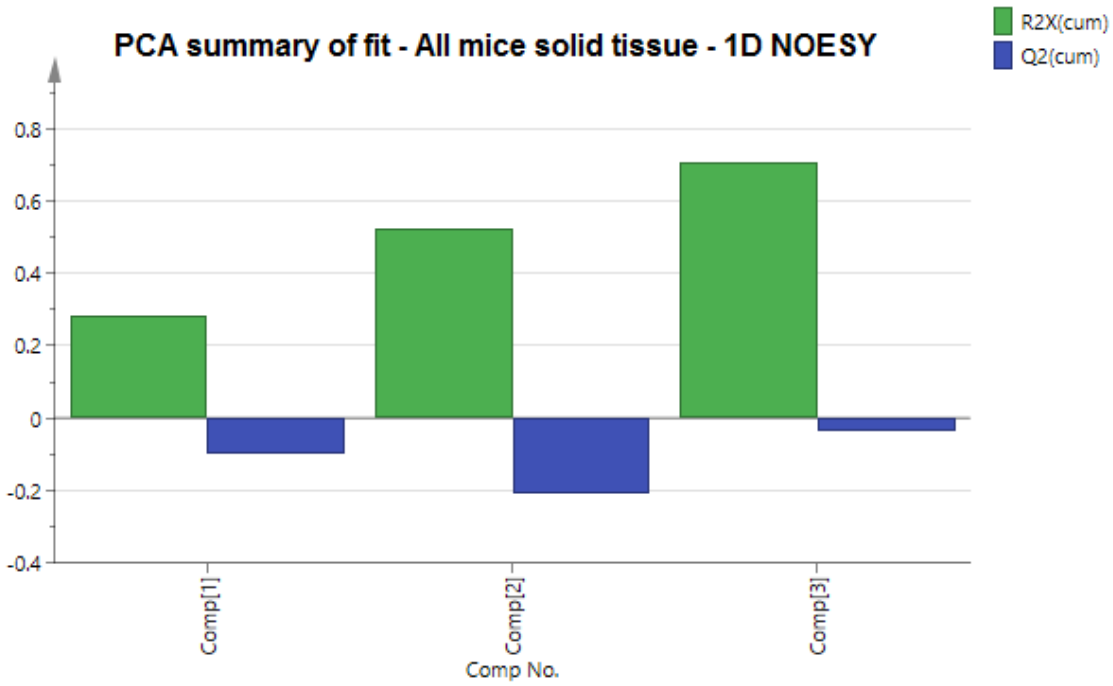

Figure 34: PCA model – All mice solid tissue – 1D NOESY sequence

Analysing the score scatter of this model showed a very weak separation between the study and control samples (figure 35). The score column for this model did not demonstrate any clustering of the samples, when arranging the scores in ascending order (figure 36).

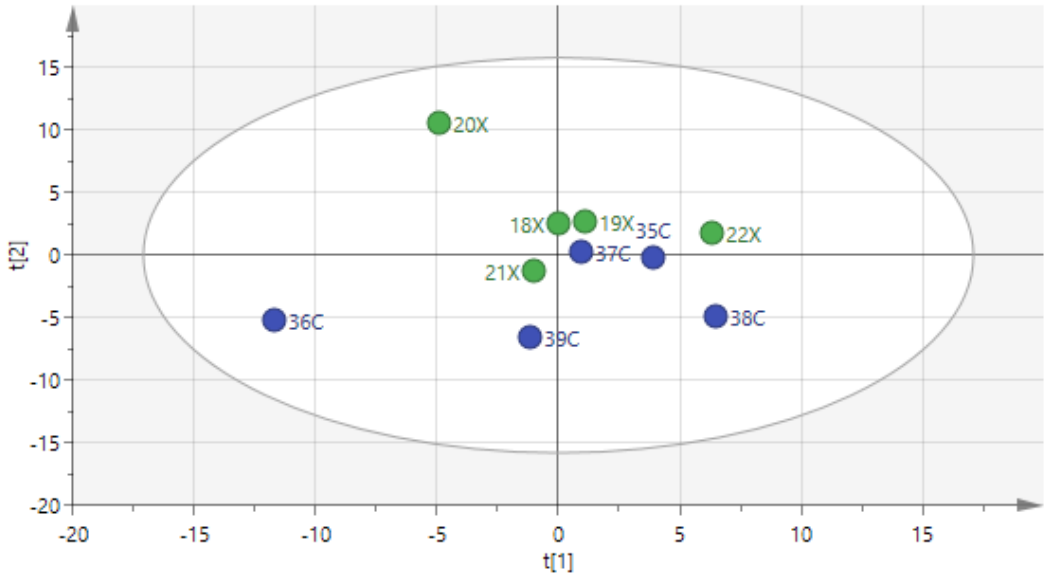

Figure 35: Score scatter of the PCA model – All mice solid tissue – 1D NOESY

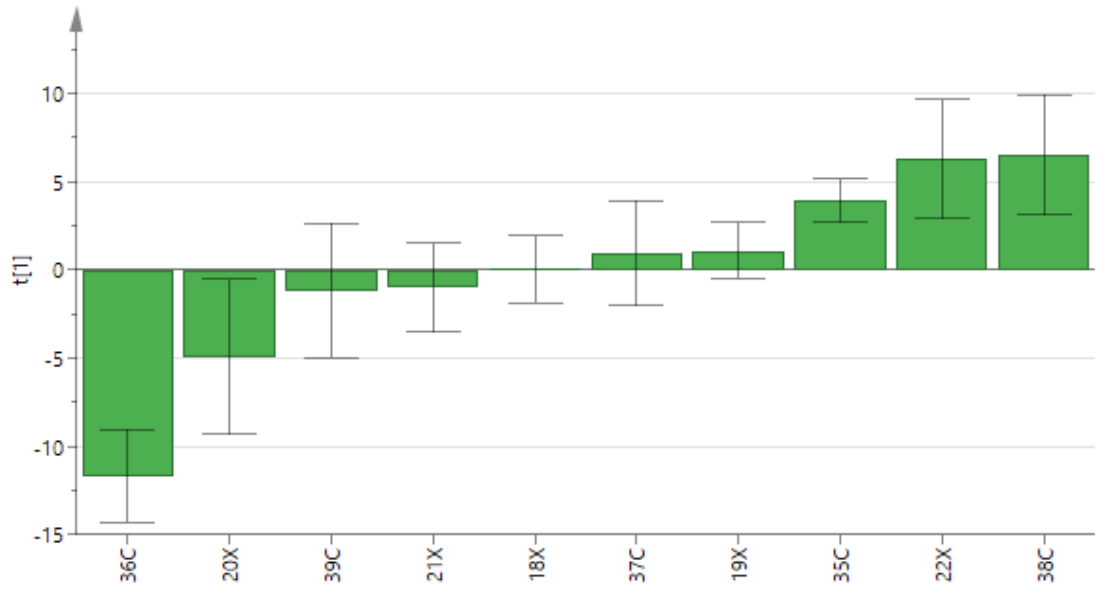

Figure 36: Score column of the PCA model – All mice solid tissue – 1D NOESY

The loading column plot of this model did not reveal any additional information. The only two signals identified as potential contributors to the weak separation were at bins 1.12 ppm (isobutyrate) and 4.28 ppm (threonine). It was, however, not possible to determine how each of them affects both groups.

4.1.2.2 PLS-DA and OPLS-DA models

A PLS-DA model for this experiment was produced, which was a stronger model than the PCA with only 1 component detected. The goodness of fit R^2X(cum) was 0.228 and R^2Y(cum) was 0.778. The predictive ability Q^2(cum) was 0.383 (figure 37). A more apparent separation was observed in this model and samples were clearly clustering according to their relevant groups. Sample 35C was the only sample which behaved as an outlier, although it did not affect group separation as shown in the score scatter (figure 38).

Similarly, the OPLS-DA model was stronger than the PCA with 1 component detected. This model did not add any further information to the experiment with 6 more forced components detected that might be affecting group separation (figure 39).

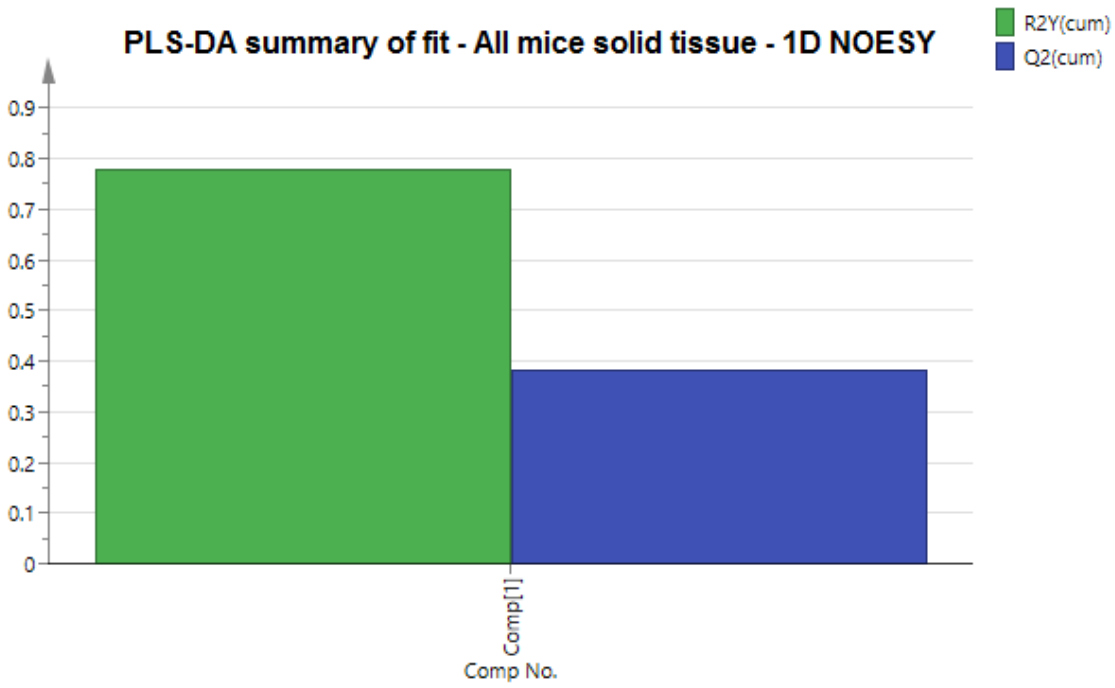

Figure 37: PLS-DA model – All mice solid tissue – 1D NOESY sequence

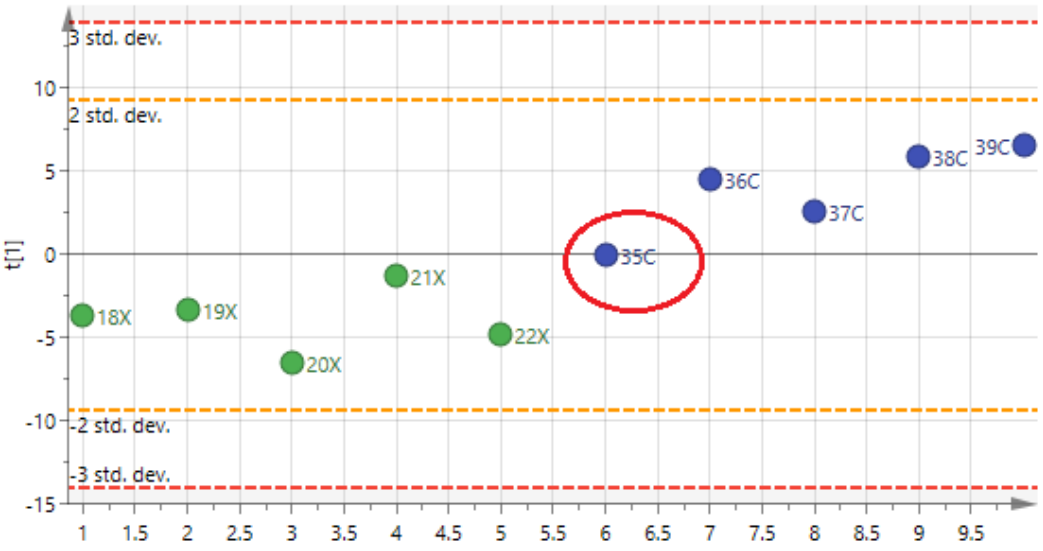

Figure 38: Score scatter of the PLS-DA model - All mice solid tissue - 1D NOESY

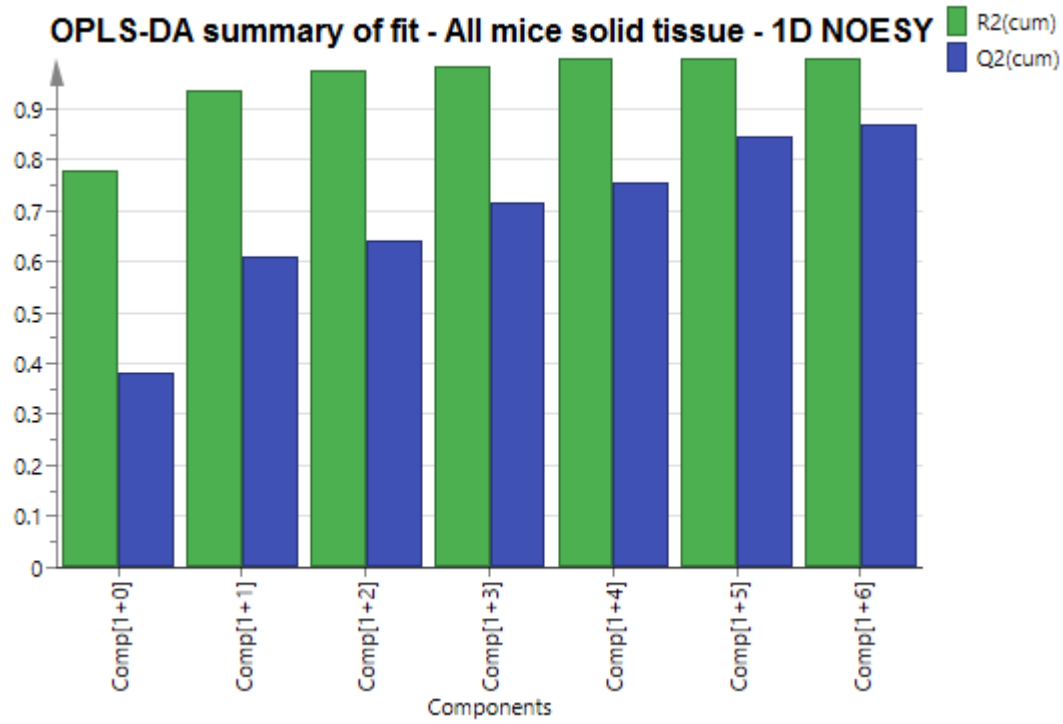

Figure 39: OPLS-DA model – All mice solid tissue – 1D NOESY sequence

The matching loading column plot for this model produced 9 signals potentially causing the discrimination (figure 40). Table 12 summarises the chemical shifts (bins) from strongest to weakest that could be responsible for differentiating the two groups, and their correlating plasma metabolites responsible for the high scores (95% Confidence Intervals) (Nicholson, et al., 1995).

Bins in the range 0.96-1.00 ppm have a doublet spectral signal are consistent with leucine, valine or isoleucine. These were stronger in the study group, but it was difficult to determine which metabolite is causing the shift. This is mainly due to a large lipid signal covering that area of the spectra. Taurine signal (3.28 ppm - triplet) was the dominant metabolite affecting the control group. The only other metabolite with an effect on the control group was acetate (1.88 ppm - singlet).

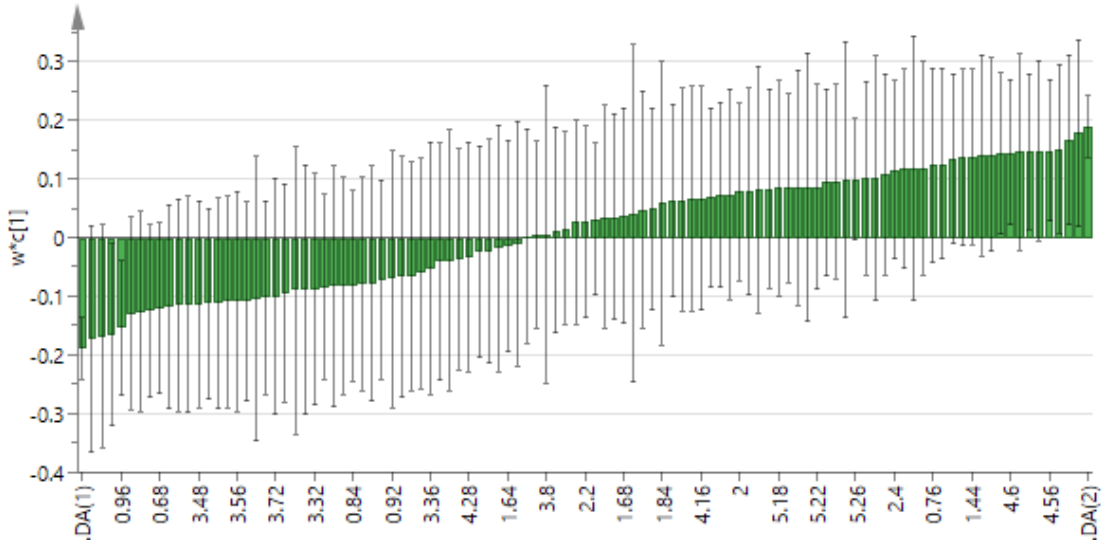

Figure 40: Loading column of the PLS-DA model – All mice solid tissue – 1D NOESY

Study			Control		
Bin	Signal multiplicity	Molecule	Bin	Signal multiplicity	Molecule
1.00	d	Leucine Valine Isoleucine	3.28	t	Taurine
0.96	d	Leucine Valine Isoleucine	1.4	none	
			2.8	none	
			4.56	none	
			4.52	none	
			4.6	none	
			1.88	s	Acetate

Table 12: Chemical shifts responsible for high scores and correlating metabolites. PLS-DA - All mice solid tissue - 1D NOESY

(s=singlet, d=doublet, t=triplet, q=quartet, m=complex multiplet)

4.2 Discussion

Animal solid tissue experiments in this study have shown weak results which were difficult to interpret, and it was not possible to generate a model that could confidently establish certain metabolites as atherosclerotic biomarkers. Promising findings were observed, however, in the 1D NOESY sequence experiment.

The effect of strong lipid signals on the spectra was noticeable and they might have covered other signals that could represent a significant biomarker. Perhaps the most interesting finding is the strong taurine signal which was present in mice plasma from the control group in the previous experiment (CPMG sequence), as well as the control mice aortic arch in this experiment (1D NOESY sequence).

This study had a small number of mice (5 study v 5 control) which could explain the models' weakness. Although, there are no other similar studies which use intact solid tissues in the NMR analysis for comparison.

Chapter 5: NMR analysis of plasma

Human samples

This chapter will describe ^{1}H-NMR spectroscopy analysis of plasma obtained from 77 patients. Samples were prepared as per Section 2.3.1 and 2.3.1.1. Data were collected as explained in Section 2.3.2. Spectra processing was done as per Section 2.5. Statistical analysis was done as per Section 2.6.

Each plasma sample was given a set of letters followed by a number for identification purpose. The letters were: (Ca) for patients with symptomatic carotid disease, (Fe) for patients with symptomatic femoral disease, and (Ctrl) for patients from the control group. The number given to each sample was according to their order of recruitment.

5.1 Results

Out of 83 patients recruited for this study, 2 from the control group did not attend their out-patient appointments, 1 from the femoral endarterectomy group was cancelled due to medical reasons, 2 patients withdrew from the study and I could not use their samples, and 1 patient from the femoral endarterectomy group went to theatre prior to me being able to take a blood sample for the study.

77 plasma samples were analysed. Patients' demographics, relevant past medical history and current medications are summarised in table 13.

More detailed statistical analysis of patients' data will be discussed throughout this chapter wherever found relevant.

		Carotid	Femoral	Control
Number of patients		42	18	17
Male/Female		27/15	15/3	8/9
Age (years)	Range	44-91	46-79	44-90
	Mean	70.7 ± 10.8	64.9 ± 10.2	67.6 ± 8.7
	Median	73	69	67
BMI ($kg.m^{-2}$)	Range	20 – 43	16.8 - 39	22.4 – 50.2
	Mean	27.9 ± 4.5	26.8 ± 5.7	31.1 ± 8.6
	Median	28.5	26.5	30.8
Smoke	Current	15	9	3
	Ex	19	8	5
	Never	8	1	9
Alcohol (unit)	Range	0-75	0-65	0-90
	Mean	12.2 ± 12.9	18.3 ± 15.1	13.7 ± 20.8
	Median	10	15	10
Hypertension	Treated	23	11	6
	Untreated	3	2	2
Diabetes Mellitus	Diet	6	0	0
	Oral	5	1	1
	Insulin	2	1	0
hyperlipidaemia		11	7	2
Antiplatelet therapy		37	16	4
Statins		38	15	8

Table 13: Patients demographics and medical background – NMR plasma study

5.1.1 Analysis of all human plasma spectra – CPMG sequence

5.1.1.1 PCA model

A PCA model was produced for all the spectra obtained from analysing human plasma using CPMG sequence. The goodness of fit R^2X(cum) was 0.808. The predictive ability Q^2(cum) was 0.269. The difference between R^2X and Q^2 suggested that there were either too much noise or many outliers affecting the signals. In the initial run of data 13 components were detected, and the control group seemed to be different from the carotid and femoral groups.

Sample Ctrl-078 noted to have a large ethanol signal compared to the rest, which suggests a high alcohol consumption prior to sampling (figure 41). This patient reported an alcohol intake of around 90 units per week, which was the highest amongst all patients. Sample Ctrl-078 was considered to be therefore an outlier with a potential significant effect on the results, and it was removed from this analysis.

A second PCA model was then produced, the goodness of fit R^2X(cum) was 0.822 and the predictive ability Q^2(cum) was 0.302. 14 components were detected in this model (figure 42).

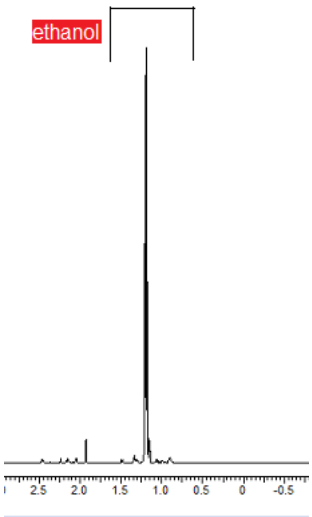

Figure 41: ethanol signal in sample Ctrl-078 (plasma)

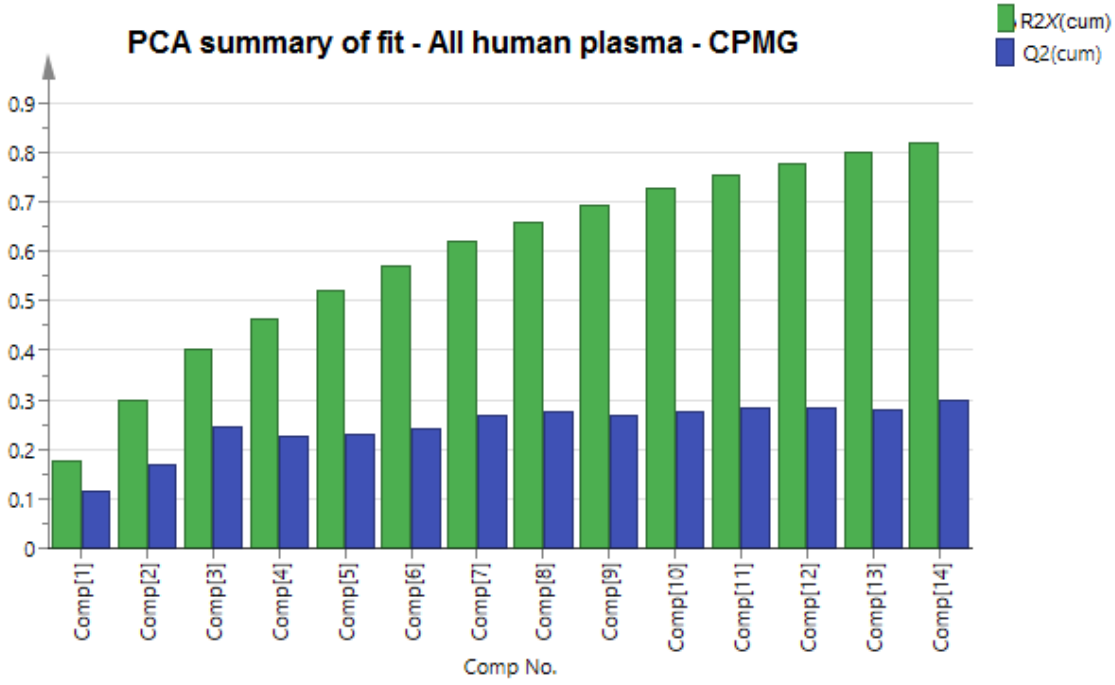

Figure 42: PCA model – All human plasma (without Ctrl-078) – CPMG sequence

The score scatter of this model showed a degree of separation and clustering between the groups, although clustering patterns were noticed within each group as well (figure 43).

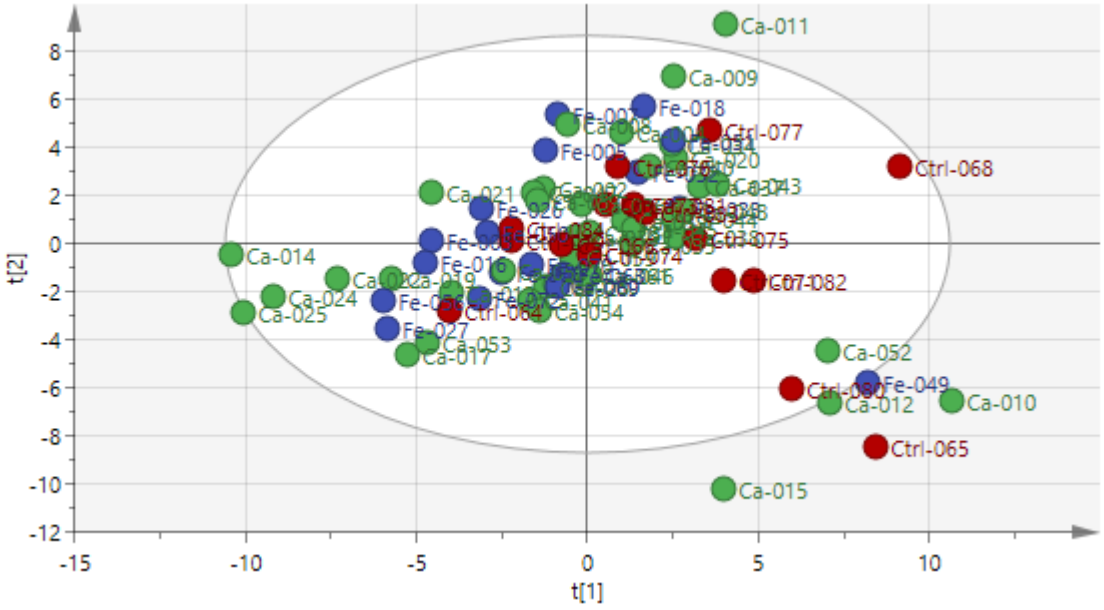

Figure 43: Score scatter of the PCA model – All human plasma (without Ctrl-078) – CPMG

4 further outliers (Ca-010, Ca-011, Ca-015, Ctrl-065) could be identified in this scatter. Analysing each spectrum and correlating patient's data, it was not possible to explain this behaviour. A third PCA model was then produced (figure 44). Based on this third model, there was no obvious improvement in the separation or clustering patterns between the groups. Therefore, these outliers were kept in the experiment and were observed for similar behaviour in other models.

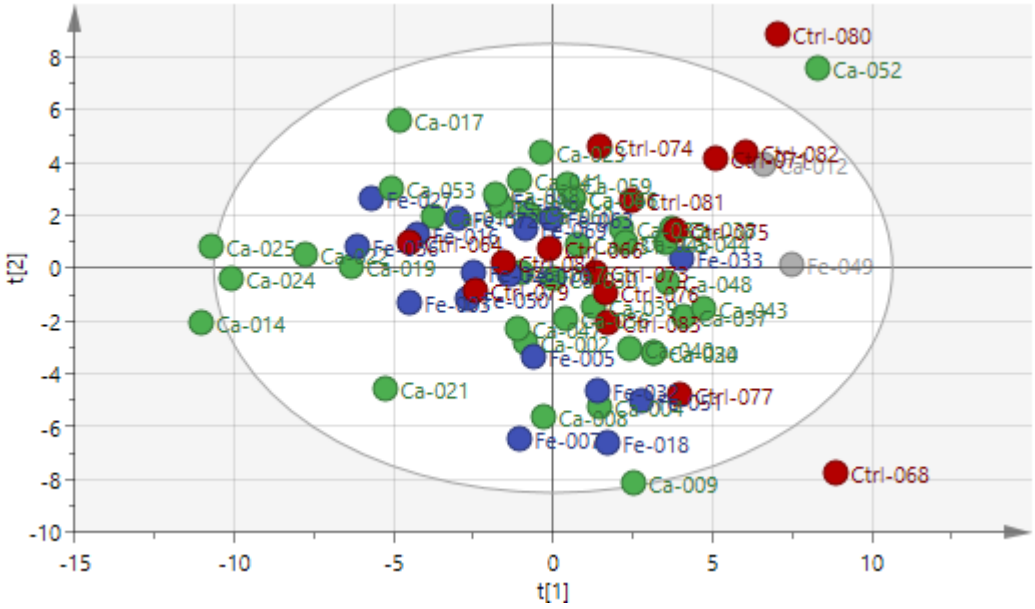

Figure 44: Score scatter of the PCA model – All human plasma (without samples Ca-010, Ca-011, Ca-015, Ctrl-065, Ctrl-078) – CPMG

The second PCA model also suggested a slight separation based on patients' gender (figure 45). However, there was a statistically significant difference in the number of males versus females in this study (49 v 27, P-value = 0.0116). This was not further analysed at this stage, and further models may be built for each gender if this pattern continues to show throughout the experiment.

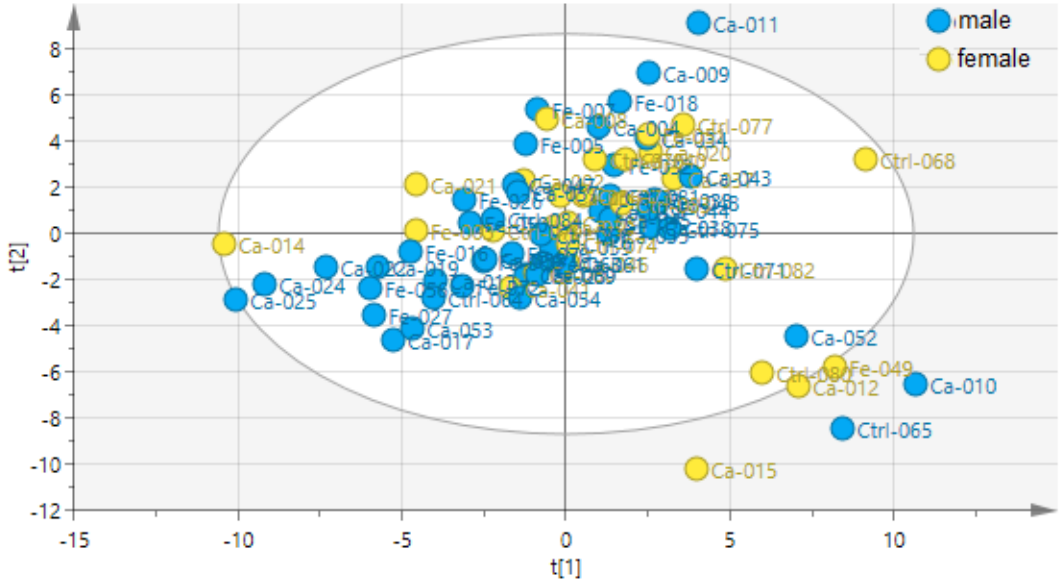

Figure 45: Score scatter of the PCA model based on gender – All human plasma (without Ctrl-078) – CPMG

5.1.1.2 PLS-DA and OPLS-DA models

A PLS-DA model was produced for all the spectra obtained from analysing human plasma using CPMG sequence. The goodness of fit R^2X(cum) was 0.136 and R^2Y(cum) was 0.177. The predictive ability Q^2(cum) was 0.0472. Similar to the PCA model, sample Ctrl-078 had a high ethanol signal and was removed from the experiment.

A second PLS-DA model was then produced excluding sample Ctrl-078. The goodness of fit R^2X(cum) was 0.143 and R^2Y(cum) was 0.17. The predictive ability Q^2(cum) was 0.0604. This was a weaker model than the PCA with only 1 component detected. There was however a clearer separation of the control group from the other two groups based on their metabolites (figure 46). This model also suggested a sub-clustering behaviour within the femoral endarterectomy group. Analysing the relevant spectra and patients' data, it was not possible to explain this behaviour within the magnetic field (figure 47).

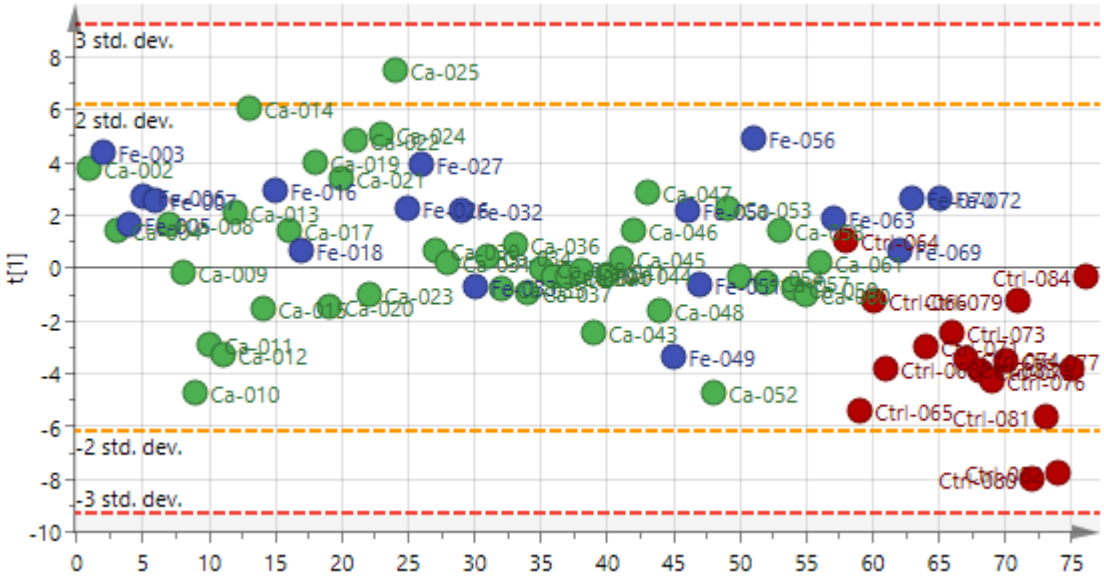

Figure 46: Score scatter of the PLS-DA model - All human plasma (without Ctrl-078) – CPMG

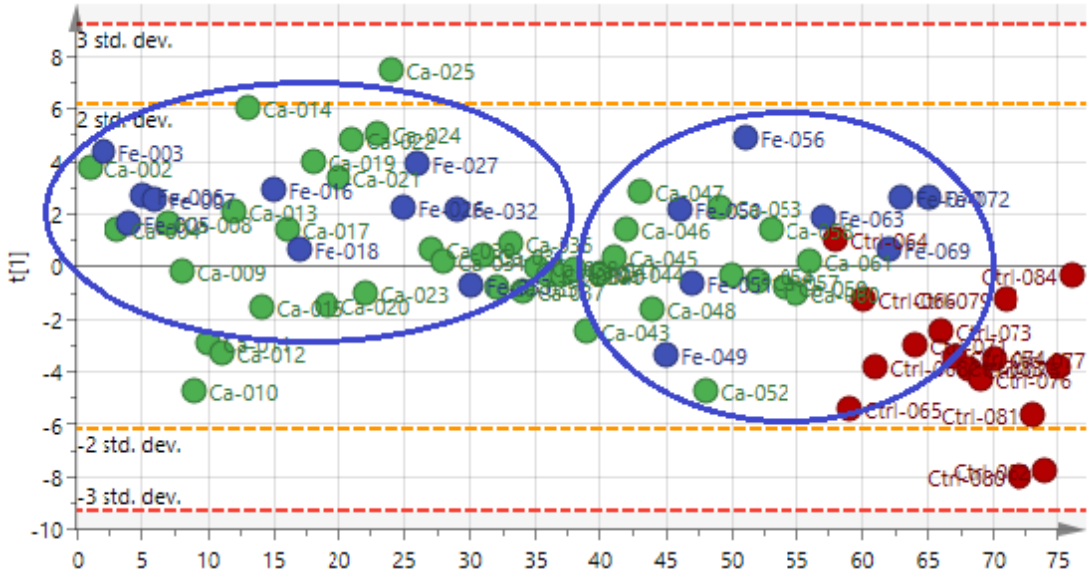

Figure 47: Score scatter of the PLS-DA model showing the sub-clustering of the femoral endarterectomy group – All human plasma (without Ctrl-078)– CPMG

The OPLS-DA model forced 2 more components and further established the separation between the control and both the femoral and carotid endarterectomy groups. However, the sub-clustering of the femoral endarterectomy group became less apparent in this model, although it highlighted a slight separation between the femoral ad carotid endarterectomy groups (figure 48).

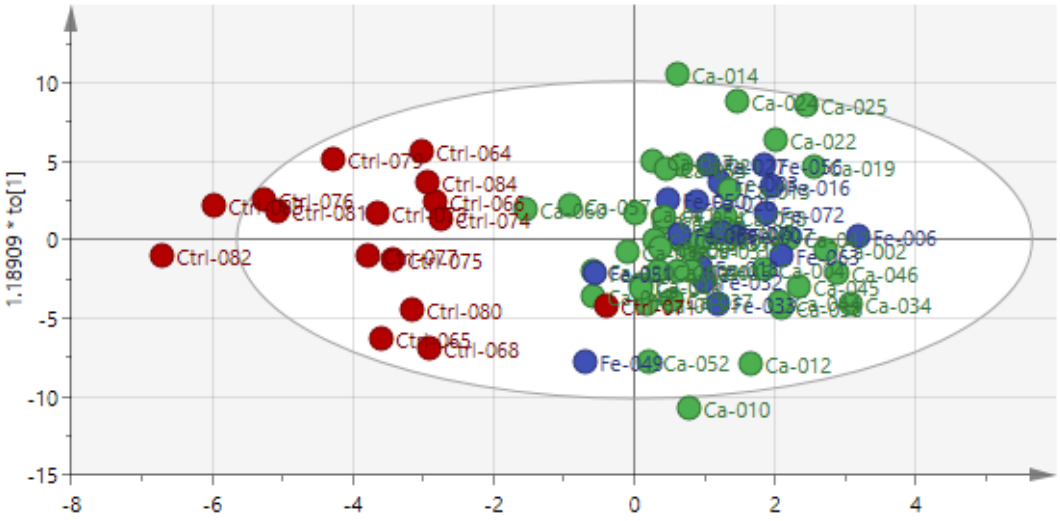

Figure 48: Score scatter of the OPLS-DA model – All human plasma (without Ctrl-078) – CPMG

The matching score and loading column plots of these models produced 15 signals potentially causing the discrimination between the control and 2 study groups (figures 49 and 50). Table 14 summarises the chemical shifts (bins) from strongest to weakest that could be responsible for differentiating the groups, and their correlating plasma metabolites responsible for the high scores (95% Confidence Intervals) (Nicholson, et al., 1995).

Bins in the range 3.02-3.05 ppm with a singlet spectral signal corresponds to either creatine or creatinine. These were found to be stronger in the control samples. Creatine is mainly produced in the liver and kidneys, and it helps in reprocessing of ATP (adenosine triphosphate) which plays an important role in the energy cycle in the body. Creatinine is a breakdown of creatine and is an important marker of the renal function clinically. Only two patients from the carotid endarterectomy group were known to have chronic kidney disease, according to its definition by the UK Renal Association (The Renal Association, 2017). This did not explain the stronger creatinine and creatine signals in the control group.

The control group had a stronger signal of the amino acid glutamate (2.18 ppm - complex multiplet), and the ketone derivative of glutaric acid 2-oxoglutarate (2.50 ppm - triplet). Choline (3.18 ppm - singlet), which is a water-soluble vitamin-like, was noticed to be stronger in the control group as well.

The study groups, on the other hand, were predominantly affected by strong glucose signals. Only one patient was diabetic in the control group compared to 15 in the study groups (13 carotid + 2 femoral). This difference though was statistically not significant (P-value = 0.1673). Another factor was that all the patients in the study groups were fasting at the time of blood sampling. While only one patient from the control group was fasting. Those two factors may well explain the stronger glucose signals. However, adding those glucose signals to the dark regions did not add or alter the information gained from this model. Therefore, further analysis of diabetic versus non-diabetic samples was not carried out at this stage.

Other signals affecting the study groups were taurine (3.26 ppm - triplet) and lactate (1.34 ppm - doublet). Lactate is usually increased when there is a higher demand for energy by tissues (exercise or hypo-perfusion for example).

It was also noticed that bins in the range 0.85-0.93 ppm had a strong lipid signal in all samples. Some signals in this range might have been covered by the lipid signal and were not exposed by this model.

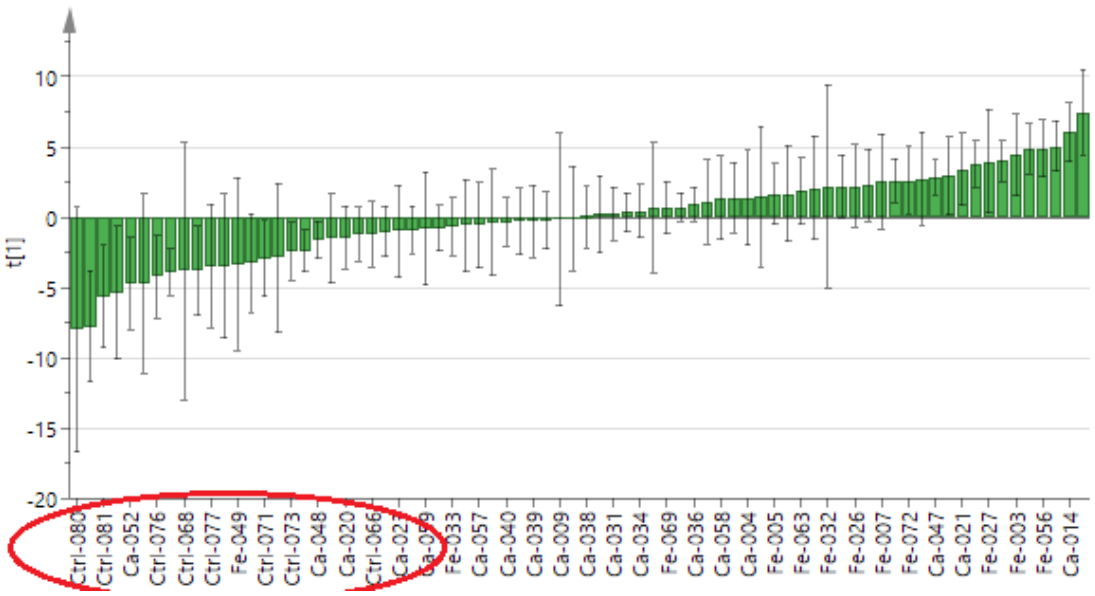

Figure 49: Score column of the PLS-DA model showing the clustering of control samples to the left when arranging the scores in ascending order

All human plasma (without Ctrl-078) – CPMG

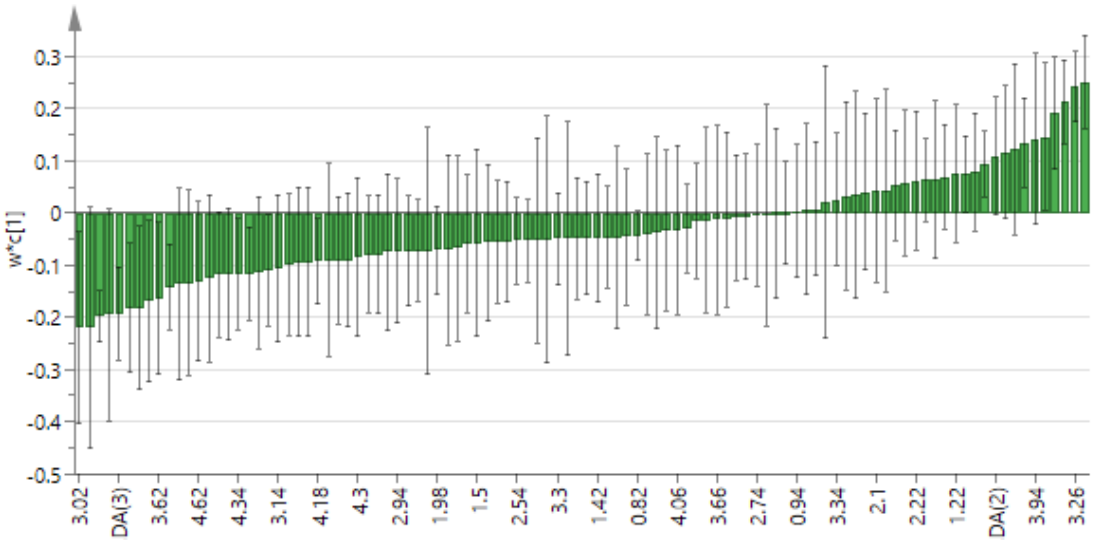

Figure 50: Loading column of the PLS-DA model - All human plasma (without Ctrl-078) – CPMG

Study (carotid and femoral)			Control		
Bin	Signal multiplicity	Molecule	Bin	Signal multiplicity	Molecule
1.34	d	Lactate	3.02	s	Creatine Creatinine
3.26	t	Taurine	2.18	m	Glutamate
3.5	dd	β-glucose	3.18	s	Choline
3.46	dd	β-glucose	2.98	none	
3.38	t	β-glucose	4.66	d	β-glucose
3.42	t	α-glucose	2.5	t	2-oxoglutarate
1.3	none		4.34	none	
			1.74	none	

Table 14: Chemical shifts responsible for high scores and correlating metabolites. PLS-DA - All human plasma (without Ctrl-078) – CPMG

(s=singlet, d=doublet, dd=doublet of doublet, t=triplet, q=quartet, m=complex multiplet)

5.1.2 Analysis of human plasma spectra (carotid v femoral) – CPMG sequence

A PCA model was produced for all the spectra obtained from analysing human (carotid and femoral endarterectomy patients) plasma using CPMG sequence. The goodness of fit R^2X(cum) was 0.777. The predictive ability Q^2(cum) was 0.264. The difference between R^2X and Q^2 suggested that there were either too much noise or many outliers affecting the signals. In the initial run of data 11 components were detected, and there was no obvious separation between the carotid and femoral samples (figure 51).

This finding was also repeated in the PLS-DA model with no component detected to suggest groups discrimination. An OPLS-DA model was then produced and only one forced component was detected. This was a very weak model with small R^2 value and negative Q^2 value (R^2X = 0.103, R^2Y = 0.302, Q^2 = -0.0635). However, a slight degree of separation was noticed in this model.

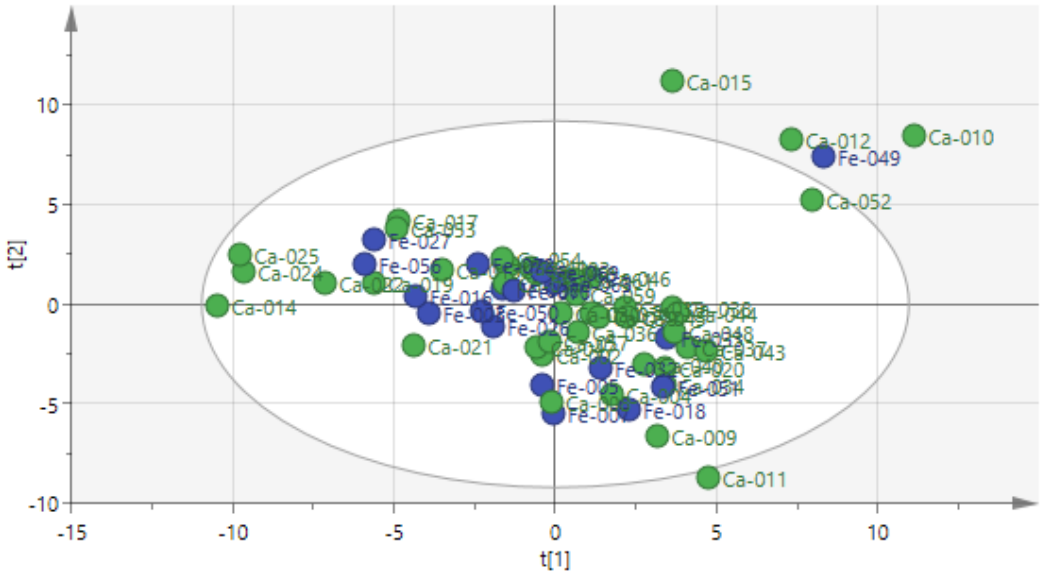

Figure 51: Score scatter of the PCA model - (carotid v femoral) plasma - CPMG

From figure 51, 5 outliers (Ca-010, Ca-011, Ca-012, Ca-015, Fe-049) could be identified in the score scatter of this PCA model. Analysing each spectrum and correlating patient's data, it was not possible to explain this behaviour. Although it was noticed that plasma samples from the first 4 outliers were processed within a short period of each other. This did not however affect other samples processed around the same time.

A second PCA model was then produced excluding those outliers. 9 components were detected in this model (R^2X = 0.715 and Q^2 = 0.178). Based on this second model, there was a degree of separation and clustering between the two groups. Although the PLS-DA model did not strengthen this separation, the OPLS-DA model detected 2 forced components and it was certainly stronger (R^2X = 0.199, R^2Y = 0.526, Q^2 = 0.0214). The separation between the two groups was more obvious too (figure 52).

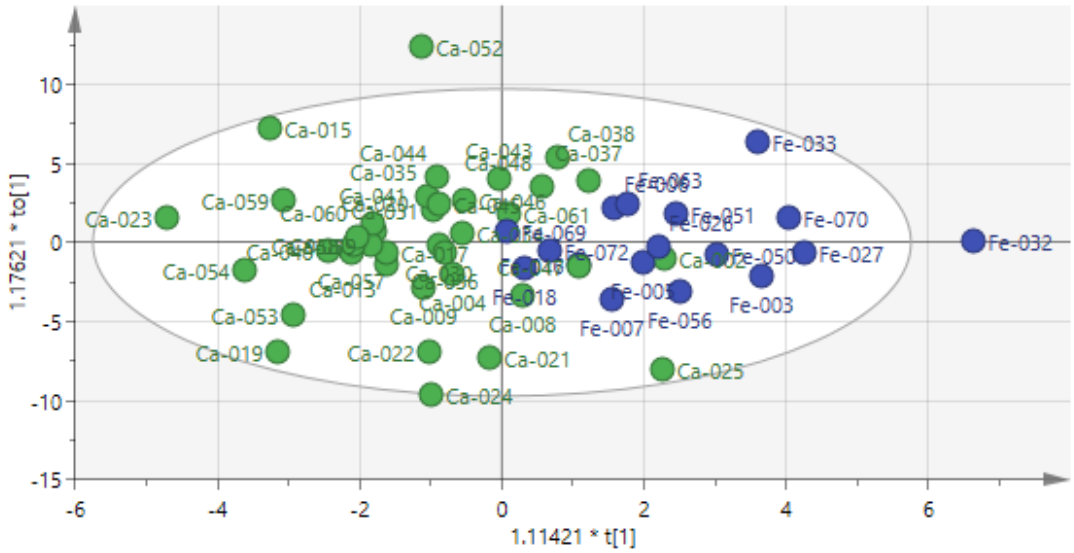

Figure 52: Score scatter of the OPLS- DA model - (carotid v femoral) plasma -(without samples Ca-010, Ca-011, Ca-012, Ca-015, Fe-049) - CPMG

Analysing the matching loading column plot, there were 6 signals affecting the carotid group that potentially could be causing the discrimination noted in the OPLS-DA model. Bins in the range 4.22-4.34 have complex multiplet signals are consistent with either lipids or threonine. The carotid group had stronger signals at 4.22, 4.26, 4.3 and 4.22 ppm. Another stronger signal in the carotid group was noticed at 3.87 ppm (doublet of doublets) which is consistent with β-glucose.

The only other signal which was stronger in the carotid group was at 1.5 ppm. This was a weak doublet signal and the closest metabolite to it was alanine.

No dominant signals (with 95% confidence intervals) were observed in the femoral group in this model.

5.1.3 Analysis of all human plasma spectra – DOSY sequence

5.1.3.1 PCA model

A PCA model was produced for all the spectra obtained from analysing human plasma using DOSY sequence. A stronger model was observed compared to the CPMG sequence experiment. The goodness of fit R^2X(cum) was 0.79 and the predictive ability Q^2(cum) was 0.39. The difference between R^2X and Q^2 was still more than 0.3 and it suggested that there were either too much noise or many outliers affecting the signals. In the initial run of data 12 components were detected with no clear separation between the groups.

Sample Ctrl-078 was again noted to have a large ethanol signal compared to the rest, which suggests a high alcohol consumption prior to sampling. Sample Ctrl-078 was removed from this analysis. A second PCA model was then produced, the goodness of fit R^2X(cum) was 0.721 and the predictive ability Q^2(cum) was 0.4. 9 components were detected in this model. The score scatter of this model did not show a clear separation of the groups, although some clustering patterns were observed (figure 53).

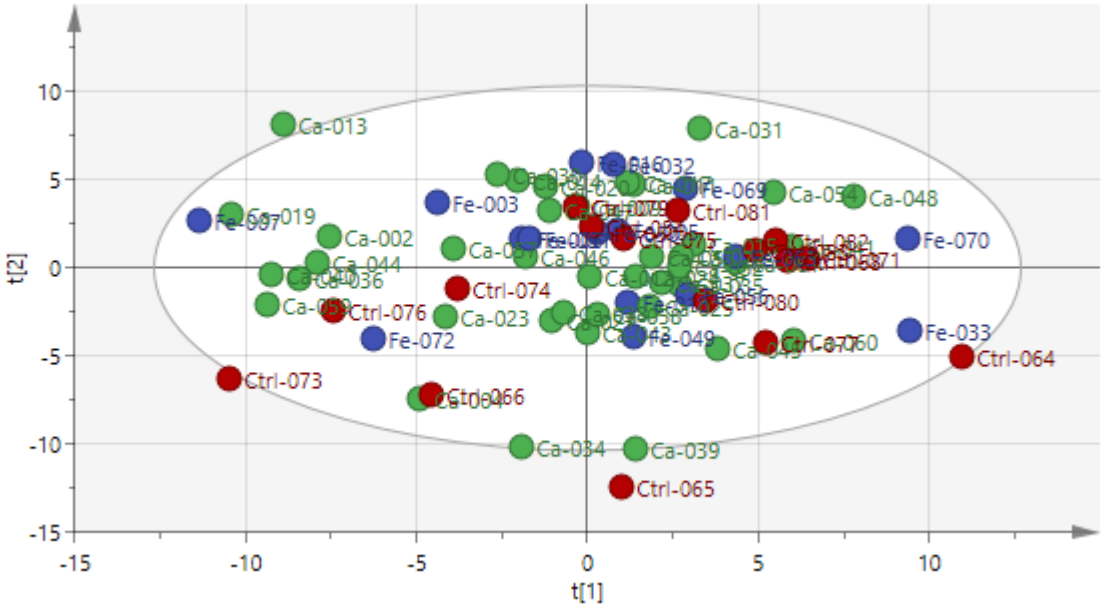

Figure 53: Score scatter of the PCA model - All human plasma (without Ctrl-078) – DOSY

Only 1 outlier (Ctrl-065) could be identified in this scatter, which was also an outlier in the PCA model of the CPMG sequence experiment. Analysing the spectrum and correlating patient's data did not explain this behaviour.

A third PCA model was then produced excluding Ctrl-065. The goodness of fit R^2X(cum) was 0.787 and the predictive ability Q^2(cum) was 0.371. 12 components were detected in this model with a slight separation between the groups noted on the score scatter (figure 54).

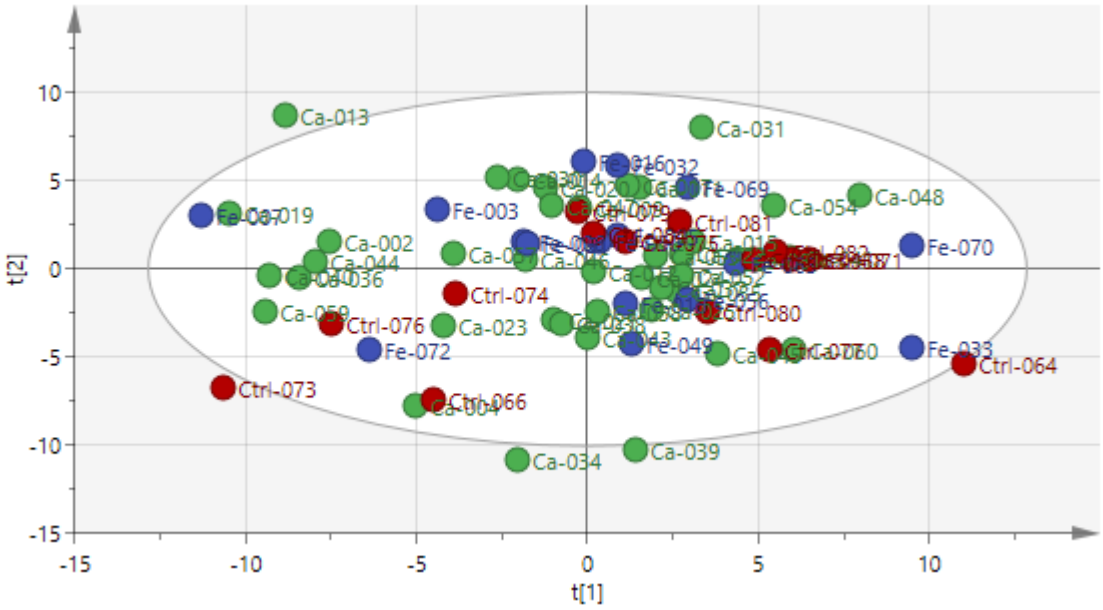

Figure 54: Score scatter of the PCA model - All human plasma (without Ctrl-078 and Ctrl-065) - DOSY

5.1.3.2 PLS-DA and OPLS-DA models

A PLS-DA model was produced for all the spectra obtained from analysing human plasma using DOSY sequence. This did not detect any components and an OPLS-DA model was then produced. This forced 2 components. The goodness of fit R^2X(cum) was 0.429 and R^2Y(cum) was 0.374. The predictive ability Q^2(cum) was 0.0986. Similar to the PCA model, sample Ctrl-078 had a high ethanol signal and was removed from the experiment.

A second PLS-DA model was then produced excluding sample Ctrl-078. This too did not detect any components and an OPLS-DA model was produced which also forced 2 components. The goodness of fit R^2X(cum) was 0.429 and R^2Y(cum) was 0.382. The predictive ability Q^2(cum) was 0.112.

A third PLS-DA model was produced excluding Ctrl-078, as this was still the only obvious outlier. This was a better model than the first two versions. only 1

component was detected, and a slightly clearer separation and clustering pattern was witnessed. The goodness of fit R^2X(cum) was 0.165 and R^2Y(cum) was 0.179. The predictive ability Q^2(cum) was 0.0475 (figure 55).

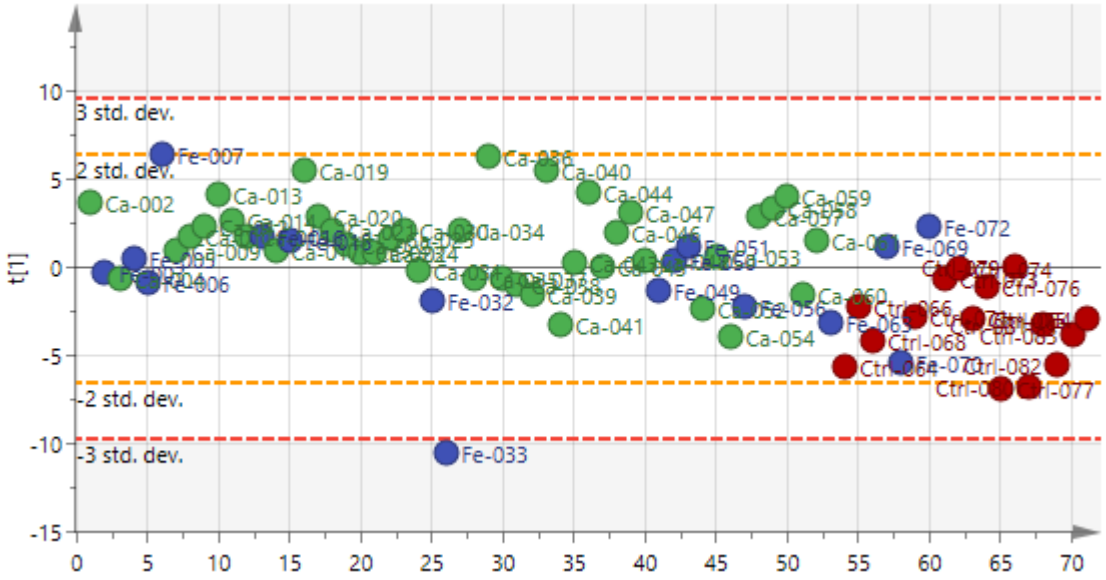

Figure 55: Score scatter of the PLS-DA model - All human plasma (without Ctrl-078 and Ctrl-065) - DOSY

The companion OPLS-DA model did show similar results, with 2 forced components detected in a stronger model ($R^2X = 0.495$, $R^2Y = 0.497$, $Q^2 = 0.108$). The separation between the two groups was more obvious too (figure 56). Observing the pattern of separation, it was evident that direct comparison between each two groups separately was more informative than all the three together.

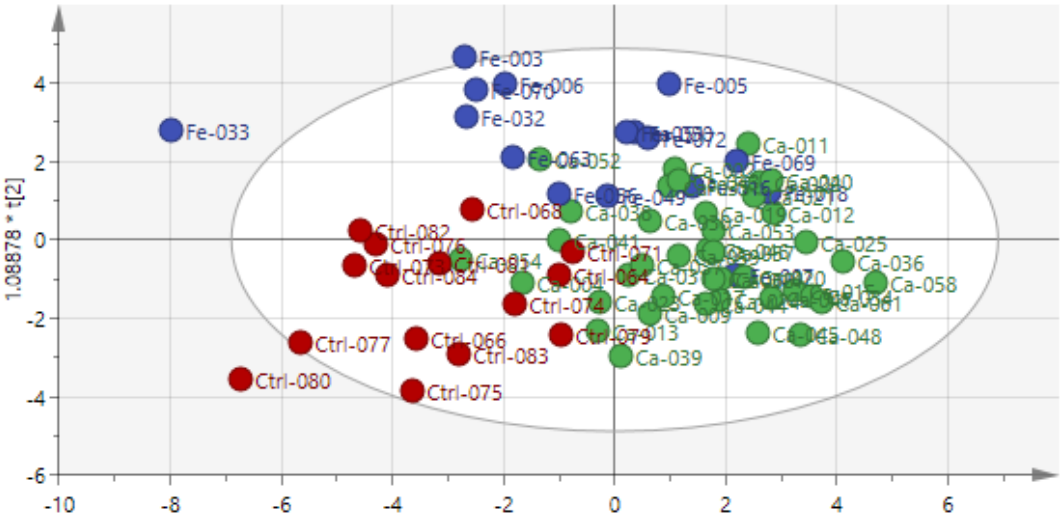

Figure 56: Score scatter of the OPLS-DA model - All human plasma (without Ctrl-078 and Ctrl-065) - DOSY

5.1.4 Analysis of human plasma spectra (carotid v control) – DOSY sequence

A PCA model was produced for all the spectra obtained from analysing human (carotid endarterectomy and control patients) plasma using DOSY sequence. The goodness of fit R^2X(cum) was 0.766. The predictive ability Q^2(cum) was 0.34. The difference between R^2X and Q^2 suggested that there were either too much noise or many outliers affecting the signals. 10 components were detected (figure 57), and there was a degree of separation between the carotid and control samples.

This separation was much clearer in the PLS-DA model which was subsequently produced (R^2X = 0.321, R^2Y = 0.639, Q^2 = 0.339), with 2 components detected (figure 58).

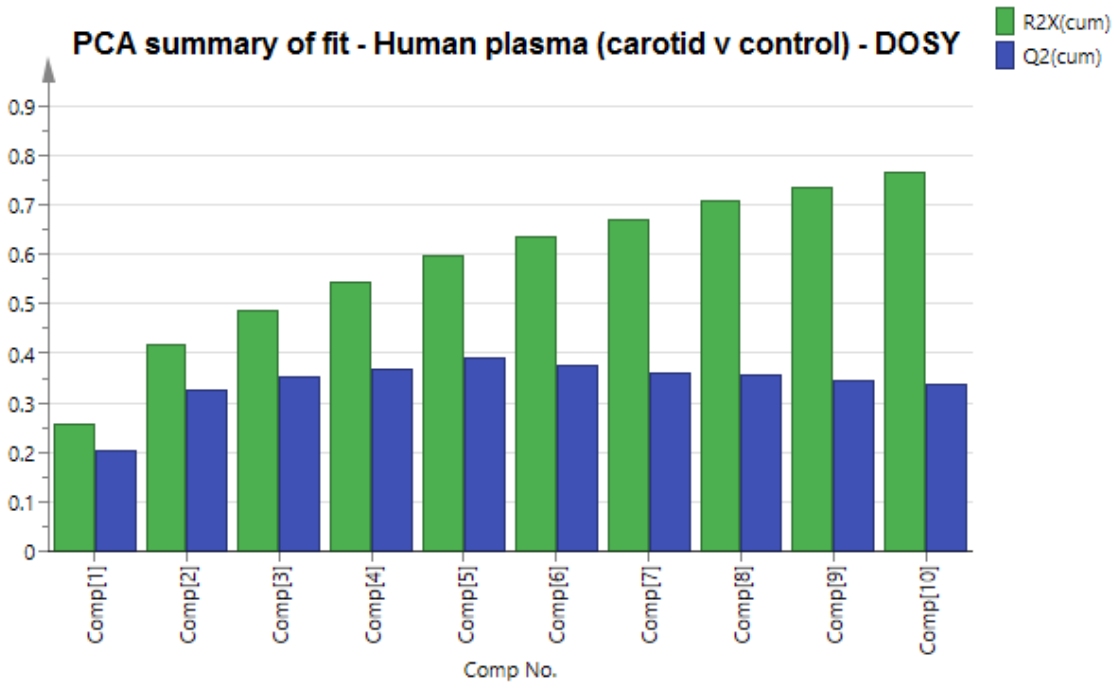

Figure 57: PCA model – Human plasma (carotid v control) - DOSY

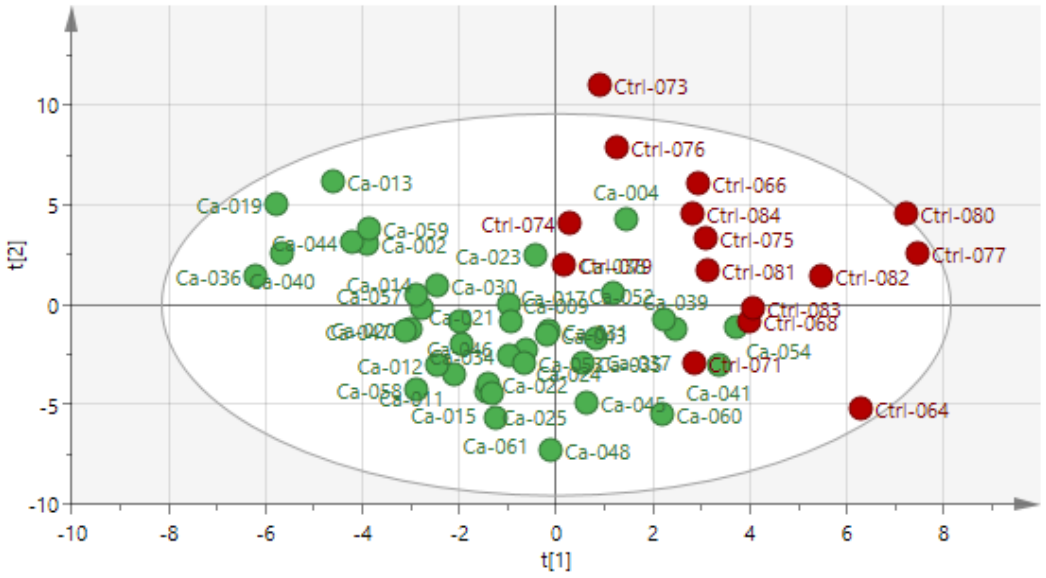

Figure 58: Score scatter of the PLS-DA model - Human plasma (carotid v control) - DOSY

The matching loading column plots of this model produced 32 signals potentially causing the discrimination between the carotid endarterectomy and the control groups (figures 59).

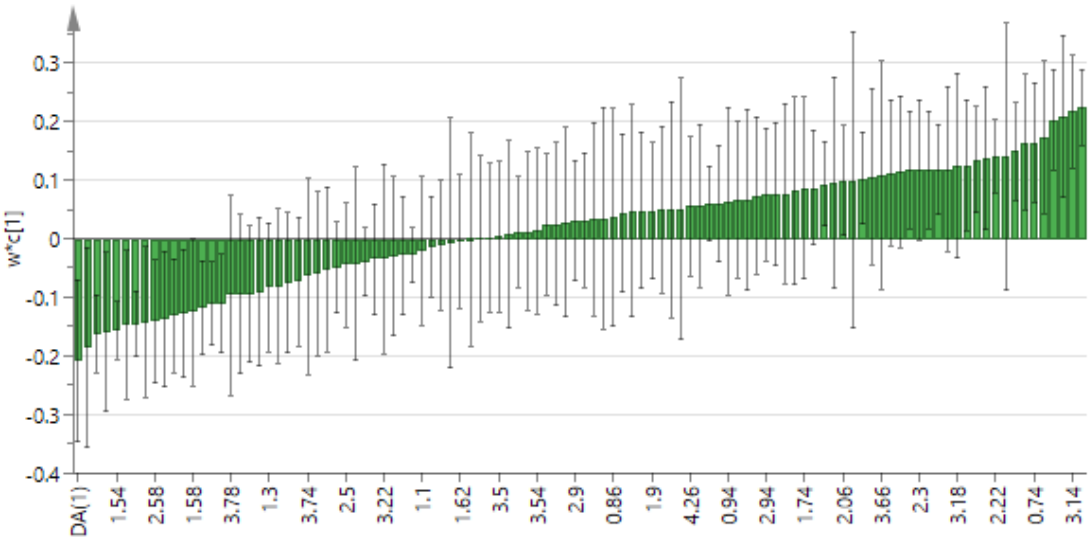

Figure 59: Loading column of the PLS-DA model – Human plasma (carotid v control) - DOSY

Table 15 summarises the chemical shifts (bins) from strongest to weakest that could be responsible for differentiating the groups, and their correlating plasma metabolites responsible for the high scores (95% Confidence Intervals) (Nicholson, et al., 1995).

It was noticeable from the table of chemical shifts in this model that lipid metabolites had stronger signals in the study group, with mainly LDL (low-density lipoprotein) and VLDL (very low-density lipoprotein) affecting their behaviour within the magnetic field. The only other two metabolites that were potentially affecting the study samples were 3-hydroxybutyrate (4.18 ppm - complex multiplet) and the amino acid isoleucine (1.94 ppm - complex multiplet).

The control group however had stronger signals of amino acids predominantly. Histidine (3.14 ppm - doublet) was the α-amino acid with the strongest effect on the control samples. Bins in the range 3.58-3.62 ppm have a doublet spectral signal are consistent with valine or threonine. Aspartate (2.62-2.66 ppm - doublet) is another α-amino acid with a stronger signal in the control samples. α-glucose was also stronger in the control group, although this could be due to the patients not being fasted ta the time of blood sampling.

Study			Control		
Bin	Signal multiplicity	Molecule	Bin	Signal multiplicity	Molecule
2.54	none		5.18	d	α-glucose
1.5	m	Lipid (mainly VLDL)	3.14	dd	Histidine
4.18	m	3-hydroxybutyrate	2.26	none	
1.54	m	Lipid (mainly VLDL)	3.42	none	
1.94	m	Isoleucine	0.74	m	Cholesterol
1.22	m	Lipid (mainly LDL)	3.38	none	
1.46	m	Lipid (mainly VLDL)	0.78	m	Cholesterol
2.58	none		2.22	none	
0.82	t	Lipid (mainly LDL)	5.14	d	α-glucose
2.42	none		1.14	none	
1.18	m	Lipid	2.66	dd	Aspartate
1.58	m	Lipid (mainly VLDL)	3.62	d	Valine Threonine
3.98	none		2.86	none	
1.26	m	Lipid	4.06	m	Glyceryl of lipids
3.06	none		3.58	d	Valine Threonine
			2.06	none	
			2.62	dd	Aspartate

Table 15: Chemical shifts responsible for high scores and correlating metabolites. PLS-DA - Human plasma (carotid v control) – DOSY

(s=singlet, d=doublet, dd=doublet of doublet, t=triplet, q=quartet, m=complex multiplet)

5.1.5 Analysis of human plasma spectra (carotid v femoral) – DOSY sequence

A PCA model was produced for all the spectra obtained from analysing human (carotid and femoral endarterectomy patients) plasma using DOSY sequence. The goodness of fit R^2X(cum) was 0.751. The predictive ability Q^2(cum) was 0.322. The difference between R^2X and Q^2 suggested that there were either too much noise or many outliers affecting the signals. 10 components were detected, and there was a slight separation between the carotid and control samples (figure 60).

This separation was not produced in the subsequent PLS-DA model, and no components were detected. The OPLS-DA model for this experiment did force 2 components and a separation became more obvious between the two groups (figure 61). This was a weak model though, with R^2X value of 0.284, R^2Y value of 0.479, and a negative Q^2 value of -0.0266.

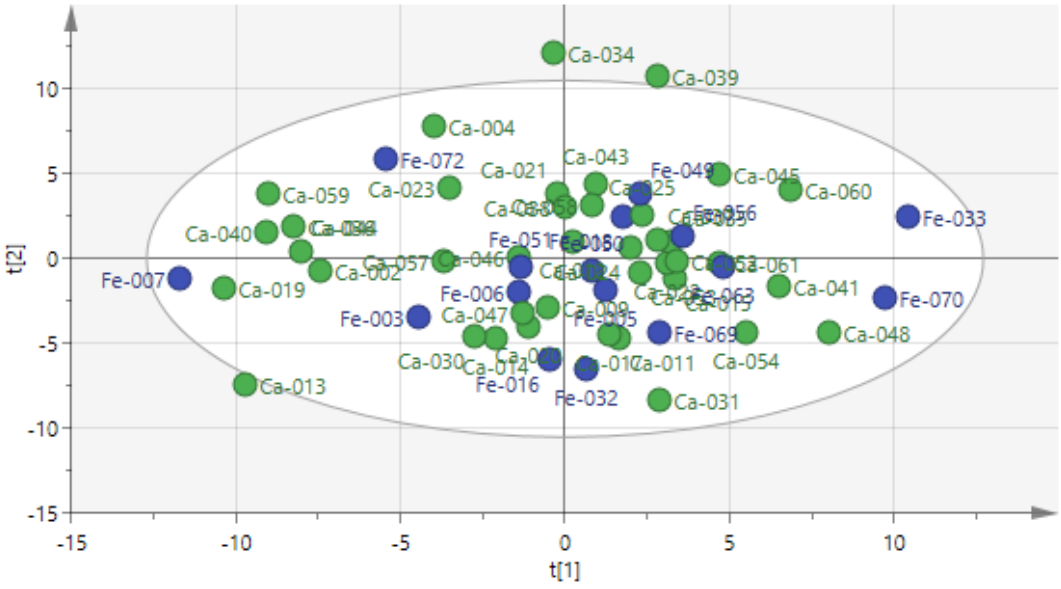

Figure 60: Score scatter of the PCA model - Human plasma (carotid v femoral) - DOSY

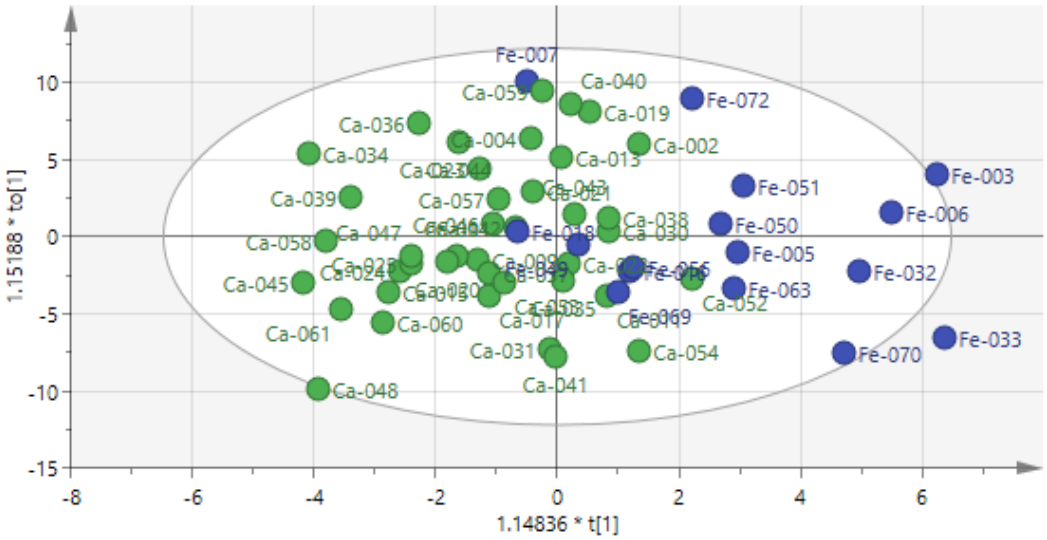

Figure 61: Score scatter of the OPLS-DA model - Human plasma (carotid v femoral) - DOSY

Detailed analysis of the matching loading column plot did not reveal many signals that could have affected the two groups, with only three signals that were thought to be affecting the possible discrimination between them. Histidine (3.14 ppm - doublet) was stronger in the femoral group. While a large lipid signal was primarily affecting the carotid samples (range 1.98-2.02 ppm - complex multiplet).

5.2 Discussion

Human plasma (carotid, femoral and control) experiments in this study have shown mixed results, some were challenging to interpret, and it was difficult to generate a model that could confidently establish certain metabolites as atherosclerotic biomarkers.

Similarity of some findings between these experiments and their matches in the animal studies were observed. DOSY sequence experiments had almost identical results to those of the animal plasma samples. The effect of strong lipid signals on the spectra was noticeable and they might have covered other signals that could represent a significant biomarker.

Taurine signal had a stronger effect on the study group (carotid and femoral) in the CPMG experiment. This was contradicting the findings in the animal models, whereas taurine was stronger in the control groups (plasma and solid tissue).

2-oxoglutarate was another signal noticed to be stronger in the control group (CPMG experiment), in both animal and human plasma models of this study. There has been no clinical research into the specific role of 2-oxoglutarate in atherosclerosis, and whether it has a protective function.

Choline was noticed to be present in the human plasma experiment as a stronger signal in the control group. Although choline intake was not found to be linked to cardiovascular disease, the long-term consumption may have a preventative role by reducing inflammation and other risk factors (Rajaie & Esmaillzadeh, 2011).

Chapter 6: NMR analysis of plaques

Human samples

This chapter will describe High Resolution Magic Angle Spinning ^{1}H-NMR spectroscopy analysis of sections of plaque samples obtained from 56 patients using CPMG and 1D NOESY pulse sequences. Samples were prepared as per Section 2.4, 2.4.1 and 2.2.4. Data were collected as explained in Section 2.3.2. Spectra processing was done as per Section 2.5. Statistical analysis was done as per Section 2.6.

Each plaque section was given two letters followed by a number and a letter for identification purpose. The letters were: (Ca) for patients with symptomatic carotid disease and (Fe) for patients with symptomatic femoral disease. The number given to each sample was according to their order of recruitment. The final letter was to echo the letter given to the section during sample preparation.

6.1 Results

Out of 64 patients recruited for this study, 6 patients (3 carotid – 3 femoral) had their operation cancelled, 1 carotid plaque sample was lost in theatre prior to collection, and 1 femoral plaque was excluded from the study as sample was too fragmented to section and process. Sections from 56 plaque samples were analysed. Total number of sections was 173 (111 carotid vs 62 femoral). Patients' demographics, relevant past medical history and current medications are summarised in table 16. More detailed statistical analysis of patients' data will be discussed throughout this chapter wherever found relevant.

		Carotid	Femoral	P-value	
Number of patients		40	16	0.0013	
Number of sections		111	62	0.0002	
Male/Female		26/14	13/3	0.0578	0.0124
Age (years)	Range	44-91	46-87		
	Mean	70.8 ± 10.9	68.9 ± 9.8	0.5594	
	Median	73	69		
BMI (kg.m^{-2})	Range	20 - 43	16.8 - 39		
	Mean	27.5 ± 3.9	26.4 ± 5.7	0.4296	
	Median	28.5	26		
Smoke	Current	14	7		
	Ex	18	7		
	Never	8	2		
Alcohol (unit)	Range	0-75	0-65		
	Mean	12.6 ± 13.1	19.4 ± 15.3		
	Median	10	14.5		
Hypertension	Treated	23	10		
	Untreated	3	1		
Diabetes Mellitus	Diet	4	0		
	Oral	4	0		
	Insulin	2	0		
hyperlipidaemia		10	6		
Antiplatelet therapy		36	15		
Statins		36	13		

Table 16: Patients demographics and medical background – NMR plaque study

6.1.1 Analysis of atherosclerotic carotid and femoral plaques – CPMG sequence

6.1.1.1 PCA model

A PCA model was produced for all the spectra obtained from the plaques using CPMG sequence. A strong model was demonstrated in this experiment with 16 components detected. The goodness of fit R^2X(cum) was 0.769. The predictive ability Q^2(cum) was 0.264. The score scatter of this model showed a clear separation between the carotid and femoral plaque. Samples Ca-036-E, Ca009-E and Ca-060-G were outliers with possible effect on the separation in this model (figure 62).

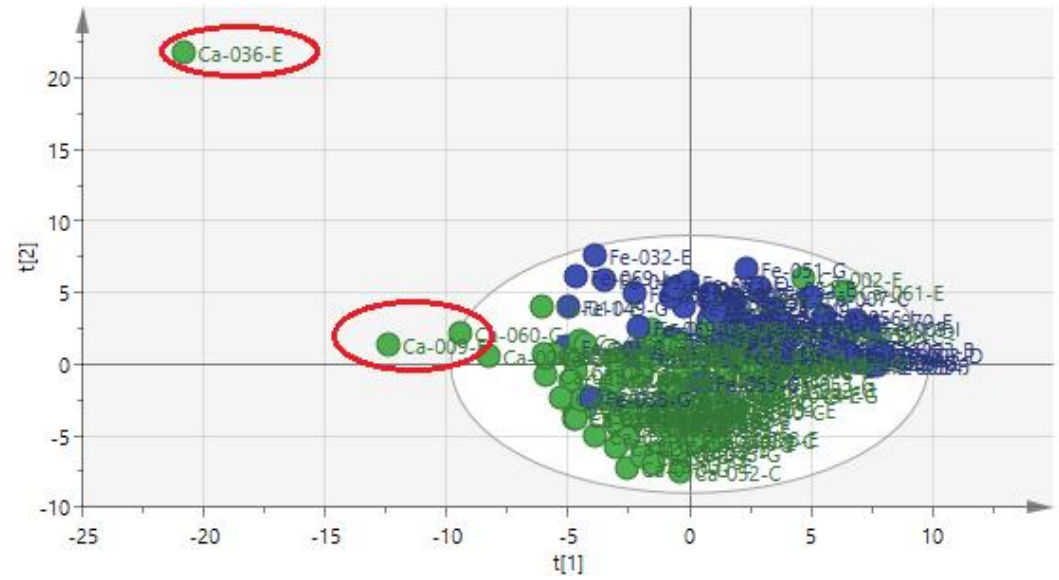

Figure 62: Score scatter of the PCA model - carotid v femoral plaques - CPMG

Those outliers were excluded and a second PCA model was produced. An improved model was demonstrated in with 16 components detected.

The goodness of fit R^2X(cum) was 0.745. The predictive ability Q^2(cum) was 0.341. The score scatter of this model continued to show a clear separation between the carotid and femoral plaque (figure 63).

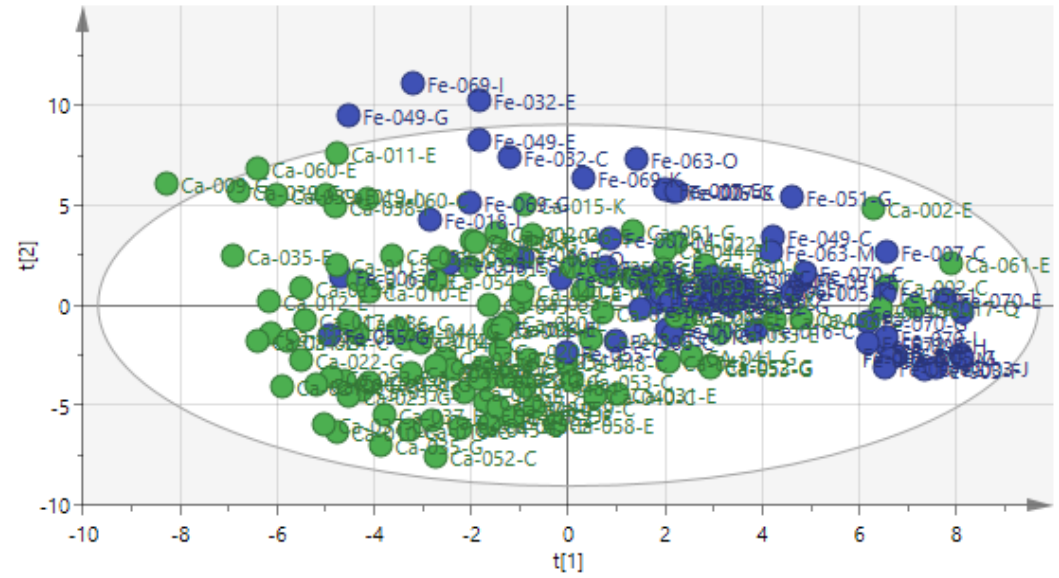

Figure 63: Score scatter of the PCA model - carotid v femoral plaques (excluding the outliers) - CPMG

6.1.1.2 PLS-DA and OPLS-DA models

After excluding the same outliers (Ca-036-E, Ca009-E and Ca-060-G, a PLS-DA model was produced for all the spectra obtained from analysing the plaques using CPMG sequence. 4 components were detected in this model. The goodness of fit R^2X(cum) was 0.347 and R^2Y(cum) was 0.828. The predictive ability Q^2(cum) was 0.668. A clear separation was observed between the two groups (figure 64).

An OPLS-DA model for this experiment showed similar observations, with no additional information to further identify the spectral signals which were potentially affecting group separation.

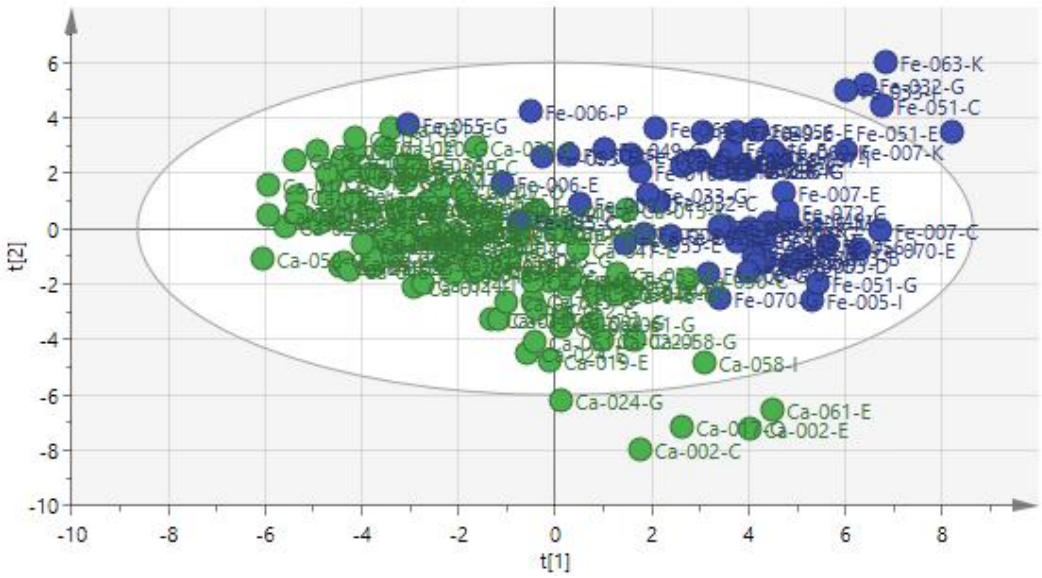

Figure 64: Score scatter of the PLS-DA model - carotid v femoral plaques (excluding the outliers) - CPMG

The matching loading column plots of these models produced 43 signals potentially causing the discrimination between the carotid and femoral groups (figure 65). Table 17 summarises the chemical shifts (bins) from strongest to weakest that could be responsible for differentiating the groups, and their

correlating plasma metabolites responsible for the high scores (95% Confidence Intervals) (Nicholson, et al., 1995).

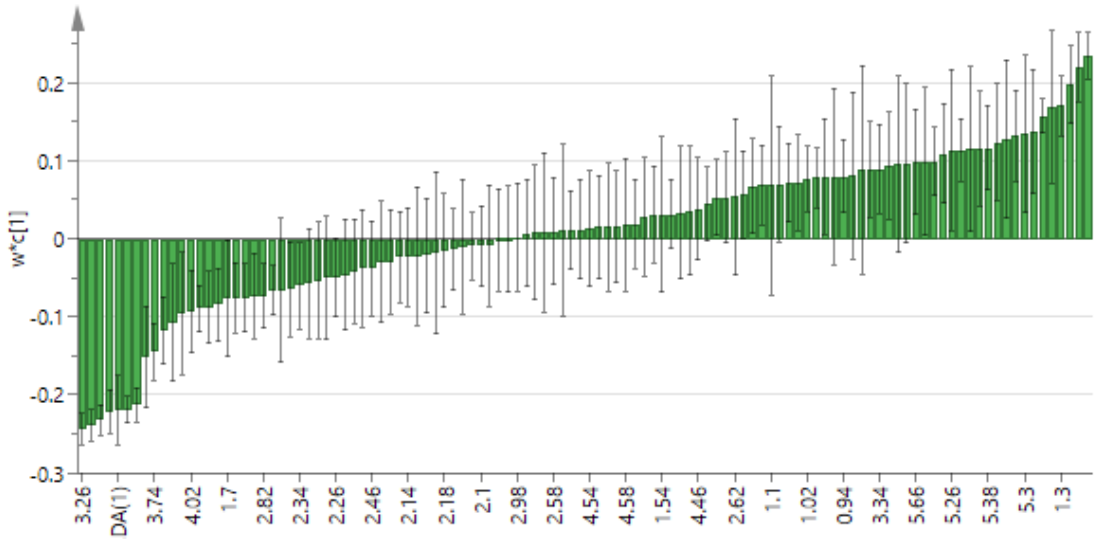

Figure 65: Loading column of the PLS-DA model - carotid v femoral plaques (excluding the outliers) – CPMG

Carotid plaques			Femoral plaques		
Bin	Signal multiplicity	Molecule	Bin	Signal multiplicity	Molecule
3.26	t	Taurine	1.38	m	Lactate
3.94	dd	Tyrosine	1.34	m	Lactate
3.66	m/t	Choline Glutamine	1.3	m	Lactate
3.9	dd	β-glucose	1.42	m	Lactate
3.98	dd	Tyrosine	0.98	m	Lipid
3.7	m	α-glucose	5.58	none	
3.22	none		5.3	m	Unsaturated lipid
3.74	m	α-glucose	5.42	none	
3.62	m/t	Choline Glutamine	5.54	none	
3.18	none		5.18	m/d	Glyceryl of lipids α-glucose
3.46	m	Proline	5.38	none	
4.02	dd	Tyrosine	5.46	none	
4.38	none		5.22	m/d	Glyceryl of lipids α-glucose
4.3	none		5.62	none	
4.34	none		5.26	M	Unsaturated lipid
1.7	none		5.5	none	
2.86	dd	Asparagine	1.26	m	Lipid
2.3	m	3-hydroxybutyrate	5.34	none	
3.42	none		5.66	none	
3.82	m	α-glucose	1.18	m	Lipid
3.86	m	α-glucose	3.34	none	
3.3	none				

Table 17: Chemical shifts responsible for high scores and correlating metabolites. PLS-DA - carotid v femoral plaques – CPMG

(s=singlet, d=doublet, dd=doublet of doublet, t=triplet, q=quartet, m=complex multiplet)

The strongest signal which possibly affected the carotid plaque samples' behaviour in the magnetic field was a triplet at 3.26 ppm. This signal corresponds to taurine. Bins in the range 3.94-3.98 with a doublet of doublets signal are consistent with tyrosine, which is an amino acid used in protein biosynthesis. This was also a dominant signal in the carotid group. In addition, the carotid samples

were affected by proline (3.46 ppm - complex multiplet) and asparagine (2.86 ppm - doublet of doublets).

Some of the signals were overlapping which made it difficult to establish which metabolite was causing the shift. Bins in the range 3.62-3.66 ppm have a complex multiplet signal are consistent with choline. However, when the area is dominated by a triplet signal it echoes glutamine. These bins were stronger in the carotid group, although the signals kept altering between the two metabolites characteristics, and it was difficult to determine which was causing the stronger effect.

The femoral group was predominantly affected by signals in the bins range of 1.30-1.42 and 5.26-5.30. There was a large lactate signal (complex multiplet) in the range 1.30-1.42 which could be the dominant metabolite influencing the femoral samples behaviour in the magnetic field. While unsaturated lipid signals (complex multiplet) were detected in the range 5.26-5.30, which also had a stronger influence on the femoral samples. Further lipid signals (complex multiplet) affecting the femoral samples were detected at bins 0.98, 1.26 and 1.18.

6.1.2 Analysis of atherosclerotic carotid and femoral plaques – DOSY sequence

6.1.2.1 PCA model

A PCA model was produced for all the spectra obtained from the plaques using DOSY sequence. A strong model was demonstrated in this experiment with 15 components detected (figure 66). The goodness of fit R^2X(cum) was 0.831. The predictive ability Q^2(cum) was 0.511. The score scatter of this model showed a clear separation between the carotid and femoral plaque. Samples Fe-049-E and Ca-030-E were outliers with possible effect on the separation in this model (figure 67). Excluding these outliers though did not affect the model's strength or separation pattern. Those outliers were kept in the experiment and monitored for similar behaviour in the subsequent analysis.

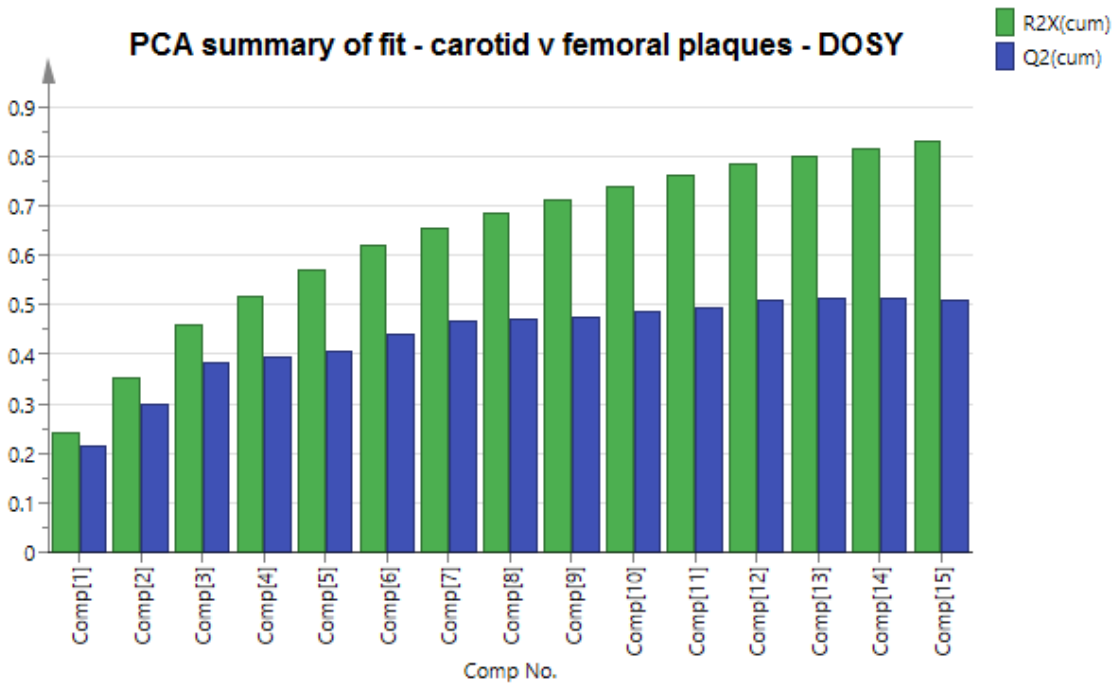

Figure 66: PCA model – carotid v femoral plaques - DOSY

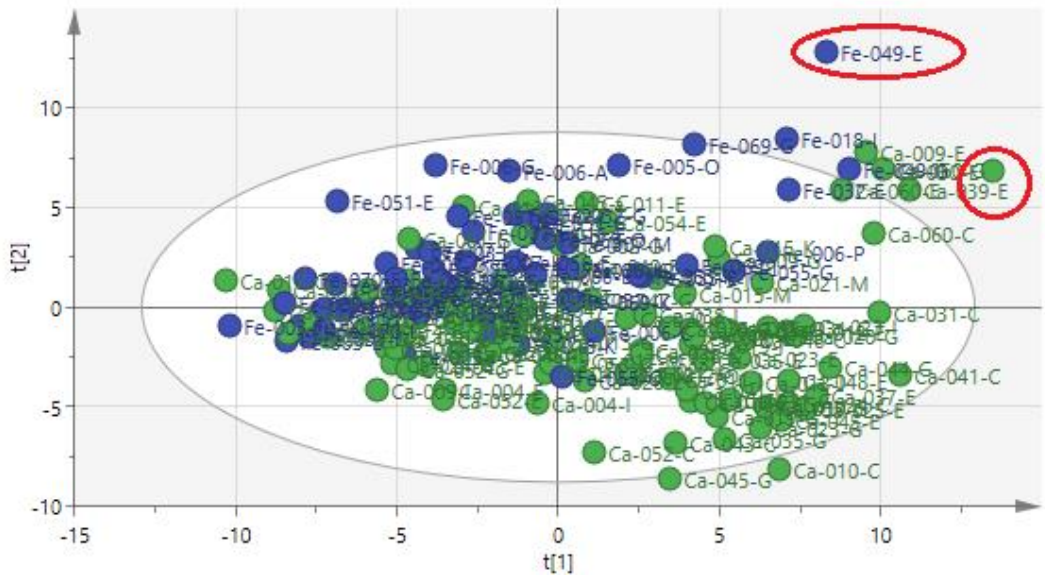

Figure 67: Score scatter of the PCA model - carotid v femoral plaques - DOSY

6.1.2.2 PLS-DA and OPLS-DA models

A PLS-DA model was produced for all the spectra obtained from analysing the plaques using DOSY sequence. 3 components were detected in this model. The goodness of fit R^2X(cum) was 0.389 and R^2Y(cum) was 0.713. The predictive ability Q^2(cum) was 0.62. A clear separation was observed between the two groups (figure 68). From the score scatter, only two samples from the femoral group were far from the other clustered samples and somehow placed closer to the carotid samples. Those two samples were belonging to the same patient Fe-055(C+G). On reviewing the medical records, this patient was the only one in the femoral endarterectomy group with an established chronic kidney disease. The plaque obtained from this patient was described by the surgeon performing the endarterectomy as “stenosed throughout with no apparent maximum point”. This may explain these samples behaviour in this model. However, a third section of this plaque (Fe-055-E) was also analysed in this experiment and it did not behave in the same way. Furthermore, excluding Fe-055-C and Fe-055-G or excluding

all the samples from patient Fe-055 did not add or affect the strength of the PLS-DA model (3 components - $R^2X(cum) = 0.39$ - $R^2Y(cum) = 0.741$ - $Q^2 = 0.658$) or the separation observed (figure 69). These samples were kept in the experiment and monitored for similar behaviour in the subsequent analysis.

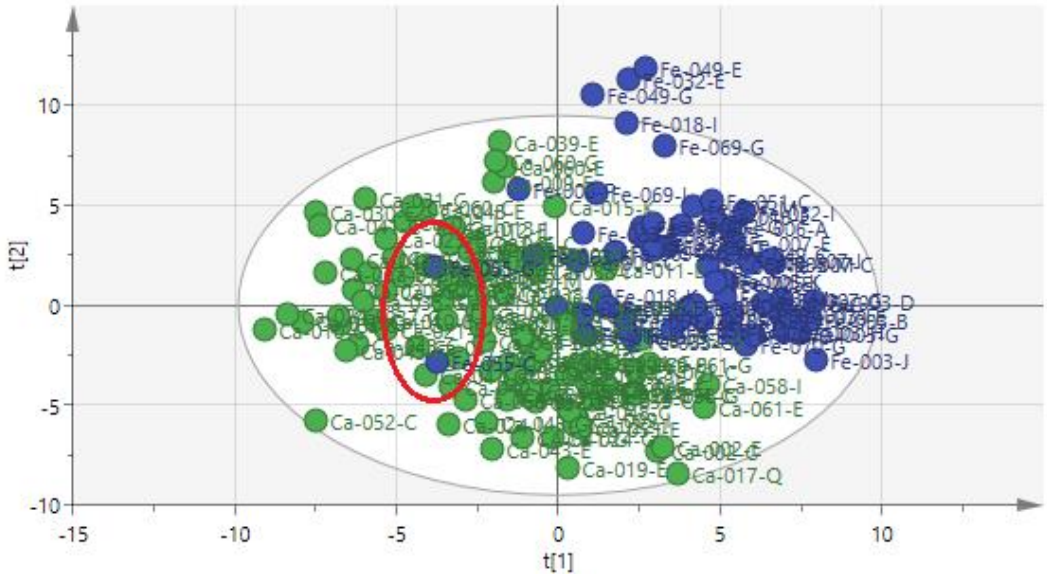

Figure 68: Score scatter of the PLS-DA model - carotid v femoral plaques - DOSY

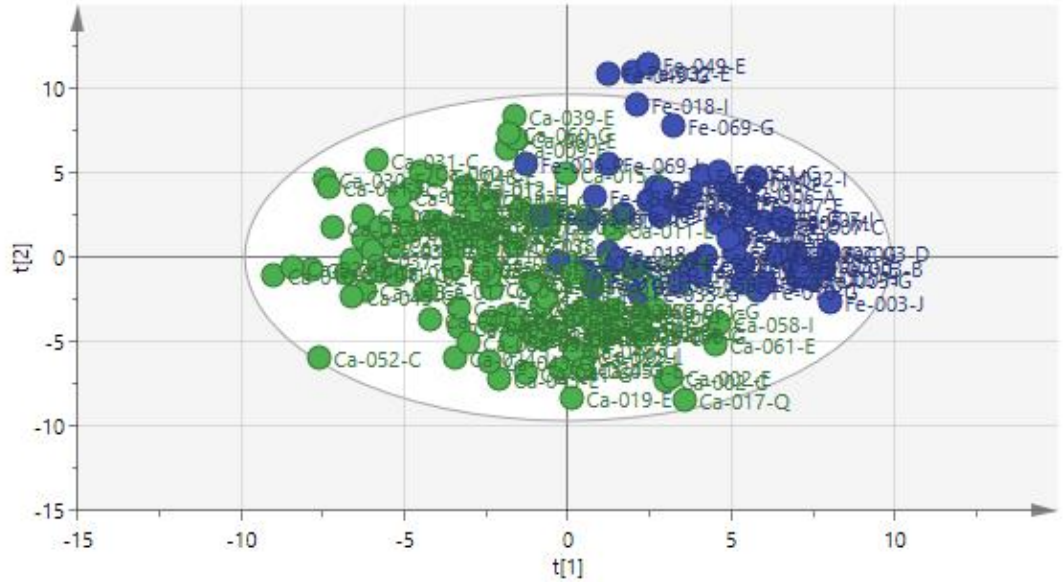

Figure 69: Score scatter of the PLS-DA model - carotid v femoral plaques (excluding patient Fe-055) - DOSY

An OPLS-DA model for this experiment showed similar observations, with no additional information to further identify the spectral signals which were potentially affecting group separation.

The matching loading column plots of these models produced 49 signals potentially causing the discrimination between the carotid and femoral samples (figure 70). Tables 18 and 19 summarise the chemical shifts (bins) from strongest to weakest that could be responsible for differentiating the groups, and their correlating plasma metabolites responsible for the high scores (95% Confidence Intervals) (Nicholson, et al., 1995).

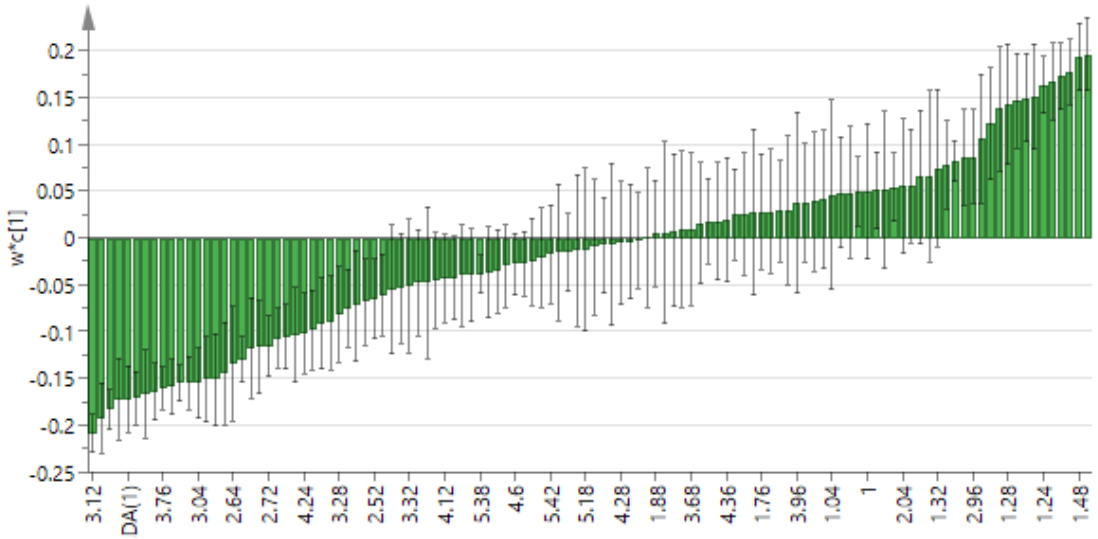

Figure 70: Loading column of the PLS-DA model - carotid v femoral plaques - DOSY

Carotid plaques					
Bin	Signal multiplicity	Molecule	Bin	Signal multiplicity	Molecule
3.12	dd	Phenylalanine Histidine	0.72	none	
3.84	none		0.56	none	
3.8	q	Alanine	2.72	d	Aspartate
0.64	none		4.16	none	
3.56	dd	Threonine α-glucose	3	none	
2.68	dd	Aspartate	0.76	none	
4.2	none		4.24	none	
3.76	q	Alanine	3.72	dd	α-glucose
3.08	none		0.52	none	
3.48	dd	Threonine α-glucose	2.6	none	
3.52	dd	Threonine α-glucose	3.28	t	Taurine
3.04	none		2.56	none	
0.6	none		4.52	d	β-glucose
0.68	none		3.4	t	Taurine
3.6	d	Threonine	2.52	none	
2.64	d	aspartate	3.24	t	Taurine
3.16	none				

Table 18: Chemical shifts responsible for high scores and correlating metabolites. PLS-DA - carotid plaques – DOSY

Femoral plaques		
Bin	Signal multiplicity	Molecule
1.52	m	Lipid (mainly VLDL)
1.48	m	Lipid (mainly VLDL)
1.2	d	3-hydroxybutyrate
2.16	m	Glutamine/Glutamate
1.24	m	Lipid (mainly LDL)
1.16	m	3-hydroxybutyrate
1.44	m	Lipid (mainly VLDL)
2.12	m	Glutamine/Glutamate
1.28	m	Lipid (mainly VLDL)
1.92	m	Isoleucine Proline Lipid
2.92	dd	Asparagine
2.8	none	
2.96	dd	Asparagine
2.2	m	Glutamine/Glutamate
1.96	m	Isoleucine Proline Lipid
1.56	m	Lipid (mainly VLDL)

Table 19: Chemical shifts responsible for high scores and correlating metabolites. PLS-DA - femoral plaques – DOSY

(s=singlet, d=doublet, dd=doublet of doublet, t=triplet, q=quartet, m=complex multiplet)

Analysing the table of chemical shifts in this model suggested that some of the signals were overlapping which made it difficult to establish which metabolite was causing the shift. The carotid endarterectomy group had stronger signals of amino acids predominantly. Bins at 3.12 with a doublet of doublets signal can be correlating to either phenylalanine or histidine. This was the strongest amino acid affecting the carotid group. Bins in the range 3.76-3.80 ppm have a quartet spectral signal are consistent with alanine. Bins in the range 3.48-3.60 ppm have a doublet of doublets spectral signal are consistent with threonine or α-glucose. These signals were stronger in the carotid group and mostly responsible for samples behaviour within the magnetic field.

Another amino acid which had stronger signal in the carotid group was aspartate (2.64-2.72 ppm - doublet of doublets). Taurine signal (3.24-3.40 - triplet) was also stronger in the carotid group, although not as dominant as it was in the CPMG sequence experiment (Section 6.1.1.2).

It was noticeable from the table of chemical shifts that lipid metabolites had stronger signals in the femoral group, with mainly LDL (low-density lipoprotein) and VLDL (very low-density lipoprotein) affecting their behaviour within the magnetic field. The other metabolites that were potentially affecting the femoral samples were 3-hydroxybutyrate (1.16 ppm - complex multiplet) and amino acids such as; glutamine/glutamate (2.12-2.2 ppm - complex multiplet) and asparagine (2.92-2.96 ppm - doublet of doublets). Bins in the range 1.92-1.96 ppm have a complex multiplet spectral signal were stronger in the femoral group. These are consistent with isoleucine, proline or lipid. Due to signals overlapping, it was difficult to establish the metabolite which was causing the shift.

6.2 Discussion

In contrast to the animal solid tissue experiment, human solid tissue experiment has shown much stronger models and clearer results. This could be purely due to the large sample size used in the human experiment. Similarities were also observed between the CPMG and DOSY sequence experiments.

The dominant lipid signals affecting the behaviour of femoral samples were repeated in both experiments. However, this was not observed in the human plasma experiment (carotid v femoral). This raises the issue of identifying solid tissue related biomarkers that are not circulating in plasma. This might also question the applicability of solid tissue NMR analysis in clinical practice.

The presence of amino acid signals in all the models of this experiment was noticed. These were mainly affecting carotid plaques, although it was challenging to detect a regular pattern of the individual amino acids.

Perhaps the most notable finding is the possible effect of taurine signals on plaques. Taurine signals have been observed in the animal (plasma and solid) as well as human plasma models in this study. Although, they have shown a much stronger effect on the carotid plaques. A finding which could be difficult to interpret considering the preventative role of taurine on cardiovascular diseases (Murakami, 2014).

Chapter 7: Other experiments

This chapter will describe other experiments carried out as part of this study.

7.1 Urine experiment

^{1}H-NMR spectroscopy analysis of urine obtained from 81 patients. Samples were prepared as per Section 2.2.3 and 2.3.1. Data were collected as explained in Section 2.3.2.

Each plasma sample was given a set of letters followed by a number for identification purpose. The letters were: (Ca) for patients with symptomatic carotid disease, (Fe) for patients with symptomatic femoral disease, and (Ctrl) for patients from the control group. The number given to each sample was according to their order of recruitment.

7.1.1 Analysis of urine samples – NOESY sequence

This experiment was run on 25 patients only. During the NMR processing and data collection it was noticed that samples were very unstable in the magnetic field. The main problem was the effect of this instability on the temperature of the NMR experiment. This was widely variable despite many attempts to re-process the samples. A large water signal was in all the examined samples which was difficult to suppress with D_2O. This was also affecting the fids obtained from the NMR and creating a lot of noise which ultimately did not allow gaining any valid results (figure 71). The concern was that these data would have not been obtained using the same methods, despite trying different techniques to control the process.

It was also not possible to identify the reason behind such a large water signal in all the samples. Although there was some variation in time of sample collection, and some patients may not have had enough starvation time.

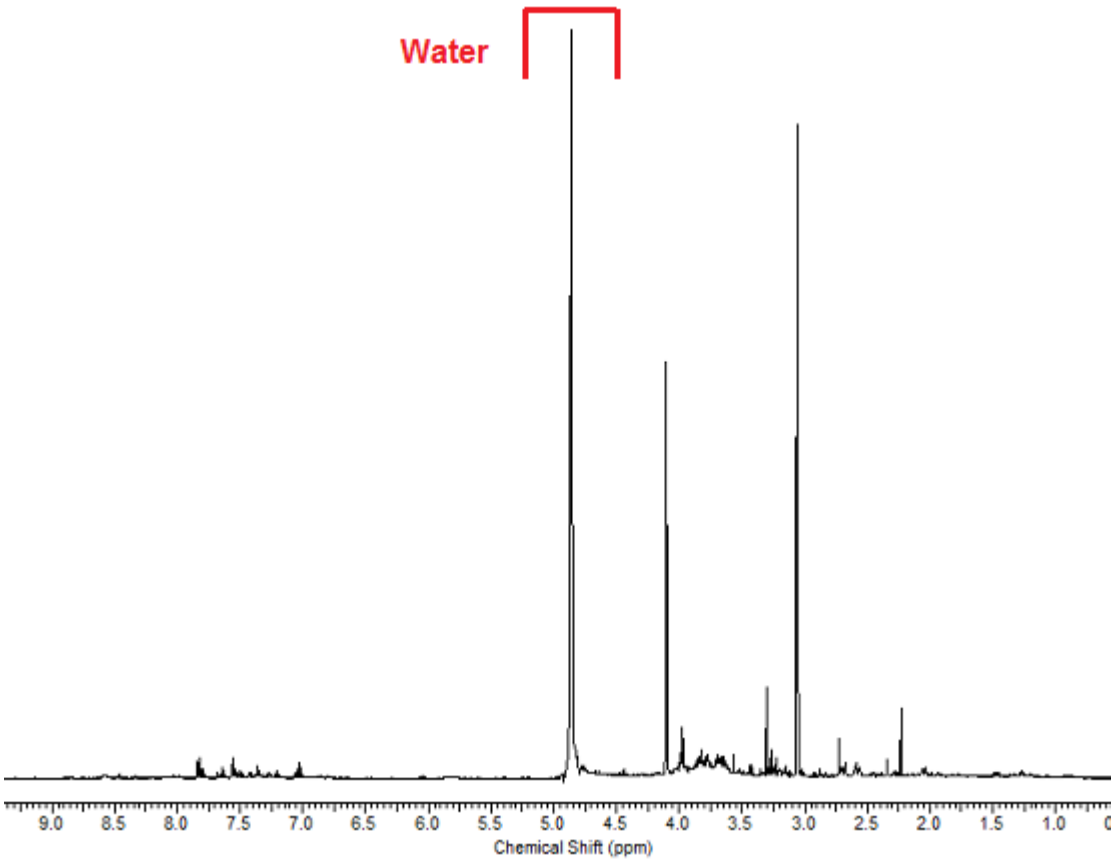

Figure 71: NMR spectra of urine sample – NOESY

After discussion with Dr Fisher regarding the problem faced while processing urine samples the experiment was discontinued, and urine data were not included in this study.

7.2 Histopathological experiment

Solid tissue samples were prepared for histopathological examination as per Section 2.2.4. Brachiocephalic artery specimens obtained from mice (6 ApoE-/- v 5 control) were included in this experiment. 216 arterial plaque sections (144 carotid v 72 femoral) obtained from 57 patients were included in this experiment. Initial histological examination was carried out on samples from 4 patients (19 slides), by Dr N West from Leeds Institute of Cancer and Pathology at the University of Leeds.

Those specimens had a significant degree of destruction, and Dr West was unable to assess them adequately for plaque stability. This could be due to a high calcium level in the specimens which affected the sectioning process, or because of the effect of formic acid used in the decalcification process.

To gain meaningful histological information from the specimens, a detailed cross examination by a second pathologist would have been necessary. Concluding this experiment therefore would have been time consuming and may not offer a confident histological examination of the specimens. The experiment was postponed, and its results will not be included in this study.

Chapter 8: Final discussion and conclusions

Identifying plaque instability in asymptomatic carotid disease was the centre of this study.

Current recommendations for surgical management of asymptomatic 50-99% carotid stenosis are guided by two factors, patient's fitness for surgical intervention and the clinical/imaging features associated with an increased risk of late stroke.

The imaging features which are specific to the plaque morphology include stenosis progression, large plaque area, large juxta-luminal black area on CT, plaque echolucency and intra-plaque haemorrhage on MRI (Naylor, et al., 2017). Despite the advances in imaging modalities and their ability to detect some features of plaque instability, full understanding of the pathophysiology of plaque instability will allow early intervention in patients with high risk of developing stroke from the unstable plaque.

To date, no serum or urine marker has been shown to predict plaque instability and the risk of future cerebrovascular events.

The work in this thesis has compared metabolic profiles of plasma and plaques from patients with symptomatic carotid stenosis undergoing endarterectomy, plasma and plaques from patients with symptomatic femoral stenosis, and plasma from patients without carotid or femoral disease (control).

We also compared plasma and solid tissues from mammalian model (mice), and further compared them to the human experiment.

This was carried out using nuclear magnetic resonance (NMR) spectroscopy to analyse the metabolic profiles of plasma and plaques, and potentially identifying predictive biomarkers of plaque instability.

8.1 NMR plasma experiments

Investigating the ability to analyse metabolic profiling in plasma using NMR spectroscopy has increased significantly in recent years. NMR studies have been focussed on coronary artery disease in general, although carotid related studies have been carried out by many researchers as explained in chapter 1.

Animal plasma experiments in this study have shown weak models and could not produce significant results that could confidently establish certain metabolites as atherosclerotic biomarkers. Sample size was certainly an important factor in this conclusion. A separate experiment was carried out alongside this study, adding data from this study to data obtained with the same methodology by A Bekhit from the University of Leeds, School of Medicine, from a different group of ApoE-/- and control mice (n=12). This experiment allowed the production of stronger models, and suggested that larger sample size perhaps would have created more reliable results.

The human plasma (carotid, femoral and control) experiments in this study as well could not confidently establish certain metabolites as atherosclerotic biomarkers. The effect of strong lipid signals on the spectra was noticeable and

they might have covered other signals that could represent a significant biomarker. However, similarities were observed between the animal and human models, and 3 metabolites (2-oxoglutarate, choline and taurine) were identified as potential biomarkers. Although there have been many studies on amino acids role in atherosclerosis development, no clinical research considered the specific role of 2-oxoglutarate and whether it has a protective function, considering its strong effect on the control subjects in both the animal and human plasma experiments.

Taurine is thought to play an important role in supressing the development of atherosclerosis and has preventative influence on cardiovascular diseases (Murakami, 2014). There have been recent NMR based studies on the effect of taurine on dyslipidaemia in mammalian models (Kim & Bang, 2017), but no similar studies investigated the effect of taurine on carotid disease. In our study taurine signals were more evident in the control group in the animal experiment.

Choline was noticed to be present in the human plasma experiment as a stronger signal in the control group. Choline effect on cardiovascular disease has always been controversial. Earlier studies advocated a preventative role, while more recent studies suggested that choline plasma metabolites are associated with a higher risk of cardiovascular disease (Guasch-Ferré, et al., 2017). Future research study may further explain the potential role of choline in carotid disease and plaque instability.

8.2 NMR solid tissue experiments

With the advances in technology, NMR based analysis of solid tissues has been increasingly investigated in recent years, although no studies tried to address the subject of this thesis. However, researchers have used the extracts of solid tissues in NMR based experiments, with no successful identification of a reliable biomarker of plaque instability.

The use of high-resolution magic angle spinning NMR spectroscopy to analyse the metabolic profiles of intact plaques is a novel approach.

Similar to the plasma experiments, animal solid tissue experiments in this study have shown weak models and could not produce significant results that could confidently establish certain metabolites as atherosclerotic biomarkers. Sample size was an important factor in this conclusion.

In contrary, human solid tissue experiments (CPMG and DOSY sequences) have shown much stronger models and clearer results. Spectra gained from these experiments were the first to be described, with no comparable studies in the literature. Metabolic profiles of plaques obtained from patients undergoing carotid and femoral endarterectomy were analysed in detail. The dominant lipid signals affecting the behaviour of femoral plaques were observed in all models. While the mixed presence of amino acid signals in all the models of this experiment was also noticed. These were mainly affecting carotid plaques, although it was challenging to detect a regular pattern and draw conclusions regarding the individual amino acids.

Perhaps the most notable finding is the possible effect of taurine on carotid plaques. Taurine signals have been observed in the animal (plasma and solid) as well as human plasma models in this study. Although, they were merely affecting the control groups. Taurine's strong influence on the metabolic profiling of carotid plaques raises the possibility of a potential biomarker of plaque instability.

In this study the maximum stenotic point was determined according to the surgeon's impression, which is essentially a subjective assessment. In addition, maximum stenosis point may not necessary reflect plaque instability. Spectra from plaque sections were treated collectively in this study, which allowed a direct comparison between carotid and femoral plaques. Spectra from individual sections were not further analysed. This is mainly due to the lack of information regarding stability/instability of each section, and therefore plaque.

Due to current clinical practice it was not feasible to obtain plaques from patients with asymptomatic carotid disease. A histological assessment of the plaques in this study would have added extra valuable information for further analysis.

Furthermore, histological assessment of the brachiocephalic samples from the mice used in this experiment will confirm the validity of the model, and may improve the weak findings of the animal experiment.

8.3 Future research

Further work is required regarding the histological examination of plaque sections. An objective assessment of the plaque instability will improve the study outcome and add a different aspect to the current results.

Moreover, being able to identify the stable sections from each plaque will allow a more detailed analysis of NMR spectra of these sections. This may further explain the findings of this study, and will help in developing future NMR based studies on the effect of taurine on atherosclerosis and plaque instability.

It will also be worth running a new experiment on the urine samples obtained during this study. Stronger NMR devices (>500 MHz) have been used in other NMR based urine studies. Following a stricter morning sample collection might make urine samples more concentrated and therefore have less water. This could tackle the problem with urine samples faced in this study.

Finally, a larger sample size mammalian study may produce stronger models and more specific results. This could be more directed towards certain metabolites detected in this study, especially amino acid pathways and their effect on plaque instability.

References

Ali, K. et al., 2012. NMR spectroscopy and chemometrics as a tool for anti-TNFα activity screening in crude extracts of grapes and other berries. *Metabolomics,* 8(6), pp. 1148 - 1161

Amarenco, P. et al., 2006. High-Dose Atorvastatin after Stroke or Transient Ischemic Attack. *N Engl J Med,* Volume 355, pp. 549 - 559

Antiplatelet Trialists' Collaboration, 1994. Collaborative overview of randomised trials of antiplatelet therapy: Prevention of death, myocardial infarction, and stroke by prolonged antiplatelet therapy in various categories of patients. *BMJ,* 308(6921), pp. 81 - 106

Aspelin, P. et al., 2003. Nephrotoxic effects in high-risk patients undergoing angiography. *N Eng J Med,* Volume 348, pp. 491 - 199

Banerjee, C. et al., 2012. Duration of diabetes and risk of ischemic stroke: the Northern Manhattan Study. *Stroke,* 43(5), pp. 1212 - 1217

Barnett, H. et al., 2000. Causes and severity of ischaemic stoke in patients with internal carotid artery stenosis. *Journal of teh American Medical Association,* Volume 283, pp. 1429 - 1436

Bartholomew, J. & Olin, J., 2006. Pathophysiology of peripheral arterial disease and risk factors for its development. *Cleve Clin J Med,* 73(4), pp. S8 -S14

Becker, F. et al., 2011. Management of critical limb ischaemia and diabetic foot. Clinical practice guidelines of the European Society for Vascular Surgery. Chapter 1: Definitions, epidemiology, clinical presentation and prognosis. *Eur J Vasc Endovasc Surg,* 42(S2), pp. S4 - S12

Beckonert, O. et al., 2010. High-resolution magic-angle-spinning NMR spectroscopy for metabolic profiling of intact tissues. *Nature Protocols,* Volume 5, pp. 1019 - 1032

Beckonert, O. et al., 2007. Metabolic profiling, metabolomic and metabonomic procedures for NMR spectroscopy of urine, plasma, serum and tissue extracts. *Nature protocols,* Volume 2, p. 2692–2703

Boja, E. & Rodriguez, H., 2012. Mass spectrometry-based targeted quantitative proteomics: Achieving sensitive and reproducible detection of proteins. *Proteomics,* Volume 12, pp. 1093 - 1110

Bond, A. & Jackson, C., 2011. The fat-fed apolipoprotein E knockout mouse brachiocephalic artery in the study of atherosclerotic plaque rupture. *J Biomed Biotechnol,* Volume 2011, p. 379069

Bosevski, M., 2014. Carotid artery disease in diabetic patients. *Pril (Makedon Akad Nauk Umet Odd Med Nauki),* 35(3), pp. 149 - 161

Bosevski, M. & Stojanovska, L., 2015. Progression of carotid-artery disease in type 2 diabetic patients: a cohort prospective study. *Vasc Health Risk Manag,* Volume 11, pp. 549 - 553

Brindle, J. et al., 2003. Rapid and noninvasive diagnosis of the presence and severity of coronary heart disease using 1H-NMR-based metabonomics. *Nat Med,* 9(4), p. 477

Brott, T. et al., 2010. Stenting versus Endarterectomy for Treatment of Carotid-Artery Stenosis. *New Engl J Med,* Volume 363, pp. 11-23

CAPRIE Steering Committee, 1996. A randomised blinded trial of clopidogrel versus aspirin in patients at risk of ischaemic events. *Lancet,* Volume 348, pp. 1329 - 1339

Carr, S. et al., 1996. Atherosclerosis plaque rupture in symptomatic carotid artery stenosis. *Journal of Vascular Surgery,* Volume 23, pp. 755 - 765

Catalano, C. et al., 2004. Infrarenal aortic and lower-extremity arterial disease: diagnostic performance of multi-detector row CT angiography. *Radiology,* Volume 231, pp. 555 - 563

Chambless, L. et al., 2002. Risk Factors for Progression of Common Carotid Atherosclerosis: The Atherosclerosis Risk in Communities Study, 1987–1998. *American Journal of Epidemiology,* Volume 155, pp. 38 - 47

Chen, X. et al., 2010. Plasma metabolomics reveals biomarkers of the atherosclerosis. *J Sep Sci,* 33(17 - 18), pp. 2776 - 2783

Claridge, T., 1999. In: *High-Resolution NMR Techniques in Organic Chemistry, 1st Edition.* Oxford, UK: Elsevier

Corsten, M., Reutelingsperger, C. & Hofstra, L., 2007. Imaging apoptosis for detecting plaque instability: rendering death a brighter facade. *Curr Opin Biotechnol,* 18(1), pp. 83 - 89

Côté, R. et al., 1995. Lack of effect of aspirin in asymptomatic patients with carotid bruits and substantial carotid narrowing. The Asymptomatic Cervical Bruit Study Group. *Ann Intern Med,* 123(9), pp. 649 - 655

Craig, A. et al., 2006. Scaling and normalization effects in NMR spectroscopic metabonomic data sets. *Anal Chem,* 78(7), pp. 2262 - 2267

Davies, M. et al., 1993. Risk of thrombosis in human atherosclerotic plaque: role of extracellular lipid, macrophages and smooth muscle cell content. *Br Heart J,* Volume 69, pp. 377 - 381

Davies, M. & Thomas, A., 1985. Plaque fissuring: the cause of acute myocardial infarction, sudden ischaemic death, and crescendo angina. *Br Heart J,* Volume 53, pp. 363 - 373

De Feijter, P. & Nieman, K., 2011. Failure of CT coronary imaging to identify plaque erosion: a resetting of expectations. *Eur Heart J,* 32(22), pp. 2736 - 2738

de Weerd, M. et al., 2014. Prediction of asymptomatic carotid artery stenosis in the general population: identification of high-risk groups. *Stroke,* 45(8), pp. 2366 - 2371

Demarin, V., Lisak, M., Morovic, S. & Cengic, T., 2010. Low high-density lipoprotein cholesterol as the possible risk factor for stroke. *Acta Clinica Croatica,* 49(4), pp. 429 - 439

Derome, A., 1987. In: *Modern NMR Techniques for Chemistry Research, 1st Edition.* Oxford, UK: Pergamon Press

DiCorleto, P. & Chisolm, G. 3., 1986. Participation of the endothelium in the development of the atherosclerosis plaque. *Prog Lipid Res,* 25(1-4), pp. 365 - 374

Diener, H. et al., 2004. Aspirin and clopidogrel compared with clopidogrel alone after recent ischaemic stroke or transient ischaemic attack in high-risk patients (MATCH): randomised, double-blind, placebo-controlled trial. *Lancet,* 364(9431), pp. 331 - 337

Diener, H. et al., 1996. European Stroke Prevention Study. 2. Dipyridamole and acetylsalicylic acid in the secondary prevention of stroke. *J Neurol Sci,* 143(1-2), pp. 1 - 13

Doll, R., Petto, R., Boreham, J. & Sutherland, I., 2004. Mortality in relation to smoking: 50 years' observations on male British doctors. *BMJ,* 328(7455), p. 1519

Dunn, W. et al., 2007. Serum metabolomics reveals many novel metabolic markers of heart failure, including pseudouridine and 2-oxoglutarate. *Metabolomics,* 3(4), pp. 416 - 426

Edwards, J., 2009. In: *Principles of NMR.* s.l.:Process NMR Associates LLC

Emwas, A., 2015. The strengths and weaknesses of NMR spectroscopy and mass spectrometry with particular focus on metabolomics research. *Methods Mol Biol,* Volume 1277, pp. 131 - 193

Eriksson, L. et al., 2006. *Multi- And Megavariate Data Analysis, 2nd Edition.* Umea, Sweden: Umetrics

ESPRIT Study Group, 2006. Aspirin plus dipyridamole versus aspirin alone after cerebral ischaemia of arterial origin (ESPRIT): randomised controlled trial. *Lancet,* Volume 367, pp. 1665 - 1673

Executive Committee for the Asymptomatic Carotid Atherosclerosis Study, 1995. Endarterectomy for asymptomatic carotid artery stenosis. *JAMA,* Volume 273, pp. 1421-1428

Fabris, F. et al., 1994. Carotid Plaque, Aging, and Risk Factors. *Stroke,* 25(6), pp. 1133 - 1140

Fancy, S. et al., 2006. Gas chromatography/flame ionisation detection mass spectrometry for the detection of endogenous urine metabolites for metabonomic studies and its use as a complementary tool to nuclear magnetic resonance spectroscopy. *Rapid Commun Mass Spectrom,* 20(15), pp. 2271 - 2280

Flu, H. et al., 2010. A systematic review of implementation of established recommended secondary prevention measures in patients with PAOD. *Eur J Vasc Endovasc Surg,* 39(1), pp. 70 - 86

Folkman, J., 1995. Angiogenesis in cancer, vascular, rheumatoid and other disease. *Nature Med,* 1(1), pp. 27 - 31

Fostegard, J. et al., 1990. Oxidized low density lipoprotein induces differentiation and adhesion of human monocytes and the monocytic cell line U937. *Proc Natl Acad Sci U S A,* 87(3), pp. 904 - 908

Fowkes, F. et al., 1991. Edinburgh Artery Study: prevalence of asymptomatic and symptomatic peripheral arterial disease in the general population. *Int J Epidemiol,* 20(2), pp. 384 - 392

Garrod, S. et al., 1999. High-resolution magic angle spinning 1H NMR spectroscopic studies on intact rat renal cortex and medulla. *Magn Reson Med,* 41(6), pp. 1108 - 1118

Gates, S. & Sweeley, C., 1978. Quantitative metabolic profiling based on gas chromatography. *Clin Chem,* 24(10), pp. 1663 - 1673

Göksan, B., Erkol, G., Bozluolcay, M. & Ince, B., 2001. Diabetes as a determinant of high-grade carotid artery stenosis: evaluation of 1,058 cases by Doppler sonography. *J Stroke Cerebrovasc Dis,* 10(6), pp. 252 - 256

Goodacre, R. et al., 2004. Metabolomics by numbers: Aquiring and understanding global metabolite data. *Trends Biotechnol,* Volume 22, pp. 245 - 252

Guasch-Ferré, M. et al., 2017. Plasma Metabolites From Choline Pathway and Risk of Cardiovascular Disease in the PREDIMED (Prevention With Mediterranean Diet) Study. *J Am Heart Assoc,* 6(11), p. pii: e006524

Halliday, A. et al., 2010. 10-year stroke prevention after successful carotid endarterectomy for asymptomatic stenosis (ACST-1): a multicentre randomised trial. *The Lancet,* 376(9746), pp. 1074 - 1084

Hansson, G., 2005. Mechanism of disease inflammation, atherosclerosis and coronary artery disease. *New England Journal of Medicine,* 352(16), pp. 1685-1695

Hawkins, I., Cho, K. & Caridi, J., 2009. Carbon dioxide in angiography to reduce the risk of contrast-induced nephropathy. *Radiol Clin North Am,* Volume 47, pp. 813 - 825

Heart Protection Study Collaborative Group, 2011. Effects on 11-year mortality and morbidity of lowering LDL cholesterol with simvastatin for about 5 years in 20,536 high-risk individuals: a randomised controlled trial. *Lancet,* 378(9808), pp. 2013 - 2020

Herisson, F. et al., 2011. Carotid and femoral atherosclerotic plaques show different morphology. *Atherosclerosis,* 216(2), pp. 348 - 354

Hiatt, W., 2001. Medical Treatment of Peripheral Arterial Disease and Claudication. *NEJM,* Volume 344, pp. 1608 - 1621

Hills, A., Shalhoub, J., Shepherd, A. & Davies, A., 2009. Peripheral Arterial Disease. *Br J Hosp Med,* Volume 70, pp. 560 - 565

Hirsch AT, H. Z. H. N. e. a., 2006. ACC/AHA 2005 practice guidelines for the management of patients with peripheral arterial disease (lower extremity, renal, mesenteric, and abdominal aortic). *Circulation,* Volume 113, pp. e463 - e654

Hollywood, K., Brison, D. & Goodacre, R., 2006. Metabolomics: current technologies and future trends. *Proteomics,* 6(17), pp. 4716 - 4723

Holmes, E. et al., 1994. Automatic data reduction and pattern recognition methods for analysis of 1H nuclear magnetic resonance spectra of human urine from normal and pathological states. *Analytical Biochemistry,* 220(2), pp. 284 - 296

Homma, S. et al., 2001. Carotid plaque and intima-media thickness assessed by B-mode ultrasonography in subjects ranging from young adults to centenarians. *Stroke,* Volume 32, pp. 830 - 835

Hopton, R. et al., 2010. Urine metabolite analysis as a function of deoxynivalenol exposure: an NMR-based metabolomics investigation. *Food Addit Contam Part A Chem Anal Control Expo Risk Assess,* Volume 27, pp. 255 - 261

Intercollegiate Stroke Working Party of the Royal College of Physicians of London, 2016. *National clinical guideline for stroke - fifth edition.* [Online] Available at: https://www.rcplondon.ac.uk/guidelines-policy/stroke-guidelines

Jahns, G. et al., 2009. Development of analytical methods for NMR spectra and application to a 13C toxicology study. *Metabolomics,* 5(2), pp. 253 - 262

Johnson, J. & Jackson, C., 2001. The apolipoprotein E knockout mouse: an animal model of atherosclerotic plaque rupture. *Atherosclerosis,* Volume 154, pp. 399 - 406

Jové, M. et al., 2013. Lipidomic and metabolomic analyses reveal potential plasma biomarkers of early atheromatous plaque formation in hamsters. *Cardiovasc Res,* 97(4), pp. 642 - 652.

Jové, M. et al., 2015. Metabolomics predicts stroke recurrence after transient ischemic attack. *Neurology,* 84(1), pp. 36 - 45

Kerwin, W., Hatsukami, T., Yuan, C. & Zhao, X., 2013. MRI of Carotid Atherosclerosis. *Am J Roentgenology,* 200(3), pp. 304 - 313

Khaleghi, M. et al., 2014. Family history as a risk factor for carotid artery stenosis. *Stroke,* 45(9), p. e198

Kiechl, S. et al., 2002. Active and passive smoking, chronic infections, and the risk of carotid atherosclerosis: prospective results from the Bruneck Study. *Stroke,* 33(9), pp. 2170 - 2176

Kietselaer, B., 2004. Noninvasive Detection of Plaque Instability with Use of Radiolabeled Annexin A5 in Patients with Carotid-Artery Atherosclerosis. *N Eng J Med,* Volume 350, pp. 1472 - 1473

Kim, K. & Bang, E., 2017. Metabolomics Profiling of the Effects of Taurine Supplementation on Dyslipidemia in a High-Fat-Diet-Induced Rat Model by 1H NMR Spectroscopy. *Taurine 10,* pp. 329 - 336

King, A., Shipley, M., Markus, H. & ACES Investigators, 2013. The effect of medical treatments on stroke risk in asymptomatic carotid stenosis. *Stroke,* 442(2), pp. 542 - 546

Kirschenlohr, H. et al., 2006. Proton NMR analysis of plasma is a weak predictor of coronary artery disease. *Nat Med,* 12(6), pp. 705 - 710

Koenig, W. & Khuseyinova, N., 2007. Biomarkers of Atherosclerotic Plaque Instability and Rupture. *Arteriosclerosis, Thrombosis, and Vascular Biology,* Volume 27, pp. 15 - 26

Kroger, K., Suckel, A., Hirche, H. & Rudofsky, G., 1999. Different prevalence of asymptomatic atherosclerotic lesions in males and females. *Vascular Medicine,* Volume 4, pp. 61 - 65

Lawes, C., Vander Hoorn, S. & Rodgers, A., 2008. International Society of Hypertension. Global burden of blood-pressure-related disease. *Lancet,* Volume 371, pp. 1513 - 1518

Lenz, E. & Wilson, I., 2007. Analytical strategies in metabonomics. *J Proteome Res,* 6(2), pp. 443 - 458

Leo, G. & Darrow, A., 2009. NMR-based metabolomics of urine for the atherosclerotic mouse model using apolipoprotein-E deficient mice. *Magnetic Resonance in Chemistry,* 47(S1), pp. S20 - S25

Lewis, G., Asnani, A. & Gerszten, R., 2008. Application of Metabolomics to Cardiovascular Biomarker and Pathway Discovery. *J Am Coll Cardiol,* 52(2), pp. 117 - 123

Libby, P., 1995. Molecular bases of acute coronary syndromes. *Circulation,* Volume 91, pp. 2844 - 2850

Li, D. et al., 2015. Metabonomic Changes Associated with Atherosclerosis Progression for LDLR(-/-) Mice. *J Proteome Res,* 14(5), pp. 2237 - 2254

Lindon, J., Holmes, E. & Nicholson, J., 2006. Metabonomics techniques and applications to pharmaceutical research & development. *Pharm Res,* 23(6), pp. 1075 - 1088

Lindon, J. & Nicholson, J., 2008. Analytical Technologies For Metabonomics And Metabolomics, And Multi-Omic Information Recovery. *TrAC-Trends in Analytical Chemistry,* 27(3), pp. 194 - 204

Li, R. et al., 1994. B-mode-detected carotid artery plaque in a general population. Atherosclerosis Risk in Communities (ARIC) Study Investigators. *Stroke,* Volume 25, pp. 2377 - 2383

Liu, A., Yu, Z., Wang, N. & Wang, W., 2015. Carotid atherosclerosis is associated with hypertension in a hospital-based retrospective cohort. *Int J Clin Exp Med,* 8(11), pp. 21932 - 21938

Lovett, J., Redgrave, J. & Rothwell, P., 2005. A Critical Appraisal of the Performance, Reporting and Interpretation of Studies Comparing Carotid Plaque Imaging with Histology. *Stroke,* Volume 36, pp. 1085 - 1091

Luque-Garcia, J. & Neubert, T., 2007. Sample preparation for serum/plasma profiling and biomarker identification by mass spectrometry. *Journal of Chromatography A,* 1153(1 - 2), pp. 259 - 276

Lusis, A., 2000. Atherosclerosis. *Nature,* 407(6801), pp. 233-241

Manly, B., 2005. Multivariate Statistical Methods: A Primer, 3rd Edition. In: Boca Raton, Florida, USA: Chapman & Hall/CRC

Marquardt, L., Geraghty, O., Mehta, Z. & Rothwell, P., 2010. Low risk of ipsilateral stroke in patients with asymptomatic carotid stenosis on best medical treatment: a prospective, population-based study. *Stroke,* 41(1), pp. e11 - e17

Marston, W. et al., 2006. Natural history of limbs with arterial insufficiency and chronic ulceration treated without revascularisation. *J Vasc Surg,* Volume 44, pp. 108 - 114

Martin, J. et al., 2009. 1H NMR metabonomics can differentiate the early atherogenic effect of dairy products in hyperlipidemic hamsters. *Atherosclerosis,* 206(1), pp. 127 - 133

Mathers, C. D., Boerma, T. & Ma Fat, D., 2009. Global and regional causes of death. *British Medical Bulletin,* Volume 92, pp. 7-32

Mayr, M. et al., 2005. Proteomic and Metabolomic Analyses of Atherosclerotic Vessels From Apolipoprotein E-Deficient Mice Reveal Alterations in Inflammation, Oxidative Stress, and Energy Metabolism. *Arterioscler Thromb Vasc Biol,* 25(10), pp. 2135 - 2142

Mayr, M. et al., 2009. Proteomics, Metabolomics, and Immunomics on Microparticles Derived From Human Atherosclerotic Plaques CLINICAL PERSPECTIVE. *Circulation,* 2(4), pp. 379 - 388

Mayr, M. et al., 2004. Vascular proteomics: linking proteomic and metabolomic changes. *Proteomics,* 4(12), pp. 3751 - 3761

McCarthy, M. et al., 1999. Angiogenesis and the atherosclerotic carotid plaque: An association between symptomatology and plaque morphology. *Journal of Vascular Surgery,* 30(2), pp. 261 - 268

Meir, K. & Leiterdorf, E., 2004. Atherosclerosis in the apolipoprotein-E-deficient mouse: a decade of progress. *Arterioscler Thromb Vasc Biol,* 24(6), pp. 1006 - 1014

Mi, T. et al., 2016. Relationship between dyslipidemia and carotid plaques in a high-stroke-risk population in Shandong Province, China. *Brain Behav,* 6(6), p. e00473

Mofidi, R. & Green, B., 2014. Carotid Plaque Morphology: Plaque Instability and Correlation with Development of Ischaemic Neurological Events. In: R. Rezzani, ed. *Carotid artery disease - From bench to bedside and beyond.* s.l.:InTech, pp. 85 - 104

Moody, P., Gould, P. & Harris, P., 1990. Vein graft surveillance improves patency in femoro-popliteal bypass. *Eur J Vasc Surg,* Volume 4, pp. 117 - 121

Moreno, P. et al., 2006. Neovascularization in human atherosclerosis. *Circulation,* Volume 113, pp. 2245 - 2252

MRC Asymptomatic Carotid Surgery Trial (ACST) Collaborative Group, 2004. Prevention of disabling and fatal strokes by successful carotid endarterectomy in patients without recent neurological symptoms: randomised controlled trial. *Lancet,* 363(9420), pp. 1491 - 1502

Murabito, J., D'Agostino, R., Silbershatz, H. & Wilson, W., 1997. Intermittent claudication. A risk profile from The Framingham Heart Study. *Circulation,* 96(1), pp. 44-49

Murakami, S., 2014. Taurine and atherosclerosis. *Amino Acids,* 46(1), pp. 73 - 80

Nakashima, Y. et al., 1994. ApoE-deficient mice develop lesions of all phases of atherosclerosis throughout the arterial tree. *Arteriosclerosis, Thrombosis, and Vascular Biology,* Volume 14, pp. 133 - 140

Naylor, A., 2011. Time to rethink management strategies in asymptomatic carotid artery disease. *Nat Rev Cardiol,* 9(2), pp. 116 - 124

Naylor, A. et al., 2017. Management of Atherosclerotic Carotid and Vertebral Artery Disease: 2017 Clinical Practice Guidelines of the European Society for Vascular Surgery (ESVS) ESVS Guideline Reviewers. *Eur J Vasc Endovasc Surg,* pp. 1 - 79

Naylor, R., 2015. Carotid artery disease: clinical features and management. *Vascular Surgery,* 33(7), pp. 340 - 344

Newman, A. et al., 1999. Ankle-arm index as a predictor of cardiovascular disease and mortality in the Cardiovascular Health Study. *Arterioscler Thromb Vasc Biol,* Volume 19, pp. 538 - 545

NICE, 2012. *www.nice.org.uk.* [Online]
Available at: https://www.nice.org.uk/guidance/cg147

Nicholson, J. et al., 1995. 750 MHz 1H and 1H-13C NMR spectroscopy of human blood plasma. *Anal Chem,* 67(5), pp. 793 - 811

Nicholson, J., Lindon, J. & Holmes, E., 1999. 'Metabonomics': understanding the metabolic responses of living systems to pathophysiological stimuli via multivariate statistical analysis of biological NMR spectroscopic data. *Xenobiotica,* 29(11), pp. 1181 - 1189

Nicholson, J. et al., 1984. Proton-nuclear-magnetic-resonance studies of serum, plasma and urine from fasting normal and diabetic subjects. *Biochem J,* 217(2), pp. 365 - 375

Norgren, L. et al., 2007. Inter-Society Consensus for the Management of Peripheral Arterial Disease (TASC II). *J Vasc Surg,* 45(S), pp. S5 - S67

North American Symptomatic Carotid Endarterectomy Trial Collaborators (NASCET), 1991. Beneficial effect of carotid endarterectomy in symptomatic patients with high-grade carotid stenosis. *N Engl J Med,* pp. 325-445

Oates, C. et al., 2009. Joint recommendations for reporting carotid ultrasound investigations in the United Kingdom. *Eur J Vasc Endovasc Surg,* 37(3), pp. 251 - 261

O'Brien, E. et al., 1994. Angiogenesis in human coronary atherosclerotic plaques. *Am J Pathol,* 145(4), pp. 883 - 894

O'Leary, D. et al., 1992b. Cholesterol and carotid atherosclerosis in older persons: The Framingham study. *Stroke,* Volume 2, pp. 147 - 153

Oliver, S., Winson, M., Kell, D. & Baganz, F., 1998. Systematic functional analysis of the yeast genome. *Trends Biotechnol,* 16(9), pp. 373 - 378

Ouwendijk, R. et al., 2005. Imaging Peripheral Arterial Disease: A Randomised Controlled Trial Comparing Contrast-enhanced MR Angiography and Multi–Detector Row CT Angiography. *Radiology,* Volume 236, pp. 1094 - 1103

Prasad, P. & Donoghue, M., 2013. A comparative study of various decalcification techniques. *Indian J Dent Res,* 24(3), pp. 302 - 308

PRoFESS Study Group, 2008. Aspirin and extended-release dipyridamole versus clopidogrel for recurrent stroke. *New England Journal of Medicine,* Volume 359, pp. 1238 - 1251

PROGRESS Collaborative Group, 2001. Randomised trial of a perindopril-based blood-pressure-lowering regimen among 6105 individuals with previous stroke or transient ischaemic attack. *Lancet,* Volume 358, pp. 1033 - 1041

Rajaie, S. & Esmaillzadeh, A., 2011. Dietary Choline and Betaine Intakes and Risk of Cardiovascular Diseases: Review of Epidemiological Evidence. *ARYA Atheroscler,* 7(2), pp. 78 - 86

Resnick, H. et al., 2004. Relationship of High and Low Ankle Brachial Index to All-Cause and Cardiovascular Disease Mortality: The Strong Heart Study. *Circulation,* Volume 109, pp. 733 - 739

Ricotta, J. J. et al., 2001. Updated Society for Vascular Surgery guidelines for management of extracranial carotid disease. *Journal of Vascular Surgery,* 54(3), pp. e1-e31

Robertson, D., 2005. Metabonomics in toxicology: a review. *Toxicol Sci,* 85(2), pp. 809 - 822

Rochfort, S., 2005. Metabolomics reviewed: A new "Omics" platform technology for systems biology and implications for natural products research. *Journal of Natural Products,* 68(12), pp. 1813 - 1820

Rosenfeld, M. et al., 2000. Advanced Atherosclerotic Lesions in the Innominate Artery of the ApoE Knockout Mouse. *Arterioscler Thromb Vasc Biol,* 20(12), pp. 2587 - 2592

Rosenfield, K. et al., 2016. Randomized Trial of Stent versus Surgery for Asymptomatic Carotid Stenosis. *N Engl J Med,* Volume 374, pp. 1011 - 1020

Rothwell, P. et al., 2004. Endarterectomy for symptomatic carotid stenosis in relation to clinical subgroups and timing of surgery. *Lancet,* 363(9413), pp. 915-924

Rothwell, P. et al., 2007. Effect of urgent treatment of transient ischaemic attack and minor stroke on early recurrent stroke (EXPRESS study): a prospective population-based sequential comparison. *Lancet,* 370(9596), pp. 1432 - 1442

Sadowski, E. et al., 2007. Nephrogenic systemic fibrosis: Risk factors and incidence estimation. *Radiology,* 243(1), pp. 148 - 157

Sakalihasan, N. & Michel, J., 2009. Functional Imaging of Atherosclerosis to Advance Vascular Biology. *Eur J Vasc Endovasc Surg,* pp. 728 - 734

Sangeetha, R., Uma, K. & Chandavarkar, V., 2013. Comparison of routine decalcification methods with microwave decalcification of bone and teeth. *J Oral Maxillofac Pathol,* 17(3), pp. 386 - 391

Sarkar, P. et al., 2017. Prophylactic role of taurine and its derivatives against diabetes mellitus and its related complications. *Food and Chemical Toxicology,* Volume 110, pp. 109 - 121

Saude, E., Slupsky, C. & Sykes, B., 2006. Optimization Of NMR Analysis Of Biological Fluids For Quantitative Accuracy. *Metabolomics,* 2(3), pp. 113 - 123

Schirmang, T. et al., 2009. Peripheral Arterial Disease: Update of Overview and Treatment. *Med Health R I,* Volume 92, pp. 398 - 402

Scholtes, V. et al., 2014. Type 2 diabetes is not associated with an altered plaque phenotype among patients undergoing carotid revascularization. A histological analysis of 1455 carotid plaques. *Atherosclerosis,* 235(2), pp. 418 - 423

Selvin, E. & Erlinger, T., 2004. Prevalence of and risk factors for peripheral arterial disease in the United States: results from the National Health and Nutrition Examination Survey, 1999–2000. *Circulation,* 110(6), pp. 738 - 743

Shah, P., 2003. Mechanisms of plaque vulnerability and rupture. *J Am Coll Cardiol,* Volume 41, pp. 15S - 22S

Shaikh, S. et al., 2012. Macrophage Subtypes in Symptomatic Carotid Artery and Femoral Artery Plaques. *Eur J Vasc Endovasc Surg,* 44(5), pp. 491 - 497

Shalhoub, J. et al., 2010. The use of contrast enhanced ultrasound in carotid arterial disease. *Eur J Vasc Endovasc Surg,* 39(4), pp. 381 - 387

Silverman, K. et al., 1985. Fat angiogenesis: a possible link to coronary atherosclerosis and thrombosis. *Circulation,* Volume 72, p. 282

Skoog, D., Holler, F. & Nieman, T., 1998. In: *Principles of Instrumental Analysis, 5th edition.* s.l.:Saunders College

Spence, J., 2015. Management of asymptomatic carotid stenosis. *Neurol Clin,* Volume 33, pp. 443 - 457

Spence, J., Song, H. & Cheng, G., 2016. Appropriate management of asymptomatic carotid stenosis. *Stroke and Vascular Neurology,* p. e000016

Spraula, M. et al., 1994. Automatic reduction of NMR spectroscopic data for statistical and pattern recognition classification of samples. *Journal of Pharmaceutical and Biomedical Analysis,* 12(10), pp. 1215 - 1225

Sritharan, K. & Davies, A., 2006. The ischaemic leg. *Br J Hosp Med (Lond),* 67(3), pp. M56 - M58

Stary, H. et al., 1995. A Definition of Advanced Types of Atherosclerotic Lesions and a Histological Classification of Atherosclerosis. A Report From the Committee on Vascular Lesions of the Council on Arteriosclerosis, American Heart Association. *Circulation,* Volume 92, pp. 1355 - 1374

Su, T., Jeng, J., Chien, K. & Libby, P., 2001. Hypertension Status Is the Major Determinant of Carotid Atherosclerosis. A Community-Based Study in Taiwan. *Stroke,* Volume 32, pp. 2265 - 2271

Tapiero, H., Mathé, G., Couvreur, P. & Tew, K., 2002. II. Glutamine and glutamate. *Biomed Pharmacother,* 56(9), pp. 446 - 457

Taylor, F. et al., 2013. Statins for the primary prevention of cardiovascular disease. *Cochrane Database Syst Rev,* Issue 1, p. CD004816

Tell, G. et al., 1994. Relation of smoking with carotid artery wall thickness and stenosis in older adults. The Cardiovascular Health Study. *Circulation,* Volume 90, pp. 2905 - 2908

Teul, J. et al., 2009. Improving metabolite knowledge in stable atherosclerosis patients by association and correlation of GC-MS and 1H NMR fingerprints. *J Proteome Res,* 8(12), pp. 5580 - 5589

The Heart Outcome Prevention Evaluation Study Investigators, 2000. Effects of an angiotensin-converting enzyme inhibitor, ramipril, on cardiovascular events in high-risk patients. *N Engl J Med,* Volume 342, pp. 145 - 153

The Renal Association, 2017. *The Renal Association - CKD Definition.* [Online] Available at: https://renal.org/information-resources/the-uk-eckd-guide/ckd-stages/

Trygg, J., Holmes, E. & Lundstedt, T., 2007. Chemometrics in metabonomics. *J Proteome Res,* 6(2), pp. 469 - 479

Türeyen, K. et al., 2006. Increased Angiogenesis and Angiogenic Gene Expression in Carotid Artery Plaques from Symptomatic Stroke Patients. *Neurosurgery,* Volume 59, pp. 971 - 977

Turner, P. et al., 2008. Dietary wheat reduction decreases the level of urinary deoxynivalenol in UK adults. *J Expo Sci Environ Epidemiol,* Volume 18, pp. 392 - 399

Ubbink, D., 2004. Toe blood pressure measurements in patients suspected in leg ischaemia: a new laser Doppler device compared with photo-plethysmography. *Eur J Vasc Endovasc Surg,* Volume 27, pp. 629 - 634

Van de Meer, I. et al., 2003. Risk factors for progression of atherosclerosis measured at multiple sites in the arterial tree: the Rotterdam Study. *Stroke,* 34(10), pp. 2374 - 2379

Van den Berg, R. et al., 2006. Centering, scaling, and transformations: improving the biological information content of metabolomics data. *BMC Genomics,* 8(7), p. 142

Van Der Greef, J. & Smilde, A., 2005. Symbiosis of chemometrics and metabolomics: past, present, and future. *Journal of Chemometrics,* 19(5 - 7), pp. 376 - 386

Viant, M. et al., 2009. International NMR-Based Environmental Metabolomics Intercomparison Exercise. *Environmental Science & Technology,* 43(1), pp. 219 - 225

Virmani, R. et al., 2000. Lessons from sudden coronary death: a comprehensive morphological classification scheme for atherosclerotic lesions. *Arterioscler Thromb Vasc Biol,* 20(5), pp. 1262 - 1275

Virmani, R., Ladich, E., Burke, A. & Kolodgie, F., 2006. Histopathology of carotid atheerosclerotic disease. *Neurosurgery,* 59(5), pp. 219 - 227

Von Maravic, C. et al., 1991. Clinical relevance of intraplaque haemorrhage in the internal carotid artery. *Eur J Surg,* 157(3), pp. 185 - 188

Vorkas, P. et al., 2016. Metabolic Phenotypes of Carotid Atherosclerotic Plaques Relate to Stroke Risk: An Exploratory Study. *Euro J Vasc Endovasc Surg,* 52(1), pp. 5 - 10

Wang, Y. et al., 2003. Spectral editing and pattern recognition methods applied to high-resolution magic-angle spinning 1H nuclear magnetic resonance spectroscopy of liver tissues. *Anal Biochem,* 323(1), pp. 26 - 32

Wardlaw, J. et al., 2006. Accurate, practical and cost-effective assessment of carotid stenosis in the UK. *Health Technol Assess,* 10(30), pp. 1 - 182

Wasserman, B., 2010. Advanced Contrast-Enhanced MRI for Looking Beyond the Lumen to Predict Stroke Building a Risk Profile for Carotid Plaque. *Stroke,* Volume 41, pp. 512 - 516

Waybill, M. & Waybill, P., 2001. Contrast media-induced nephrotoxicity: identification of patients at risk and algorithms for prevention. *J Vasc Interv Radiol,* Volume 12, pp. 3 - 9

Webb-Robertson, B. et al., 2005. A study of spectral integration and normalization in NMR-based metabonomic analyses. *Journal of Pharmaceutical and Biomedical Analysis,* 39(3 - 4), pp. 830 - 836

Wijeyaratne, S., Abbott, C. & Gough, M., 2002. A modification to the standard technique for carotid endarterectomy allowing the removal of intact endarterectomy specimens: Implications for research and quality control of preoperative imaging. *Euro J Vasc Endovasc Surg,* Volume 23, pp. 370 - 371

Willeit, J. & Kiechl, S., 1993. Prevalence and risk factors of asymptomatic extracranial carotid artery atherosclerosis. A population-based study. *Arterioscler Thromb,* Volume 13, pp. 661 - 668

Wishart, D., 2007. Proteomics and the human metabolome project. *Exp Rev Proteomics,* Volume 4, pp. 333 - 335

Würtz, P. et al., 2011. Characterization of systemic metabolic phenotypes associated with subclinical atherosclerosis. *Mol Biosyst,* 7(2), pp. 385 - 393

Wu, Y. et al., 2007. Characterization of Plaques Using 18F-FDG PET/CT in Patients with Carotid Atherosclerosis and Correlation with Matrix Metalloproteinase-1. *J Nucl Med,* Volume 48, pp. 227 - 233

Yang, Y. et al., 2014. Molecular BioSystems Serum metabonomic analysis of apoE-/- mice reveals progression axes for atherosclerosis based on NMR spectroscopy. *Mol Biosyst,* Volume 10, pp. 3170 - 3178

Yuan, J. et al., 2017. Imaging Carotid Atherosclerosis Plaque Ulceration: Comparison of Advanced Imaging Modalities and Recent Developments. *American Journal of Neuroradiology,* 38(4), pp. 664 - 671

Zhang, F. et al., 2009. Metabonomics study of atherosclerosis rats by ultra fast liquid chromatography coupled with ion trap-time of flight mass spectrometry. *Talanta,* 79(3), pp. 836 - 844

Zha, W. et al., 2009. Metabonomic characterization of early atherosclerosis in hamsters with induced cholesterol. *Biomarkers,* 14(6), pp. 372 - 380